



Woodchip denitrification filter- performance evaluation

Third year of operation

Prepared for DairyNZ

April 2019

Prepared by:
Neale Hudson
Stephan Heubeck
Evan Baddock

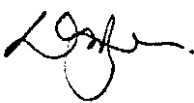
For any information regarding this report please contact:

Neale Hudson
Environmental Chemist/Group Manager
Catchment Processes
+64-7-856 1772
neale.hudson@niwa.co.nz

National Institute of Water & Atmospheric Research Ltd
PO Box 11115
Hamilton 3251

Phone +64 7 856 7026

NIWA CLIENT REPORT No: 2019086HN
Report date: April 2019
NIWA Project: DNZ18202

Quality Assurance Statement		
	Reviewed by:	Kit Rutherford
	Formatting checked by:	Alison Bartley
	Approved for release by:	David Roper

Contents

- Executive summary 9**

- 1 Introduction 12**
 - 1.1 Nutrient attenuation..... 12
 - 1.2 Report structure 14

- 2 Materials and methods 15**
 - 2.1 Location of the nitrate-N filter..... 15
 - 2.2 Description of the nitrate-N filter 15
 - 2.3 High frequency, real time analysers of inflow and outflow nitrate concentration 20
 - 2.4 Data storage and manipulation 20
 - 2.5 Modelling nutrient loads 21
 - 2.6 Estimating filter performance..... 23

- 3 Climate summary..... 25**

- 4 Woodchip filter hydrology..... 28**

- 5 Hyperspectral and water quality sonde data..... 30**
 - 5.1 Hyperspectral data..... 30
 - 5.2 Dissolved oxygen concentrations 32
 - 5.3 Dissolved organic matter concentrations..... 34
 - 5.4 pH measurement 35

- 6 Other woodchip filter bed characteristics 37**
 - 6.1 Water temperature..... 37
 - 6.2 Electrical conductivity..... 37
 - 6.3 Turbidity..... 39

- 7 Nitrate-N filter performance assessment..... 40**
 - 7.1 Estimation of mass loads 40
 - 7.2 Ammoniacal-N 41
 - 7.3 Nitrate-N 45
 - 7.4 Total nitrogen 60
 - 7.5 Effect of water level adjustment on woodchip filter 62

- 8 Treatment performance – opportunities for optimisation 65**

9	Summary	67
10	Acknowledgements	70
11	Glossary of abbreviations and terms	71
12	References	72
Appendix A	Instrumentation deployed at nitrate-N woodchip filter	75
Appendix B	Hyperspectral measurement devices	77
	The measurement principle	77
	Issues associated with use of the Spectra::lyser device	79
Appendix C	Derivation of a process-based denitrification model	80
Appendix D	Climate data	83
Appendix E	Woodchip filter hydrology	86
Appendix F	Explanation of box and whisker plot	89
Appendix G	Woodchip filter bed water level changes in response to rainfall events	90
Appendix H	Electrical conductivity measurements	91
	EC vs flow – Inflow	93
	EC vs Flow - Outflow	94
Appendix I	Turbidity-flow relationships	95
Appendix J	N-filter load estimation – concentration data	96
	Concentration vs flow relationships	96
	Measured vs Model estimated concentrations	100
	Ammoniacal-N.....	100
Appendix K	Efficacy of woodchip filter, inflow AMLE vs outflow process model estimates – Nitrate-N only	129
Appendix L	Nitrate-N removal performance	134
Appendix M	Relationship between woodchip filter performance and temperature	142
	Tables	
Table 7-1:	Summary statistics for estimated ammoniacal-N inflow and outflow flux.	44
Table 7-2:	Nitrate-N removal efficacy for the entire assessment period derived from hourly average values.	51

Table 7-3:	Nitrate-N removal performance over the three-year assessment period.	58
Table 7-4:	Woodchip filter performance in terms of TN removal and removal efficacy.	61
Table 9-1:	Summary of median measured and predicted concentrations and performance metrics.	67
Table 9-2:	Comparison of measured nitrate-N removal with other published performance data.	69
Table E-1:	Summary statistics for woodchip filter inflow and outflow.	86
Table J-1:	Summary statistics for all grab sample concentration data for woodchip filter inflow and outflow.	98
Table J-2:	Woodchip filter performance data - ammoniacal-N.	118
Table J-3:	Summary statistics for woodchip filter performance - nitrate-N removal, entire assessment period.	120
Table J-4:	Summary statistics for woodchip filter performance - nitrate-N removal, by season.	121
Table J-5:	Woodchip filter performance data - nitrate-N.	125
Table J-6:	Woodchip filter performance data - total-N.	127

Figures

Figure 2-1:	Location of the nitrate-N filter in Southland.	16
Figure 2-2:	Location of nitrate-N filter relative to the paddock which is the principal source of shallow groundwater draining into the filter.	17
Figure 2-3:	Schematic of nitrate-N filter showing dimensions and key components of the as-built filter.	18
Figure 2-4:	Photograph of nitrate-N filter showing key components of the monitoring equipment at the as-built filter.	19
Figure 3-1:	Annual total rainfall, 2001-2018 inclusive.	25
Figure 3-2:	Comparison of monthly total rainfall measured on site January 20016 to December 2018, and long-term statistical values.	26
Figure 3-3:	Comparison of monthly average soil moisture recorded at Invercargill airport between January 20016 and December 2018, and the long-term average value (2001-2018, black line).	27
Figure 4-1:	Comparison of inflow to and outflow from the woodchip filter.	28
Figure 4-2:	Time-series of water levels in the woodchip filter, recorded in the NE (inlet) SE (outlet) corner of the bed.	29
Figure 4-3:	Distribution of theoretical retention time in the woodchip filter (left), and relationship between retention time and season (right).	29
Figure 5-1:	Inflow and outflow nitrate-N concentrations and flux.	30
Figure 5-2:	Estimate of nitrate-N removal efficacy derived from TriOS inflow and outflow measurements.	31
Figure 5-3:	Comparison of nitrate-N removal efficacy derived from TriOS inflow and outflow measurements (blue) and estimates from a mixed regression model based on grab sample concentrations (red).	32
Figure 5-4:	Comparison of inflow and outflow dissolved oxygen concentrations, and relationship to inflow events.	33

Figure 5-5:	Comparison of inflow and outflow fluorescent dissolved organic matter concentrations.	35
Figure 5-6:	Comparison of inflow and outflow pH.	36
Figure 6-1:	Comparison of hourly average inflow and outflow temperatures.	37
Figure 6-2:	Comparison of hourly average inflow and outflow electrical conductivity.	38
Figure 6-3:	Time series of daily median turbidity values, woodchip filter inflow, classified according to season.	39
Figure 7-1:	Ammoniacal-N inflow flux to woodchip filter, estimated using two models.	42
Figure 7-2:	Ammoniacal-N outflow flux from woodchip filter, estimated using two models.	42
Figure 7-3:	Comparison of woodchip filter inflow and outflow ammoniacal-N flux estimated using bootstrap regression models.	43
Figure 7-4:	Performance of the woodchip filter in terms of ammoniacal-N removal, reported as proportion of inflow load by month (left) and season (right).	45
Figure 7-5:	Nitrate-N inflow flux to woodchip filter, estimated using two models.	46
Figure 7-6:	Nitrate-N outflow flux from woodchip filter, estimated using two models.	47
Figure 7-7:	Comparison of woodchip filter measured and predicted nitrate-N outflow concentrations.	48
Figure 7-8:	Time series of measured (red dots) and predicted (blue crosses) woodchip filter nitrate-N outflow concentrations at normal (A) and log ₁₀ scale (B).	48
Figure 7-9:	Time series of measured and predicted woodchip filter nitrate-N outflow flux.	49
Figure 7-10:	Relationship between nitrate-N removal (blue), estimated as the difference between inflow and outflow nitrate-N flux, and hydraulic retention time (grey).	52
Figure 7-11:	Seasonal variation in nitrate-N removal efficacy (A) and nitrate removal rate (B).	53
Figure 7-12:	Relationship between nitrate-N removal efficacy (red) and hydraulic retention time (grey).	54
Figure 7-13:	Relationship between nitrate-N removal and hydraulic retention time (A), and nitrate-N removal efficacy and hydraulic retention time (B).	54
Figure 7-14:	Comparison of median nitrate-N inflow and outflow flux by month.	55
Figure 7-15:	Median nitrate-N removal, estimated as the difference between inflow and outflow flux by month.	56
Figure 7-16:	Average nitrate-N removal efficacy, estimated as the percent of inflow flux removed by the filter by month.	56
Figure 7-17:	Seasonal nitrate-N flux (A), removal (B) and efficacy (C).	57
Figure 7-18:	Relationship between nitrate-N removal performance and inflow, 2016 data only.	59
Figure 7-19:	Influence of temperature on nitrate-N removal performance.	59
Figure 7-20:	TN inflow flux to the woodchip filter, estimated using two models.	60
Figure 7-21:	Comparison of woodchip filter inflow and outflow TN flux estimated using bootstrap regression models.	60
Figure 7-22:	Time-series of daily average inflows and outflows, and water levels in the woodchip filter, recorded in the NE (inlet) SE (outlet) corner of the bed.	63
Figure 9-1:	Relationship between nitrate-N removal rate and active bed volume by year.	68

Figure A-1:	Schematic from NEON logger schema indicating location and type of measurement equipment. A and B indicate location and type of additional equipment.	76
Figure D-1:	Monthly average rainfall, 2001-2018 inclusive.	83
Figure D-2:	Comparison of on-site monthly total rainfall, 2016-2018 inclusive, with rainfall recorded at Invercargill airport.	83
Figure D-3:	Difference between monthly total rainfall measured on site with rainfall measured at Invercargill airport.	84
Figure D-4:	Long-term average daily temperature and soil moisture recorded at Invercargill airport for the period 2001-2018.	84
Figure D-5:	Comparison of monthly average temperatures recorded at Invercargill airport between January 20016 and December 2018, and the long-term average value (black line).	85
Figure E-1:	Hourly average flow recorded for woodchip inflow and outflow.	87
Figure E-2:	Daily average flow recorded for woodchip inflow and outflow.	87
Figure E-3:	Seasonal average flow recorded for woodchip inflow and outflow.	88
Figure E-4:	Distribution of inflow values for the entire assessment period (left) and by season (right).	88
Figure F-1:	Explanation of a box-and-whisker plot.	89
Figure G-1:	Time-series of hourly average inflows and outflows, and water levels in the woodchip filter, recorded in the NE (inlet) SE (outlet) corner of the bed.	90
Figure H-1:	Relationship between daily average inflow and outflow electrical conductivity according to season.	91
Figure H-2:	Relationship between daily average inflow and outflow electrical conductivity according to season.	92
Figure H-3:	Relationship between daily average inflow and outflow nitrate-N according to season.	92
Figure H-4:	Relationship between daily average inflow and electrical conductivity according to month and year.	93
Figure H-5:	Relationship between daily average outflow and electrical conductivity according to month and year.	94
Figure I-1:	Relationship between daily median turbidity and woodchip inflow classified according to season.	95
Figure J-1:	Comparison of measured concentration and flow values for three forms of nitrogen.	97
Figure J-2:	Comparison of inflow and outflow concentrations for all grab samples (mg/L).	99
Figure J-3:	Comparison of measured and predicted inflow ammoniacal-N concentration.	101
Figure J-4:	Comparison of measured and predicted outflow ammoniacal-N concentration.	103
Figure J-5:	Comparison of measured and predicted inflow nitrate-N concentration.	105
Figure J-6:	Comparison of measured and process-model predicted outflow nitrate-N concentration.	107
Figure J-7:	Relationship of measured and process-model predicted outflow nitrate-N concentrations and flow, all values.	108

Figure J-8:	Comparison of measured and predicted inflow total-N concentration.	110
Figure J-9:	Comparison of measured and predicted outflow total-N concentration.	112
Figure J-10:	Performance of the woodchip filter in terms of ammoniacal-N removal, grams per day.	113
Figure J-11:	Performance of the woodchip filter in terms of ammoniacal-N removal, reported as proportion of inflow load.	113
Figure J-12:	Time-series of hourly average outflow nitrate-N flux derived from a mixed regression model. The black dots are grab sample flux estimates.	114
Figure J-13:	Time-series of hourly average inflow and outflow nitrate-N flux derived from two bootstrap regression models.	114
Figure J-14:	Nitrate-N inflow and outflow flux from woodchip filter, estimated using two models.	115
Figure J-15:	TN outflow flux from the woodchip filter, estimated using two models.	115
Figure J-16:	Comparison of woodchip filter inflow and outflow TN flux estimated using AMLE regression models.	116
Figure J-17:	TN removal by woodchip filter - inflow minus outflow TN flux, estimated using bootstrap regression models.	116
Figure J-18:	Efficacy of TN removal by woodchip filter, expressed as proportion of inflow flux removed, estimated using bootstrap regression models.	117
Figure K-1:	Relationship between nitrate-N removal (red) and hydraulic retention time (cyan).	129
Figure K-2:	Median nitrate-N removal efficacy, estimated as the percent of inflow flux removed by the filter by month.	130
Figure K-3:	Nitrate-N removal efficacy for various time periods.	131
Figure K-4:	Distribution of retention time by year.	132
Figure K-5:	Distribution of nitrate-N removal performance data by year.	132
Figure K-6:	Relationship between nitrate-N removal performance and retention time by year.	133

Executive summary

NIWA was commissioned to evaluate the performance of a woodchip denitrification filter in the Waituna Lagoon catchment, Southland. The assessment covered a three-year period (2016-2018). This report summarises the findings from the entire assessment period, but incorporates insights gained from measuring additional variables in the final year (turbidity, pH and DO) and from using novel measuring techniques (continuous nitrate-N sensors) to complement the techniques used in the first two years. The third year of the study was intended to corroborate the findings from the earlier two years and check whether filter performance remained similar. The second assessment period included an altered hydrological regime, where the water level in the bed was lowered to provide increased storage volume, with an expectation that the increased storage would improve treatment efficacy.

Treatment efficacy was assessed in terms of loads of ammoniacal-N, nitrate-N and total N entering and leaving the woodchip filter. These loads were quantified at hourly timestep using two broad modelling approaches, and several discrete model types. First, regression models were developed between flow (measured continuously) and concentration (sporadic grab samples) and used to estimate time-series of inflow and outflow flux. Treatment efficiency was calculated as the difference between inflow and outflow flux, expressed in terms of mass of material removed, at a daily time-step. These types of model were adequate for ammoniacal-N and total nitrogen. Second, a process-based denitrification model was developed using literature equations and calibrated to match measured fluxes. This was required to provide accurate estimates of nitrate-N, which was the focus of this work. The results of the study are summarised for the entire assessment period in Table i. It is important to realise that the performance of the woodchip filter was highly variable over the assessment period, principally because of fluctuating hydraulic and contaminant mass loading rates, and other season effects.

Table i: Summary of median measured and predicted concentrations and performance metrics.

Negative values indicate net increase in concentration between inflow and outflow. N/A indicates value not calculated.

Nitrogen form	Estimation method	Median concentration (mg/L)		Mass removal (g/d)	Specific removal (g/m ³ /d)	Efficacy (%)
		Inflow	Outflow			
Ammoniacal-N	Model	0.02	0.125	-2.0	N/A	-314
	Grab	0.019	0.078	N/A	N/A	N/A
Nitrate-N	Model	2.3	0.7	32.7	0.9	72
	Grab	2.2	0.78	N/A	N/A	N/A
Total N	Model	2.41	1.09	32.1	N/A	54.4
	Grab	2.45	1.12	N/A	N/A	N/A

The estimate of mass load reduction or treatment efficacy is to a small extent influenced by the models selected, but all models gave similar results in terms of mass of material removed, trend over time and specific assessment period (e.g., summer or winter).

As reported in the summary of the first year of operation, the woodchip filter was a net source of ammoniacal-N. Although discharge of ammoniacal-N to water is undesirable (ammoniacal-N is toxic

to aquatic organisms), the relatively small mass loads (typically in a range from 1-2 g/d) suggest that the discharge is unlikely to have measurable effects on the receiving stream (Waituna Creek), where the current load is of the order 6,000 g/d (estimated using data from other sources).

Regression models provided credible estimates of inflow TN flux under all conditions, and outflow TN flux except during periods of low outflow, when the models predicted slightly higher flux than those calculated from measured TN using grab samples. Removal of TN was variable over time, determined principally by influent load, retention time, and temperature. Over the full trial period, approximately 33% of the TN was removed, reducing the influent flux from approximately 150 g/d to 100 g/d.

Determination of nitrate-N treatment efficacy was more difficult than for ammoniacal-N or TN. None of the regression model approaches trialled provided acceptable estimates of outflow nitrate-N concentrations or flux, particularly under low-flow conditions. The reason is that the regression models assume linear relationships between concentration, flow and temperature but ignore non-linear microbial transformations within the filter (notably denitrification). All the regression model approaches under-predicted nitrate removal.

Denitrification is a microbially mediated process, and the rate of reaction is determined by inflow nitrate-N concentrations, organic carbon supply, dissolved oxygen concentrations, temperature and retention time. A process-based denitrification model was developed that allowed outflow nitrate-N concentration and flux to be predicted from influent nitrate-N concentration, temperature, retention time and organic carbon supply. Over the entire period mean and median nitrate-N removal rates were estimated to be 75 g/d and 33 g/d respectively, while mean and median removal efficacies (proportion of influent load removed) were 65% and 70% respectively. Although the removal efficacy was lower in winter than summer (because inflows were high, retention time was low, and temperature was low), the mass of nitrate-N removed was high in winter and in high flows because of the large mass of nitrate-N in the inflow during these periods.

Treatment efficacy is influenced strongly by retention time – greater time allows the fixed microbial biomass to utilise the influent nitrate-N load. We found that reducing the bed water depth reduced the effective treatment volume, with two outcomes:

- the nitrate-N removal rate expressed in g/d decreased as bed depth decreased, and
- the treatment efficacy expressed as g/m³/d also decreased.

Reducing the water depth in the woodchip filter bed increased potential storage volume, but decreased active bed volume, treatment capacity and efficacy. We postulate that the population of denitrifying bacteria in the upper filter layer that only became saturated during high inflows was not able to increase quickly enough to utilise the additional nitrate-N load. We conclude that reducing the bed depth in order to provide additional storage for high inflows increases the cost of treatment and is not cost-effective because the storage capacity created is un- or under-utilised much of the time.

During the second assessment period, several additional water quality variables and novel measurement techniques were used to provide further insights into filter operation and to determine their usefulness for treatment assessment purposes. We demonstrated that continuous hyperspectral analysers provided reliable nitrate-N concentration estimates. These devices are well-suited for moderate duration deployments (weeks to months), creating the potential to provide very detailed flow-treatment efficacy information.

The data and information that has been derived from this assessment will allow the design and operation of future woodchip denitrification filters to be further refined and optimised.

1 Introduction

To improve water quality outcomes, inputs of nutrient from various land uses may need to be managed and reduced. Various on-farm tools are available to reduce the nitrogen and phosphorus (N and P) in water leaving paddocks and entering streams, including constructed and natural wetlands, riparian buffers, or addition of reactive materials (McKergow et al. 2008).

While the science behind many attenuation tools is reasonably well understood, their performance at field-scale is less certain. Farmers require certainty regarding the efficacy and cost-effectiveness of different mitigation options, before they will adopt new strategies for reducing contaminant losses. Industry bodies (e.g., DairyNZ, Fonterra), regulatory agencies (Department of Conservation, Regional Councils etc.) and researchers, consultants and farm advisers all need to have confidence in the mitigation measures that are currently available and likely to be deployed. Field trials are required under conditions relevant to New Zealand pastoral farming to verify performance, refine design, demonstrate applicability and provide realistic information regarding construction and maintenance costs.

NIWA was commissioned by DairyNZ and the Living Water - Department of Conservation - Fonterra Partnership to design, install and operate a woodchip-filled nitrate-N filter, and a smaller phosphorus filter to treat drainage from pasture. The latter was filled with a modified zeolite medium – the modification involves inclusion of aluminium as the primary phosphorus binding agent. Once the two filters were installed and operational, NIWA was to manage/operate a monitoring programme that would provide the data and information required to estimate the N and P removal efficacy of these filters. The selection of the filter deployment sites, and design and construction of these filters was described previously (Tanner et al. 2013; McKergow et al. 2015; McKergow et al. 2016). Performance of the filters for the period January 2016 to April 2017 (viz., after initial 10- and 16-month periods of operation (P and N filters respectively)) was reported previously (Hudson et al. 2017). The current report summarises the outcomes of monitoring conducted for the period April 2017 to December 2018 as an extension of the earlier work.

In addition to summarising and quantifying the nutrient removal efficacy of two filter media, this report also describes several instruments that were deployed to make additional measurements that provided information regarding the inflow and discharge of organic carbon, nitrate-N and several other water quality variables. This was done to contribute to our understanding of the performance of a biological process. The data summarised includes real-time high frequency measurement of several variables, and identifies how this technology may be used to assess environmental performance relatively cost-effectively.

1.1 Nutrient attenuation

Tile drains are an important feature of Southland's agricultural landscape, providing drainage essential for pasture production. Subsurface drainage reduces surface runoff, notably peak outflow rates. However, improved drainage accelerates the transport of nutrients off-farm, particularly nitrate-nitrogen. This form of nitrogen is readily mobilised through the soil profile with drainage water. Tile drainage effectively shortens nutrient discharge pathways (reducing denitrification capacity), thereby increasing the delivery of nitrogen to surface waters (Maalim and Melesse 2013; Christianson et al. 2016; Villeneuve 2017). Arenas Amado et al. (2017) demonstrated that tile drains delivered up to 80% of the stream N load while providing only 15–43% of the streamflow. The use of

treatment systems to intercept and treat tile drain discharges would have wide scale applicability if it could be demonstrated that this was a cost-effective and practical.

Nutrient attenuation or removal can be enhanced by the addition of reactive materials to flowpaths, such as tile drains. Materials are added to target one nutrient and increase the efficacy of one attenuation process, typically the addition of labile carbon for N removal by denitrification, or addition of reactive materials to facilitate P removal by adsorption.

Adsorption of P is the physical or chemical binding of molecules to the surface of solids (soil, sand, clay, pumice, limestone, shells, and modified materials such as aluminised clays). A wide range of materials are available, but any material selected should have a moderate to high affinity for P, be relatively abundant, be readily available at low cost, be non-toxic, be suitable for reuse with no risk to soil or water quality in either the short or long term, and ideally be a renewable and natural material (Ballantine and Tanner 2010). Melter slag, fly ash and alum have been through basic 'proof of concept' testing, but field scale performance assessments are required to confirm their effectiveness.

Denitrification is the conversion of simple organic carbon and an electron acceptor (such as nitrate), to energy, carbon dioxide and gaseous oxides (nitric oxide (NO) and nitrous oxide (N₂O)) or nitrogen gas (N₂) (Christianson 2011). A diverse range of microorganisms (bacteria, proteobacteria, archaea and fungi) are capable of denitrification. Optimal denitrification conditions for these specialist microbes include:

1. Slow release carbon source.
2. Nitrate source.
3. Anoxic (low oxygen concentration) conditions.

Passive filter systems have been extensively trialled at laboratory- and mesocosm-scales around the world. Recently, larger-scale trials have been initiated in the US for treatment of diffuse agricultural run-off and drainage from cropped lands, and preliminary implementation guidelines have been developed (Christianson et al. 2012a; Christianson et al. 2012b). Although performance is promising, it is expected to be highly dependent on the seasonality and variability of drainage flows. To date these systems have not been applied to treat agricultural tile drain runoff in New Zealand.

Denitrification walls and small-scale woodchip filters have been evaluated under New Zealand conditions. Denitrification walls (trenches filled with sawdust and soil mix) are best constructed where the full extent and flow direction of nitrate-polluted groundwater (including shallow sub-surface drainage) can be determined, such as sites used for intensive land application of wastewater, cattle feedlots, and old fertiliser dumps (e.g., Schipper and Vojvodic-Vukovic 1998).

Small-scale woodchip filters have been evaluated in the Waikato (Sukias et al. 2005; Sukias et al. 2006). Three medium (1.2% of catchment area) and one small (0.6% of catchment area) pilot-scale woodchip filters receiving tile drain flow on a dairy farm in the Waikato were monitored. Annual mass loads of nitrate-N were reduced by 55-79% over a two-year period, representing average annual removal rates in the range of ~0.09-0.3 g N/m³/d. Increases in levels of ammonium-N and, in the first year of operation organic-N, reduced the efficacy of total N removal (16-49%).

High denitrification rates (in the range of 2-10 g N/m³/d) were recorded in other field-scale trials under continuous flow where nitrate concentrations were high are non-limiting (Schipper et al. 2010).

1.2 Report structure

This report considers several factors that had the potential to impact on the efficacy and performance of the woodchip filter. These include climate, resulting soil moisture and nutrient generation from soils, and ultimately the hydraulic and contaminant load to which the filter bed was subject. Performance was assessed in terms of three forms of nitrogen.

To create a flow of logic, the report has been divided into several sections, where these aspects are considered separately. In several areas, the materials in the report body are supported by additional information presented in Appendices.

Section 2 describes the materials and methods used in the assessment, including a brief description of the development of a process-based denitrification model. Other load estimation techniques are also described.

Section 3 summarises the climate (specifically rainfall, temperature and soil moisture), and the implications of climate on woodchip filter performance.

Section 4 discusses the impact of rainfall and drainage on filter hydrology because flows and residence times are key determinants of denitrification performance.

In **Section 5 and Section 6** the results of several other water quality measurements are summarised. These variables were either originally considered to have potential in terms of predicting filter performance or to provide additional data that could be used to estimate woodchip filter efficacy, or to assist with explanation of the filter performance.

In **Section 7** the efficacy of the woodchip filter is discussed in terms of ammoniacal-N (Section 7.2), nitrate-N (Section 7.3), and total N (Section 7.4). The effect of water level on filter performance is discussed in Section 7.5.

Section 8 uses the performance information described in earlier sections to discuss opportunities for improving the performance of this nutrient mitigation tool.

Thirteen appendices summarise details of the materials, methods and assessment procedures, and summarise much of the outcomes of those assessments.

2 Materials and methods

The materials and methods were previously described (Hudson et al. 2018), and similar processes were used throughout the project. However, some method differences and additional measures were used in the last phase of the study as described below. Successful deployment of additional instruments occurred during July and August 2018.

The design, dimensions and equipment installed in the nitrate-N filter were described previously (McKergow et al. 2015), and limited information derived from initial reports is included below to facilitate use.

2.1 Location of the nitrate-N filter

The location of the nitrate-N filter in rural Southland is shown in Figure 2-1, and the location of the filter relative to the main source of drainage water and Waituna Creek is shown in Figure 2-2.

2.2 Description of the nitrate-N filter

The woodchip filter was constructed by excavating a vertical-sided pit that was lined with a polythene membrane and filled with screened pine wood chip (from which leaf material, fines and bark material was excluded).

Dimensions and key features of the woodchip filter are shown in Figure 2-3. A manifold - a perforated drainage pipe, was installed to distribute the inflowing drainage water across the width of the bed. The efficacy of this distribution manifold was not investigated or estimated.

Components of the monitoring system are shown in Figure 2-4, which also indicates the polythene cover that was used to exclude direct infiltration by rainfall and overland flow from the adjacent paddock. Waituna Creek is also shown in the background, incised into the farmland.

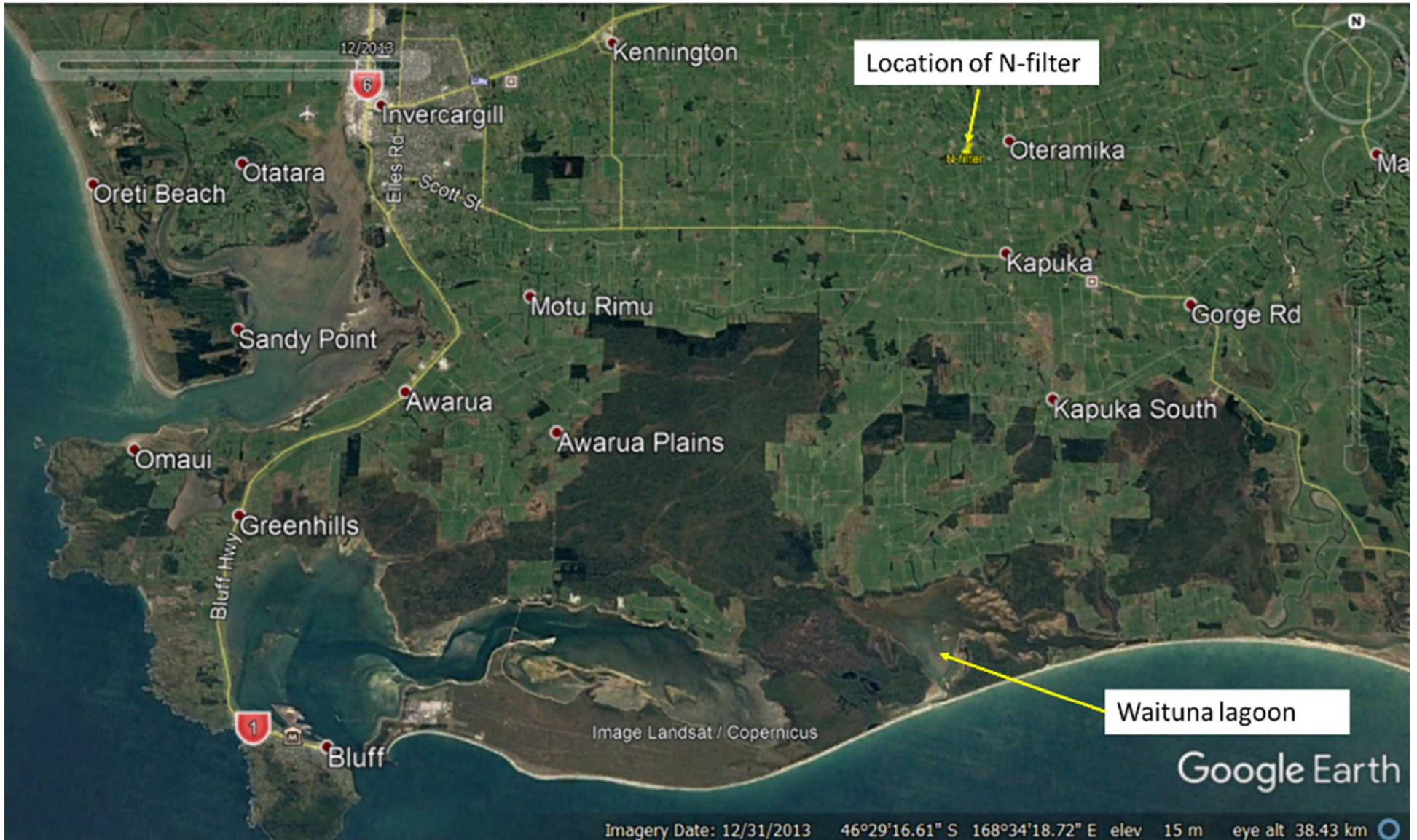


Figure 2-1: Location of the nitrate-N filter in Southland.



Figure 2-2: Location of nitrate-N filter relative to the paddock which is the principal source of shallow groundwater draining into the filter. Waituna Creek flows from right to left.

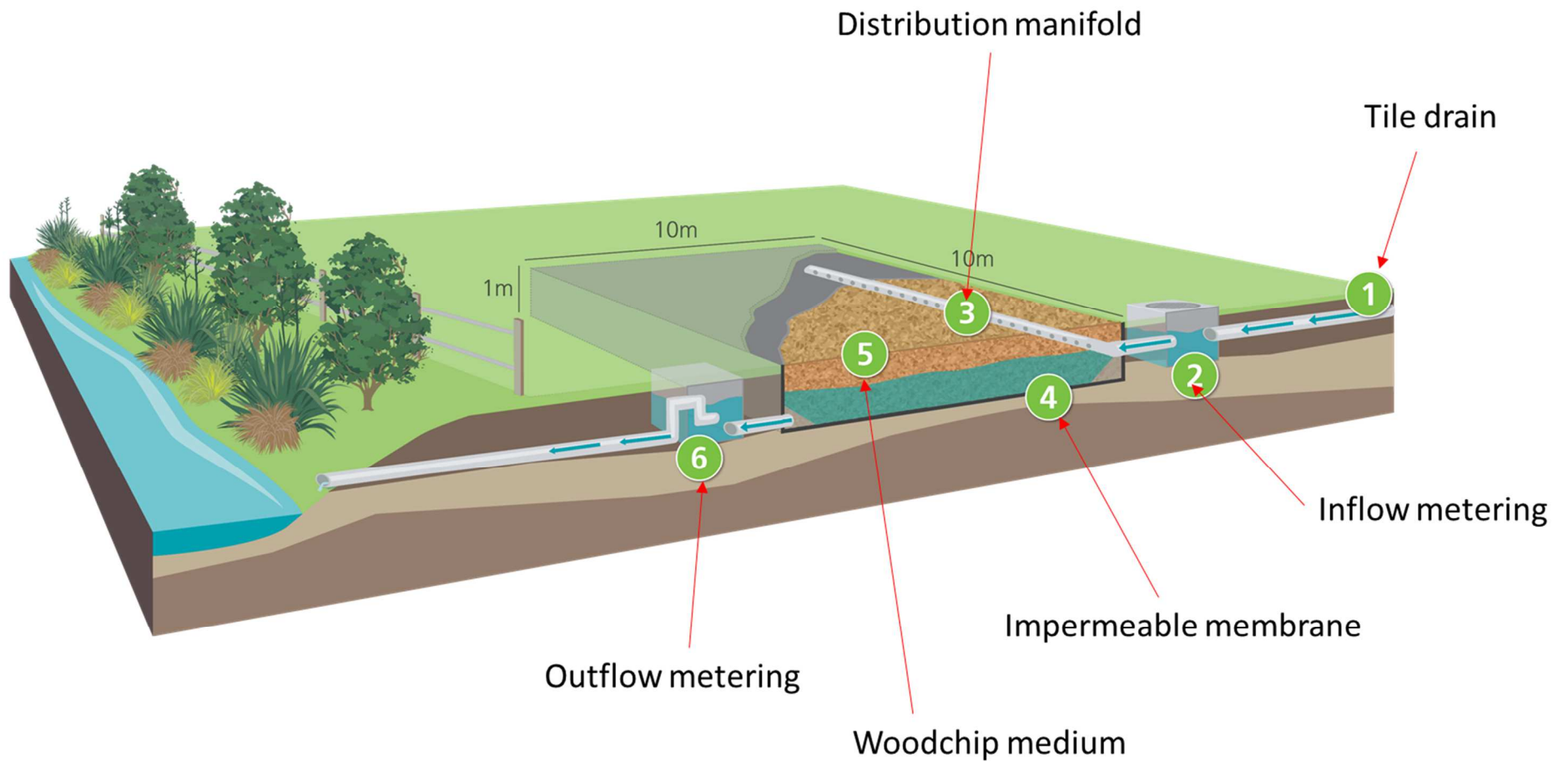


Figure 2-3: Schematic of nitrate-N filter showing dimensions and key components of the as-built filter.

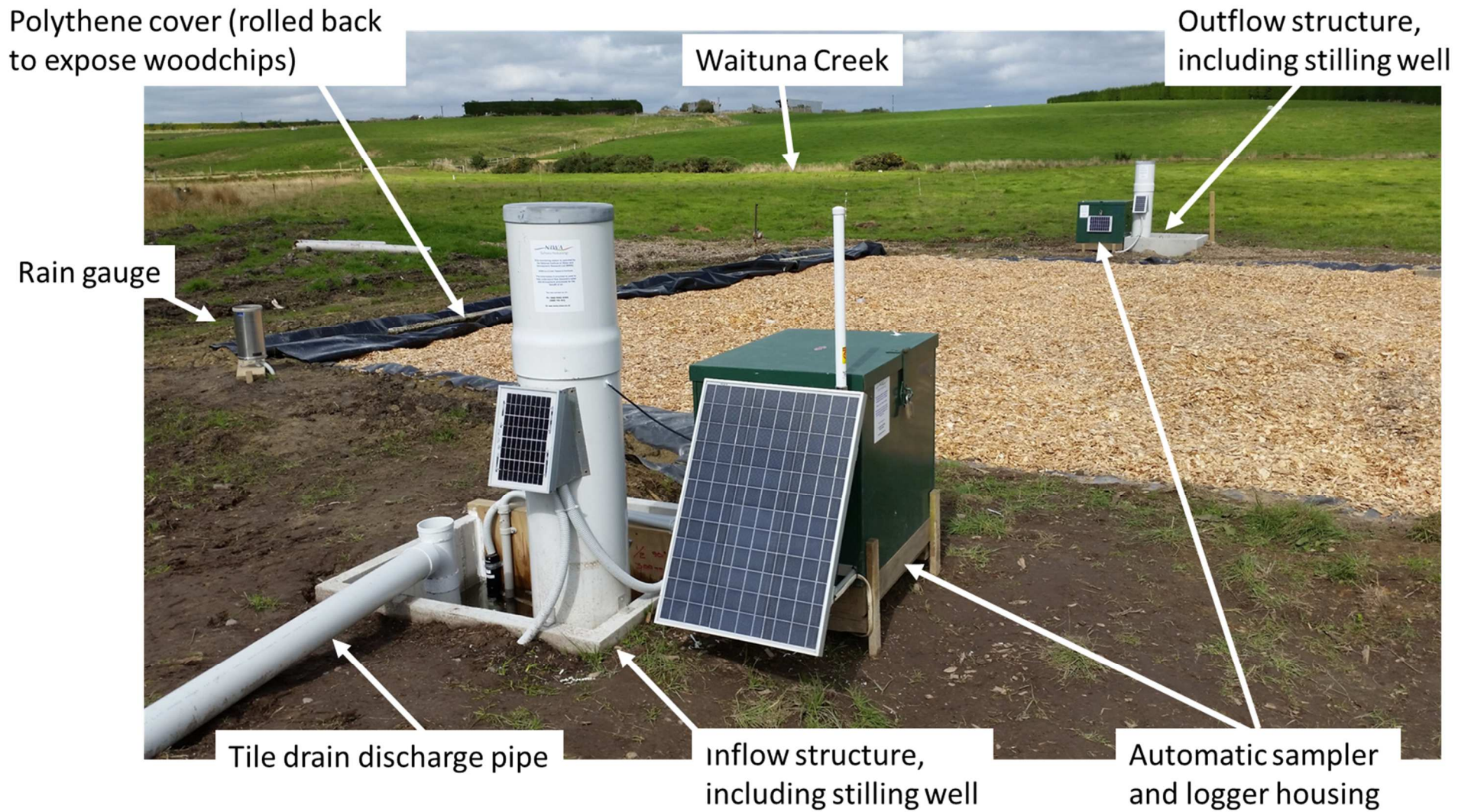


Figure 2-4: Photograph of nitrate-N filter showing key components of the monitoring equipment at the as-built filter.

2.3 High frequency, real time analysers of inflow and outflow nitrate concentration

In the offer of service NIWA proposed that the capability of high frequency, real time nitrate-N analysers be assessed in the context of estimating inflow and outflow nitrate concentrations and loads. The use of these devices for surface water assessments has been well established internationally (e.g., Pellerin et al. 2014; May et al. 2015; Tan et al. 2015; Miller et al. 2016; Pons et al. 2017; Schwab et al. 2017) and in New Zealand (Burkitt et al. 2017; Hudson and Baddock 2019).

NIWA also proposed to deploy water quality sondes (able to measure and record values for several water quality variables unattended) on the N-filter inflow and outflow, specifically to determine inflow and outflow dissolved oxygen concentrations, and to estimate variability of dissolved organic carbonaceous material over one or more rainfall events.

2.3.1 Hyperspectral analysers – Spectra::lyser®

Two instruments and associated equipment was shipped to Waituna and deployed. Unfortunately, equipment failure and cell phone signal strength prevented data acquisition. The problems associated with remote operation of this equipment is described in more detail in Appendix A.

2.3.2 Hyperspectral analysers – TriOS OPUS® device

Following the failure of the Spectra::lyser devices, an alternate brand of equipment (TriOS OPUS®) was trialled. The TriOS brand of equipment makes use of the same measurement principle as the Spectra::lyser, but takes measurements over a narrower spectral range but at higher resolution (refer to Appendix A for further details). An attractive characteristic of the TriOS brand device was the “plug-and-play” capability. Devices were deployed at the inlet and outlet sites, and data were recorded at five-minute intervals. These data were transferred via the NEON logger and telemetry system, together with the other data measured on site, allowing measurement to be visualised remotely in near real-time.

2.3.3 Exosonde II multiparameter water quality sondes

An Exosonde II device was deployed at the woodchip filter inlet and the outlet. Data were recorded at five-minute intervals and stored on the in-built sonde logger for subsequent retrieval and analysis. Data measured on site include temperature, electrical conductivity, pH, dissolved oxygen, turbidity and dissolved organic matter.

2.4 Data storage and manipulation

Data acquired on site and transferred via the NEON logger and telemetry system were stored on the secure NEON server. These data were downloaded from the server as required in CSV format. Data were either manipulated in Microsoft Excel or Systat for Windows v13. Data were recorded at five-minute frequency which created a file with more than 300,000 rows of data. It proved cumbersome manipulating a datafile of this size in Excel, and although Systat for Windows performed better, Windows-based software took excessive time to render graphs prepared using data acquired at that intensity.

Recent work undertaken at NIWA had demonstrated that for most situations, hourly average data provided adequate information. Very transient events would obviously not be represented perfectly, but from the earlier work in the woodchip filter, five-minute temporal resolution was not necessary (Hudson et al. 2017). Most of the manipulation, calculation and summaries were therefore undertaken using hourly average data. The data file for a three-year period was more manageable – approximately 26,000 rows of data.

2.5 Modelling nutrient loads

2.5.1 Regression modelling

In the first assessment of the woodchip filter (Hudson et al. 2017), several approaches for modelling inflow and outflow contaminant loads were described. These included:

- Simple concentration vs flow regression relationships, with or without log transformations.
- Mixed regression models, where two or more regression models were applied according to flow conditions, to better predict outflow concentrations and loads under summer low-flow conditions.

These models generally take the form:

$$\text{LnC} = a_0 + a_1 \text{LnQ} \quad \text{Equation 2-1}$$

where a_0 and a_1 are coefficients (dimensionless), C is concentration (mass/volume), and Q is flow or discharge (volume/time). Ln indicate log (base ten or natural log).

For conservative variables, it may not be necessary to include other explanatory variables, whereas for nutrients, inclusion of other explanatory variables may be essential (e.g., time, temperature etc.).

The LOADEST software system (Runkel et al. 2004) was used in the initial assessment, to estimate inflow loads. In the final assessment, additional models were used that included simple regression models, and regression models that allowed random selection of multiple pairs of concentration and flow values to provide large numbers (typically >100) of regression models.¹ Use of the last approach allows estimation of uncertainty of model prediction.

Use of regression-based models was continued in this study, to allow comparison with the earlier assessment. However, it was apparent that these simple models were not able to adequately describe performance under summer, low flow conditions, particularly following changes made to the bed water level. This made it necessary to investigate other modelling approaches.

The woodchip filter is a biological treatment system, and it is necessary to include processes that hydrological models do not routinely include. These include coefficients and variables related to reaction rates, retention time, the concentration of organic carbon and temperature. Inclusion of these factors provides a treatment process model, rather than a hydrological model. Considerable effort was expended developing a process-based model that allowed use of inflow concentration

¹ BOOTSTRAP regression modelling, from an Excel-based spreadsheet application developed by Dr Kit Rutherford, Emeritus researcher at NIWA.

values to predict outflow concentrations. This was an additional strand of work not addressed in the earlier assessment.

2.5.2 Process-based models

The process-based model was derived using information from the literature regarding denitrification. Several approaches for modelling denitrification exist, such as microbial growth models, soil structure models, and process models (Heinen 2006). Simplified process models do not consider microbial processes and are therefore easier to use. These models assume that denitrification is determined principally by easily measured variables, including soil saturation (used as a proxy for soil dissolved oxygen concentration), nitrate-N concentrations and the soil or water temperature based. Use of these models is also favoured because they encapsulate the averaging of denitrification that is inherent in a volume of medium in which denitrification occurs.

Following a critical review of 50 soil denitrification models, Heinen (2006) generalised these models as indicated in Equation 2-2:

$$D_a = \alpha \int N \int S \int T \int pH \quad \text{Equation 2-2}$$

where

D_a = actual denitrification rate

α = a parameter used to account for organic carbon and depth of the denitrifying medium etc., (as required), and

$\int N \int S \int T \int pH$ = dimensionless reduction functions related to nitrate-N concentration, soil moisture content, soil temperature and pH respectively.

Actual denitrification has a range of units, determined by the application of the model to a point, layer, or loss of nitrate-N from soil solution.

For this assessment, we have relied on the approach used in the SWAT catchment model (Neitsch et al. 2011), modified by that of Appelboom et al. (2010); the latter approach was developed to improve estimation of denitrification rates in sediments and overlying water columns.

An estimation method derived from the Theoretical Documentation for the SWAT catchment model (p195, Neitsch et al. 2011), modified using the approaches of Appelboom et al. (2010), Birgand (2000), and Kelly et al. (1987) was used to estimate nitrate-N removal by the woodchip filter using Equation 2-3. The derivation of the model is summarised in Appendix C.

$$[NO_{3_{out}}] = [NO_{3_{in}}] \times (\exp(-0.016 \times RT \times T_{out})/D \times [DOC]) \quad \text{Equation 2-3}$$

where

0.016 is the average mass transfer coefficient from Appelboom et al. (2010) (m/d)

RT is retention time (days), estimated from measured inflow rate (L/s), measured real-time woodchip filter water level (m) (D below), and nominal 100 m² filter surface area.

T_{out} is the outflow temperature (°C)

D is the water depth in the wood chip filter bed (m), and

[DOC] is the concentration of dissolved organic carbon (g/m³).

Nitrate-N removal rates were estimated using seasonally varying, measured inflow DOC concentrations, but these provided no advantage in terms of improved model goodness of fit over use of an average value derived from measurements made over the assessment period.

2.6 Estimating filter performance

Having used models to estimate the flux (instantaneous load) of three nitrogen forms for the filter inflow and outflow, it was possible to estimate filter performance. Performance is described in terms of the mass of material removed (Equation 2-4) or the mass of material lost as a proportion of the inflow (Equation 2-5):

$$\text{Filter performance} = \text{mass in inflow} - \text{mass in outflow} \quad (\text{g/d}) \quad \text{Equation 2-4}$$

In the report the result obtained following application of Equation 2-4 is referred to as **mass removal**, and in this instance, removal is summarised at daily timestep (i.e., it represents the sum of multiple values for mass removal during a 24-hour period).

$$\text{Filter performance} = \frac{\text{mass in inflow} - \text{mass in outflow}}{\text{mass in inflow}} \times 100 \quad (\%) \quad \text{Equation 2-5}$$

In the report the result obtained following application of Equation 2-5 is termed **efficacy** (defined below); this term describes mass removal in terms of the proportion of inflow load that is removed. Once again it is summarised at daily time step.

A third method for reporting performance is mass removal as a function of active woodchip filter bed volume (i.e., the volume of the filter bed that is immersed in water). Section 4 describes water depth in the filter bed over time. Equation 2-6 describes mass removal as a function of treatment volume:

$$\text{Filter performance} = \frac{\text{mass in inflow} - \text{mass in outflow}}{\text{active filter bed volume}} \quad (\text{g/m}^3/\text{d}) \quad \text{Equation 2-6}$$

It is worth defining two words that are often (erroneously) used interchangeably – efficacy and efficiency.

Efficacy describes:

- the power or capacity of something to produce a desired effect
- the possession of a quality that gives the produced results, or the potential to lead to an effective outcome.

Efficiency describes:

- producing an output in a competent and qualified way
- acting or producing with a minimum of waste, expense, or unnecessary effort.

When assessing the performance of a product, efficacy is the preferred term; efficacy is used in this manner in the medical field, e.g., “the efficacy of this drug is enhanced when it is taken with a meal”. We have used the term efficacy exclusively when describing the performance of the woodchip filter in terms of changing the load of influent material. In some cases, efficacy may be negative, such as when the mass of one or more contaminant increases through the treatment process.

3 Climate summary

Meteorological data were collected on-site, and these were compared with long-term climate data acquired from the nearest station with a long-term record – Invercargill Aero Automatic Weather Station (AWS), some 23 km due west of the N-filter site. Figure 3-1 summarises total annual precipitation for Invercargill AWS over the period 2001-2018 inclusive. With few exceptions, rainfall measured on site was similar to, or less than, that recorded in Invercargill. The actual measured rainfall is compared in Figure D-2 and Figure D-3 (Appendix C).

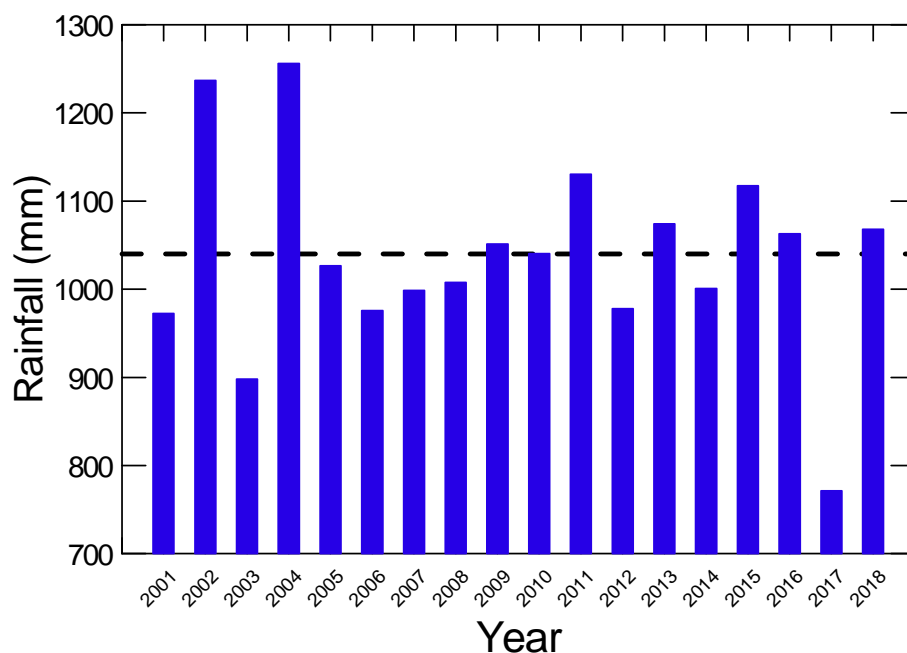


Figure 3-1: Annual total rainfall, 2001-2018 inclusive. Data sourced from “Invercargill Aero AWS”, Site 684305. The dashed horizontal line is the annual average for this period (1037 mm).

Monthly total rainfall measured through the assessment period is summarised in Figure 3-2 together with monthly median and above and below normal rainfall amount values derived from the long-term rainfall record. Key points to note:

- Rainfall measured in 2016 and 2018 was close to average, but well-below average rainfall was received in 2017.
- With the exception of January 2017 (well-above median rainfall) and July 2017 and September 2017 (approximately median rainfall), rainfall in all other months in that calendar year were below or well-below median.
- Significantly low rainfall persisted into January 2018.
- After January 2018, rainfall was generally equal to median or well-above median.

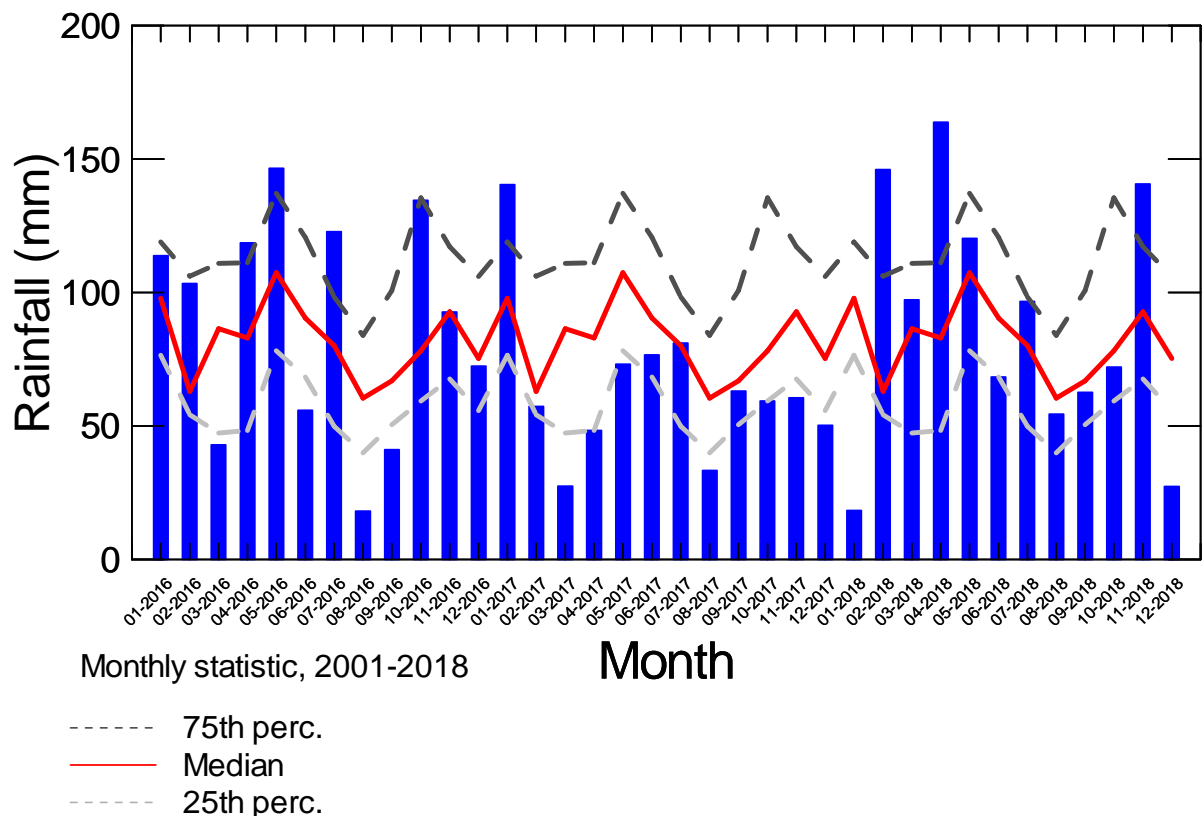


Figure 3-2: Comparison of monthly total rainfall measured on site January 20016 to December 2018, and long-term statistical values. Long-term statistical data sourced from “Invercargill Aero AWS”, Site 684305.

The rainfall trends are to some extent reflected in daily average temperatures and average soil moisture record from Invercargill airport (Figure D-4 and Figure D-5, Appendix C). Several months in 2017 were considerably warmer than the long-term average, and this was reflected in the soil moisture recorded from late 2017 through to October 2018 (Figure 3-3). Measured soil moisture was considerably less than the long-term average for summer 2017/18 through to late spring 2018/19. This is likely to have influenced tile drainage, both in quantity of water, and the mass of nitrate-N transported in the drainage water. One of the prerequisites for denitrification, and a factor that determines the extent of denitrification in soil is soil moisture (e.g., the Technical Guidance for the SWAT catchment model, Section 3.1.4. (Neitsch et al. 2011)). In general, when the water-filled porosity is greater than 60%, denitrification will be observed in a soil. This happens because oxygen diffuses through water 10,000 times slower than through air, and as soil water content increases, anaerobic conditions increasingly develop.

The influence of climate on the inflow to the woodchip filter is discussed in Section 4.

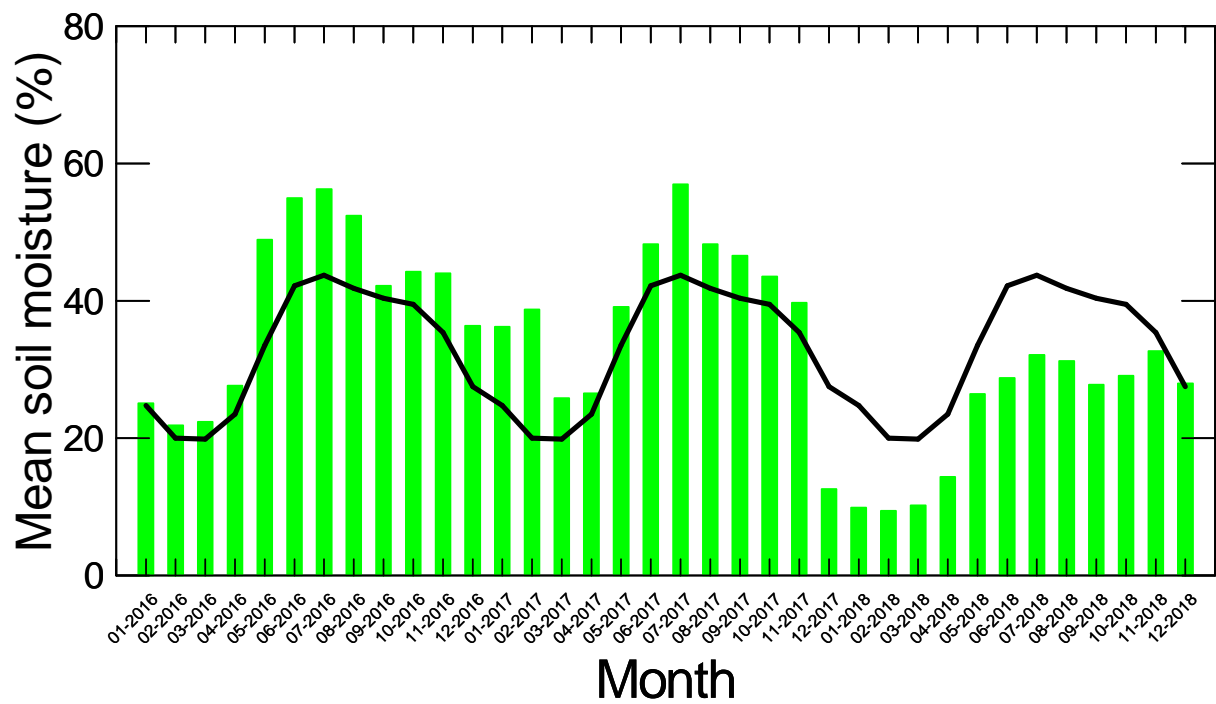


Figure 3-3: Comparison of monthly average soil moisture recorded at Invercargill airport between January 20016 and December 2018, and the long-term average value (2001-2018, black line). Data sourced from “Invercargill Aero AWS”, Site 684305.

4 Woodchip filter hydrology

Woodchip filter inflow and outflow was measured at five-minute intervals. To make the files more manageable, these data were aggregated to hourly values. This had negligible impact on load estimation or understanding the response of the woodchip filter to rainfall. Inflow and outflow data are summarised at an hourly time-step in Figure 4-1 and at monthly and seasonal time-steps in Figure E-2 and Figure E-3. Summary statistics are provided in Table E-1.

In general inflow and outflow match closely, although there is indication that the inflow was more “flashy” than the outflow after May 2017. The minor differences observed between inflow and are considered to have negligible effects on the load estimation because they occurred during low-flow periods. If the flows are small, the loads of materials of interest are also likely to be small.

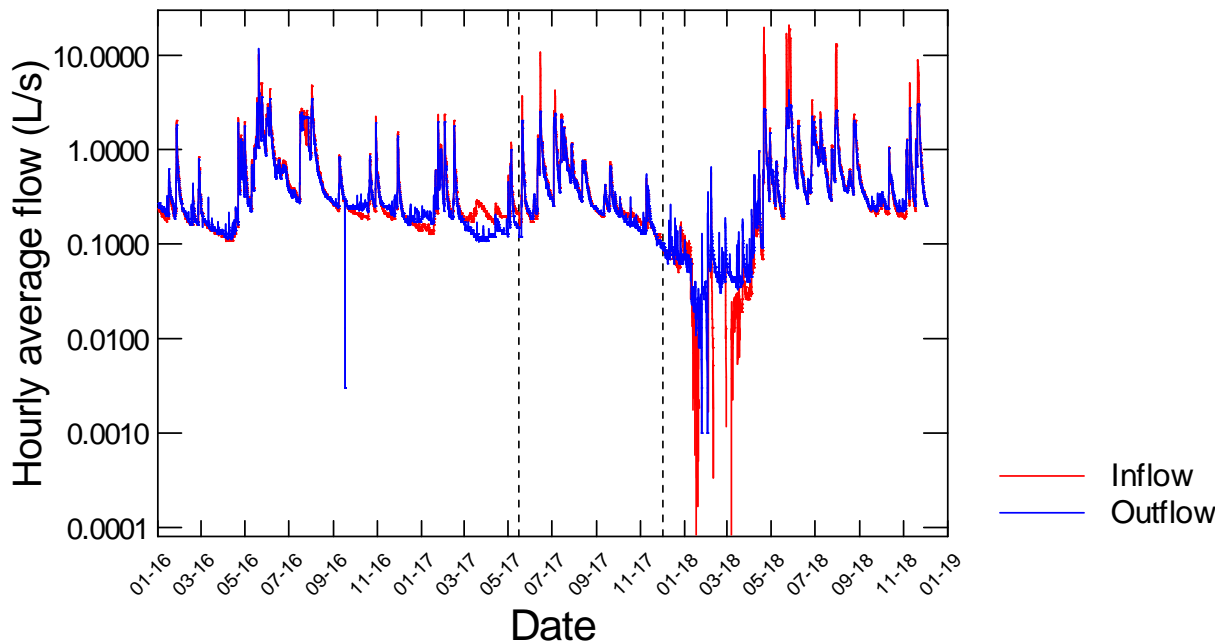


Figure 4-1: Comparison of inflow to and outflow from the woodchip filter. Hourly average flows were derived from five-minute data. Note y-axis has \log_{10} scale.

Figure 4-2 provides a time series of water levels within the woodchip filter bed. The two vertical lines demarcate three periods discussed below and are subsequently described as High, Medium and Low water level conditions.

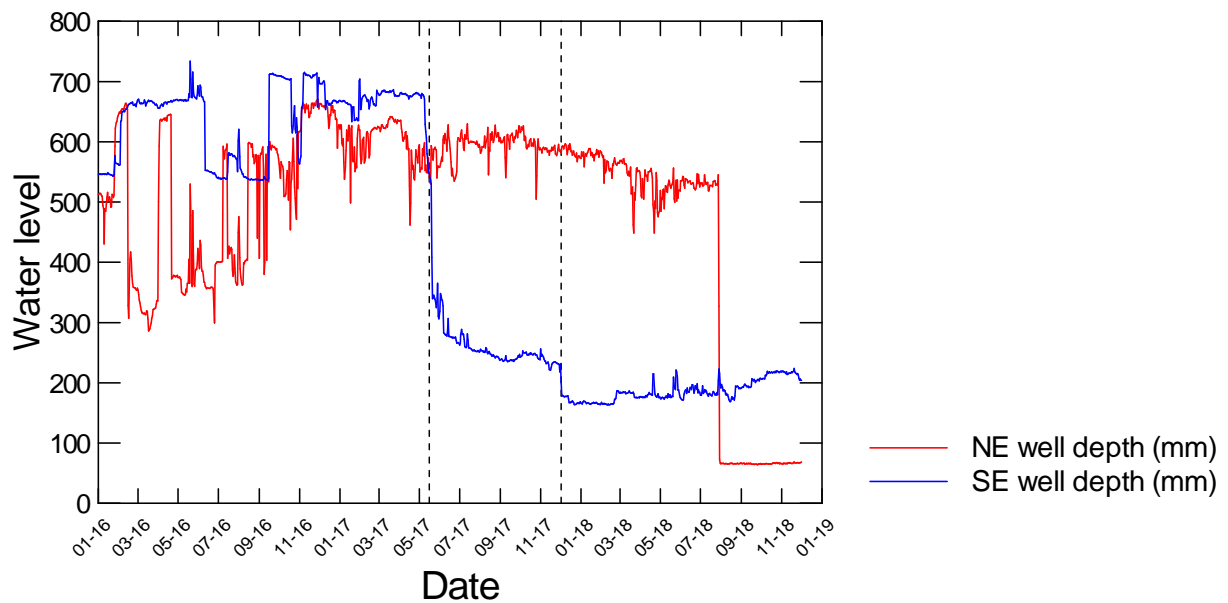


Figure 4-2: Time-series of water levels in the woodchip filter, recorded in the NE (inlet) SE (outlet) corner of the bed. These are daily average values derived from five-minute data. The vertical broken lines indicate 15/05/2017 and 1/12/2017 respectively. The inlet recorder was disabled in August 2018.

Previously we described the effect that retention time or residence time of water within the filter bed had on performance (Hudson et al. 2017). Performance improves with retention time. This is discussed further in this report in Sections 7.3 and 7.5. Here we characterise the relationship between flow, water level and residence time. The distributions of measured inflows are summarised in Figure E-4. More than 80% of the time flow is less than 1 L/s, and higher inflows occur primarily in autumn and winter. Figure 4-3 shows the distribution of retention times over the entire assessment period, and for each season. Less than 10% of inflow remains within the bed in winter, approximately 30% of inflow remains in the bed for at least two days, while approximately 35% of flow remains in the filter bed for four days or longer. These retention times are theoretical (viz., filter volume divided by outflow rate), assuming that flow occurs evenly across the bed width, without preferential flow paths.

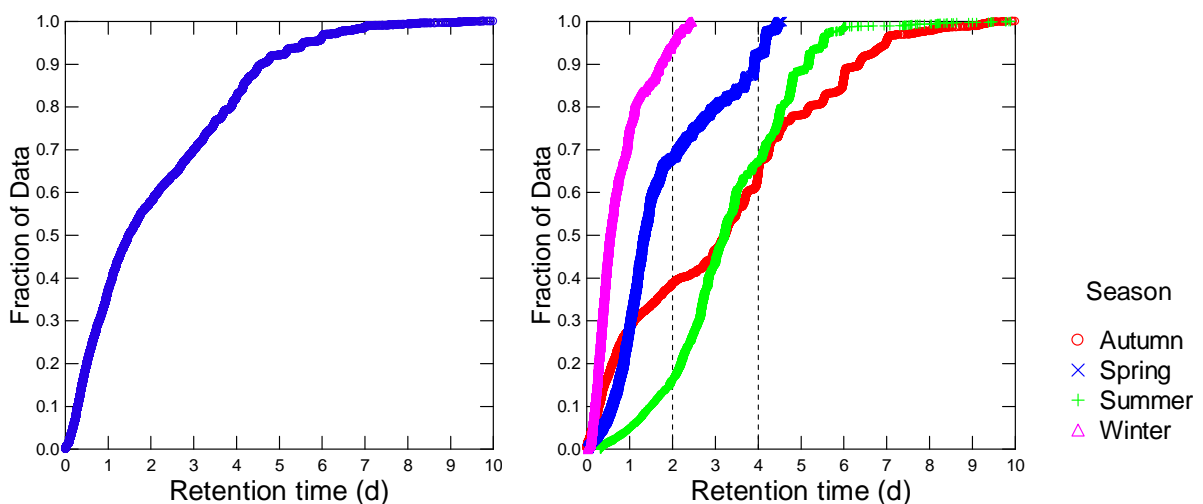


Figure 4-3: Distribution of theoretical retention time in the woodchip filter (left), and relationship between retention time and season (right). Note that x-axis of figure on right has \log_{10} scale. The dashed vertical lines indicate two- and four-day retention time respectively.

5 Hyperspectral and water quality sonde data

5.1 Hyperspectral data

In Figure 5-1 grab sample and TriOS estimates of concentration and flux of nitrate-N are shown for a six-week period during July-August 2018.

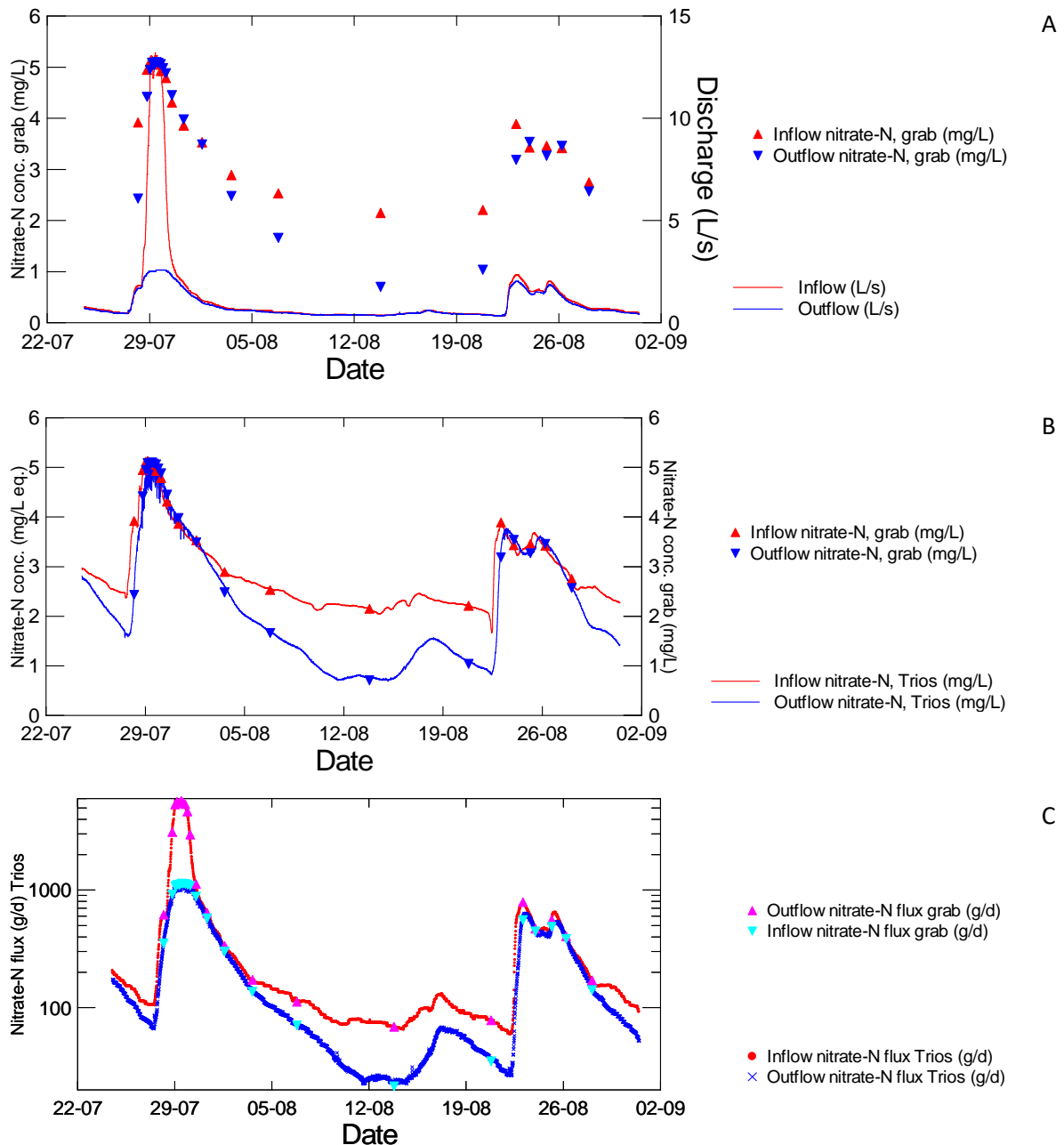


Figure 5-1: Inflow and outflow nitrate-N concentrations and flux. A) Grab sample concentrations for July and August 2018, B) five-minute TriOS nitrate-N estimates of nitrate-N and grab sample concentrations, and C) instantaneous nitrate-N load derived from TriOS measurements and grab sample concentrations. Note the y-axis in C) has a \log_{10} scale.

Referring to Figure 5-1, the grab samples (A) indicate a difference between inflow and outflow concentrations and how this difference varies during the discharge events, (B) indicates very good agreement between grab sample concentrations and TriOS estimates in both inflow and outflow, and (C) indicates how either method provides reliable estimates of flux or instantaneous load. For estimation of total load using grab samples, however, it would be necessary to fill the gaps between the grab samples using a suitable interpolation technique.

In Figure 5-2 the removal efficacy of the filter bed is expressed as the difference between instantaneous inflow and outflow load (i.e., as described in Equation 2-4). Section 7 describes treatment efficacy in detail. It is useful, however, to consider these data here so that the use of continuous water quality sensors for this purpose can be explored; these results are included in subsequent discussion as well.

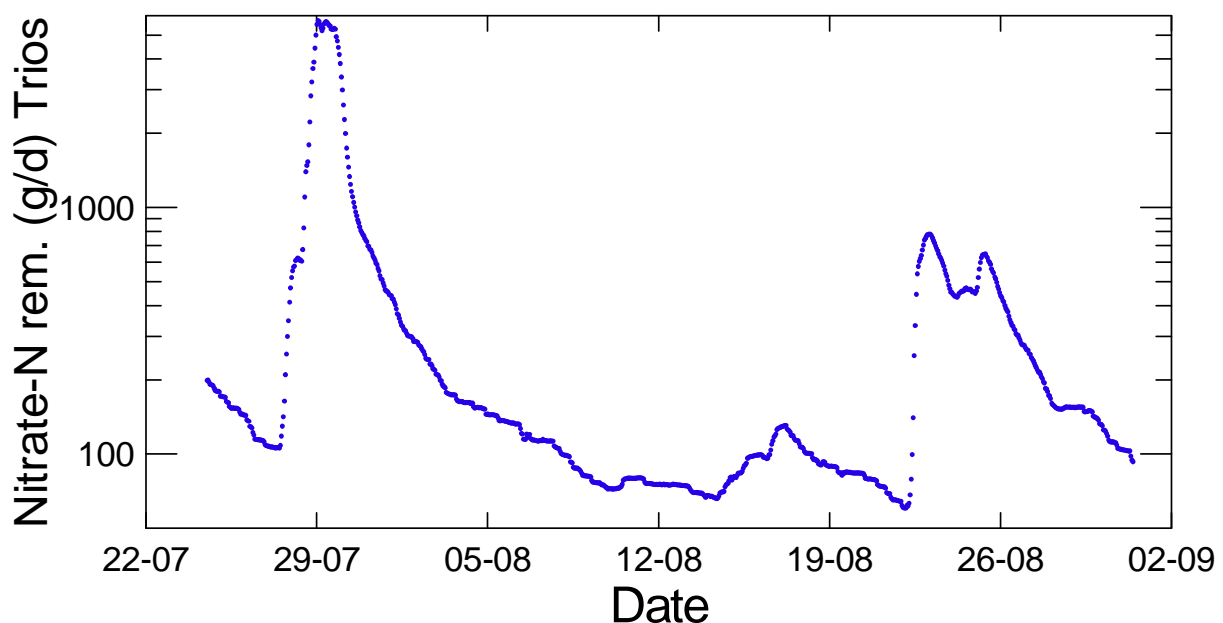


Figure 5-2: Estimate of nitrate-N removal efficacy derived from TriOS inflow and outflow measurements. The removal efficacy is the difference between the inflow and outflow mass load estimated at five-minute intervals.

One might have expected that little nitrate removal would occur at peak flow. For example, on 25/08 and 26/08 the inflow and outflow flux in Figure 5-1 look similar but they are plotted on a log scale. The difference between inflow and outflow flux in Figure 5-2 indicates, however, that the greatest removal (expressed as g/d) occurs during high flow events. This is the consequence of the high inflow load delivered to the woodchip filter. Even though the outflow nitrate-N load is high, Figure 5-2 demonstrates that a substantial mass of nitrate-N is removed. In later sections the performance of the woodchip filter is described as a function of retention time. During high flow events, although the efficacy of removal (viz., removal as a percentage of inflow load) is lower because retention times are short, the woodchip filter is still able to remove a substantial amount of nitrate-N.

In Figure 5-3, the efficacy of the woodchip filter is described in terms of the proportion of influent load removed, expressed as a percentage of influent load. The efficacy indicated by the continuous TriOS data is compared with that estimated from load estimates derived from two regression models. The latter models cover the entire three-year period of operation but only those data that overlap with the TriOS data are shown. The timing and magnitude of peaks and troughs agree

tolerably. Overall the TriOS data indicate higher removal than the regression model. The likely reason is the inability of the regression model to represent the nitrate-N removal process adequately. This is discussed in detail in Section 7.3.

These data and results indicate that high frequency hyperspectral analysers may be used to directly evaluate the performance of mitigation devices such as woodchip filters, offering several benefits, including provision of near real-time results, and accurate characterisation of peak concentrations and loads during periods of low nitrate-N concentration and flow. These data can be used to develop regression or process models to estimate performance, or to directly quantify performance under a range of typical conditions.

It would be prudent to always collect grab samples for laboratory analysis to ensure that the results derived from the TriOS sensors were credible – a hyperspectral device will always provide an output, but even though some devices have sophisticated correction and error-detection algorithms, erroneous data may still be recorded. The grab sample results provide necessary validation.

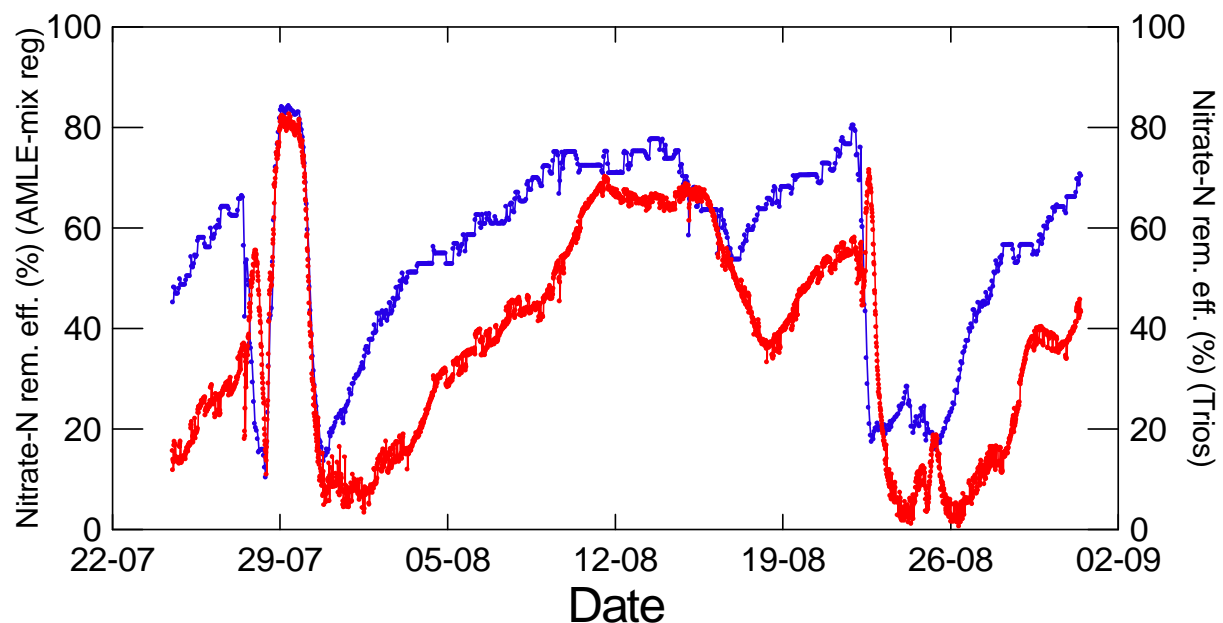


Figure 5-3: Comparison of nitrate-N removal efficacy derived from TriOS inflow and outflow measurements (blue) and estimates from a mixed regression model based on grab sample concentrations (red). Removal efficacy is expressed as the proportion (%) of influent mass removed.

5.2 Dissolved oxygen concentrations

Several prerequisites exist for denitrification, including anoxic conditions. The genes encoding denitrifying enzymes are repressed in the presence of oxygen, and nitrous oxide reductase is inactivated in the presence of molecular oxygen (Lu et al. 2014; Ward 2015), reducing treatment efficacy. Dissolved oxygen concentrations were not measured during the initial assessment period, and the possibility existed that high inflows may introduce substantial amounts of dissolved oxygen which could in turn impair treatment efficacy.

YSI brand EXO2 data sondes were deployed on the woodchip inflow and outflow for approximately six weeks during July through September 2018.² This coincided with the nitrate-N sensor deployment period. Figure 5-4 provides a time series of inflow and outflow dissolved oxygen concentrations for a period that includes two inflow events. Points to note:

- dissolved oxygen concentrations in the inflow were consistently low (less than 1% saturation)
- rainfall and drainage events caused transient and very slight increases in dissolved oxygen concentration in the inflow
- the outflow was anoxic except during rainfall and drainage events
- the increased inflow during rainfall events was sufficient to provide a “pulse” of partially oxygenated water that was conveyed through the filter bed and emerged at the outflow
- by inference, the concentration in the outflow was related to the mass of oxygen that entered the filter bed, and that was influenced by the inflow volume (the dissolved oxygen concentration in the inflow is almost invariant)
- as a consequence, the dissolved oxygen concentration in the discharge was greatest in the event of 29/7/2018, when inflow was approximately five times greater than during the event during the week of 19/08/18
- outflow concentrations were strongly influenced by the peak inflow – during both events, anoxic conditions resumed in the outflow with a day or two of the peak discharge.

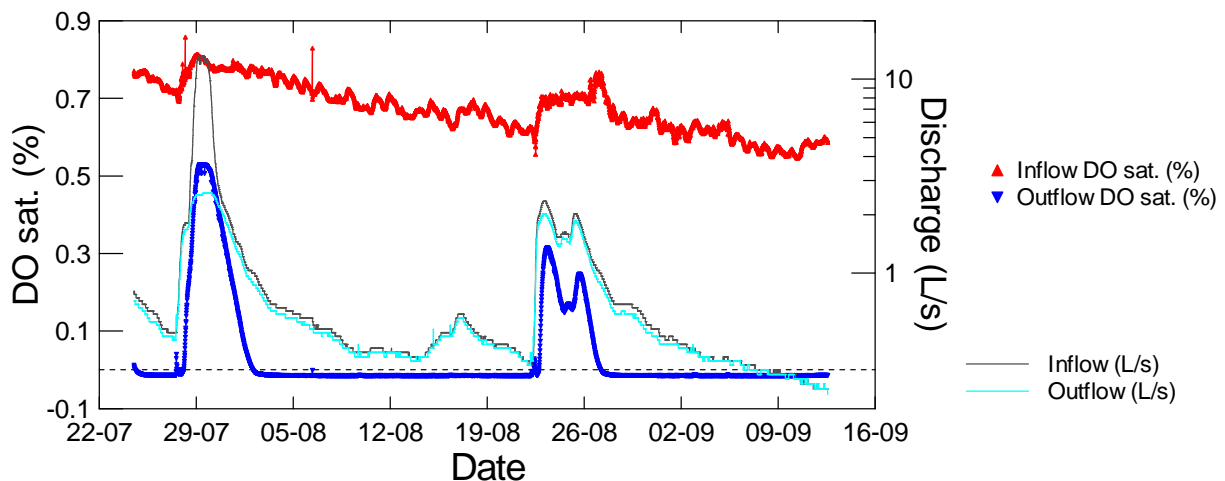


Figure 5-4: Comparison of inflow and outflow dissolved oxygen concentrations, and relationship to inflow events. Dissolved oxygen concentrations are expressed in terms of percent saturation.

² Sonde deployment period - 2018/07/24 12:00 - 2018/09/12 13:45

Tile drainage (viz., the inflow to the filter bed) is likely to be anoxic because the shallow groundwater has been subject to biological activity during drainage, and bacteria are likely to consume the available oxygen as they metabolise the organic carbon leached from and present in the soil. Although the tile drain is likely to have an air space above the water (because it is unlikely to be full except during peak flows), a significant mass of oxygen is unlikely to diffuse up the pipe to alter the dissolved oxygen status of the drainage water. The drainage water drops into a sump that contains the v-notch weir – this is where dissolved oxygen measurement occurred and is probably where the limited aeration occurred (oxygenation of water is strongly determined by water phase turbulence).

5.3 Dissolved organic matter concentrations

The EXO2 sonde has a sensor that is able to estimate fluorescent dissolved organic matter (fDOM). Results are reported in quinone sulphate units (QSU) – quinone sulphate fluoresces strongly, and provides a stable, easy to measure standard. Although the precise relationship between fDOM and dissolved organic matter or dissolved organic carbon needs to be determined experimentally and will vary according to the water sample and water source, the fDOM values provide insights regarding the organic carbon concentration in the woodchip inflow and outflow. Figure 5-5 provides a time-series of fDOM results for the woodchip inflow and outflow for the period July-September 2018. Points to note:

- With the exception of very transient peak inflow conditions on 29/07/18 and 25/08/18, outflow fDOM concentrations were higher than inflow concentrations.
- There is a slight time delay between peak and minimum inflow and outflow concentrations. The time delay appears to vary according to inflow conditions – during periods of high inflow, the delay is smaller during low flows (e.g., compare the peaks for the 29/07/18 event and the smaller inflow events that occurred in the week of 12/08/18).

In Section 4 the change in water level in the woodchip filter over time was discussed briefly and is discussed further in Section 7.5. Decreasing the volume of water in the filter bed will cause less of the woodchip to be submerged. It is possible that this could reduce the input of organic carbon from the wood chip medium to the nitrate-containing liquid in the bed, potentially “starving” the denitrifying bacteria of excess organic carbon, essential for denitrification. These results suggest that during periods when elevated nitrate-N loads enter the woodchip filter, the concentrations of fDOM in both the inflow and outflow increase. The additional fDOM is likely to satisfy the increased demand for dissolved organic carbon, provided the fDOM represents biologically available carbon. The fDOM derived from the tile drain is likely to be relatively resistant to microbial metabolism because it is the product of biological processes that occurred in the soil profile prior to drainage. It would be useful to assess the recalcitrance of the organic carbon to microbial processes using tests such as biochemical oxygen demand (e.g., five-day biochemical oxygen demand or BOD₅), which would indicate the proportion of organic carbon amenable to aerobic microbial processes within a timescale relevant to operation of a wood chip filter.

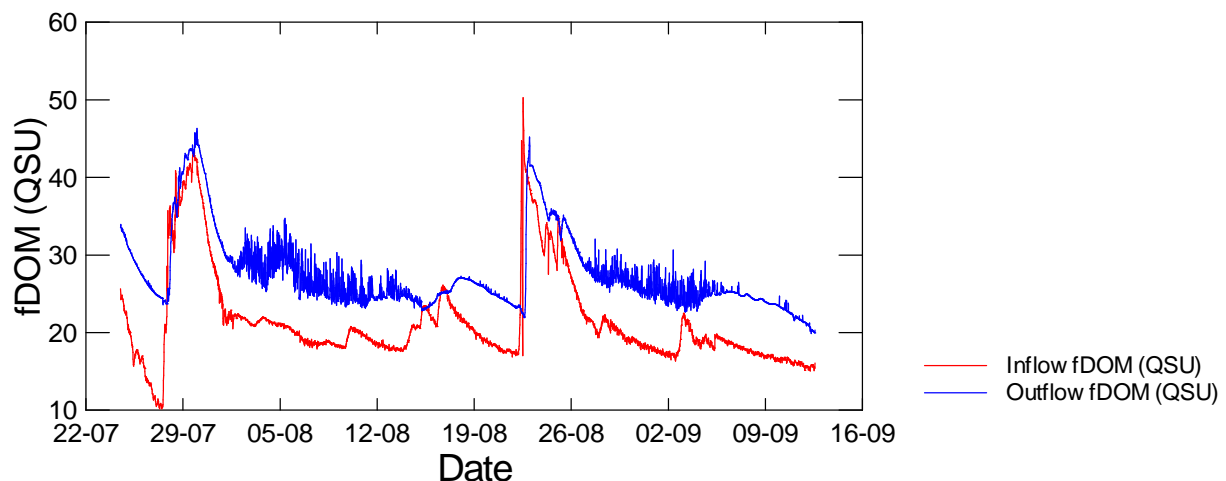


Figure 5-5: Comparison of inflow and outflow fluorescent dissolved organic matter concentrations. Fluorescent dissolved organic matter concentrations are reported in quinone sulphate units (QSU).

5.4 pH measurement

The relationship between pH and denitrification is complex and although pH influences rates and products of denitrification, the influence of pH is difficult to predict. (Šimek and Cooper 2002).

For the period that pH was assessed in the woodchip filter (Figure 5-6), we saw:

- an overall decrease in pH in the outflow
- relatively constant pH in the inflow
- small changes in pH over the assessment period, spanning up to 0.5 pH units in the outflow, and approximately 0.2 pH units in the inflow.

It is possible that the decrease in pH in the outflow represents the change in conditions within the woodchip filter over the winter drainage period, but absence of independent verification of pH does not allow sensor drift to be excluded.³ Additional monitoring during other seasons would be required to determine this. From the denitrification performance measured at the same time using the TriOS nitrate analysers, however, the decreasing pH observed over this period did not appear to have had a measurable effect on the denitrification performance. pH in the inflow and outflow were however lower than the values considered optimal for wastewater denitrification (pH 7). pH values outside the optimal range in wastewater situations are related to use of readily bioavailable carbon sources (such as methanol), and are generally linked with accumulation of intermediate denitrification products, such as nitrous oxide and nitrite-N ((Lu et al. 2014) – the latter was not observed in the nitrate-filter outflow.

³ Although the pH in the outflow was not checked independently, the probe passed quality assurance tests on return to the laboratory (in accord with standard practice), therefore we can assume that the decrease in pH over the deployment period was real.

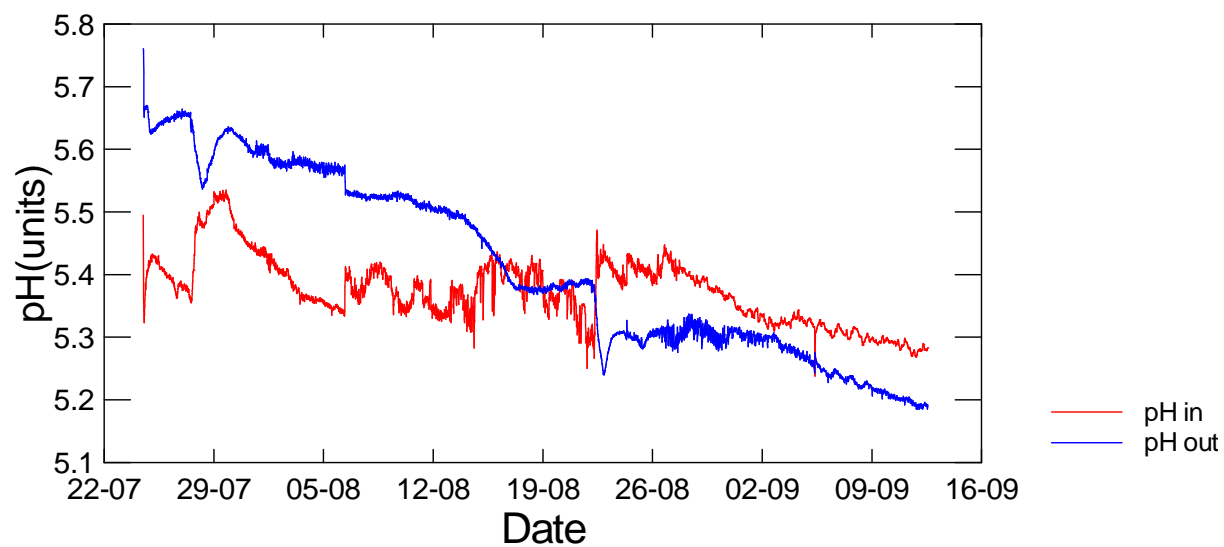


Figure 5-6: Comparison of inflow and outflow pH.

6 Other woodchip filter bed characteristics

Several other water quality variables were measured routinely during the three-year operation period, including water temperature, electrical conductivity and turbidity.

6.1 Water temperature

The temperatures of the inflow and outflows were measured continuously at five-minute intervals. These data are summarised in Figure 6-1, which indicates:

- close correlation between inflow and outflow temperatures
- strong seasonal variation of approximately 7°C.

Temperature has an effect on the efficacy of biological treatment systems – treatment performance decreases with temperature, with most bacteria operating most efficiently at temperatures between 25 and 37°C. This is discussed in Section 7.

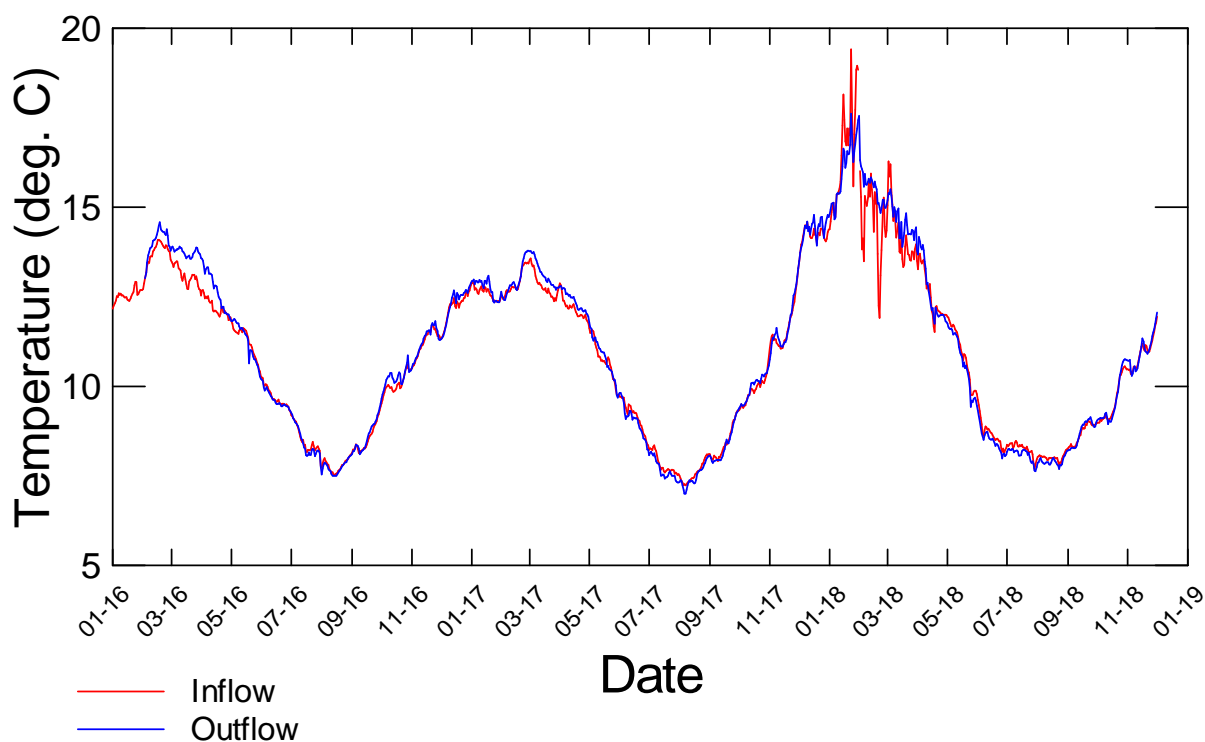


Figure 6-1: Comparison of hourly average inflow and outflow temperatures. These values were derived from five-minute data.

6.2 Electrical conductivity

Electrical conductivity or specific conductance provides a measure of the capacity of a liquid to transmit an electrical current, which in turn is an index of the concentration of ions in solution. In the system related to the woodchip filter, salts and minerals would be derived principally from the soil profile draining into the tile drain (including materials deposited on the soil surface, such as animal urine and fertilisers), and the processes occurring within the filter bed.

Figure 6-2 provides a time-series of inflow and outflow electrical conductivity values over the entire assessment period. Points to note:

- inflow electrical conductivity is always higher than in the outflow
- both inflow and outflow electrical conductivity responds positively (increases) as flow increases
- during the drought of summer 2017/2018, the sensor was not submerged at all times, and electrical conductivity in the outflow increased as the concentrations of salts and other charged dissolved materials increased during the low-flow period
- at the end of the drought, the electrical conductivity in the inflow and the outflow increased considerably (March 2018), presumably in response to the mobilisation of dissolved materials in soil profile and tile drainage.

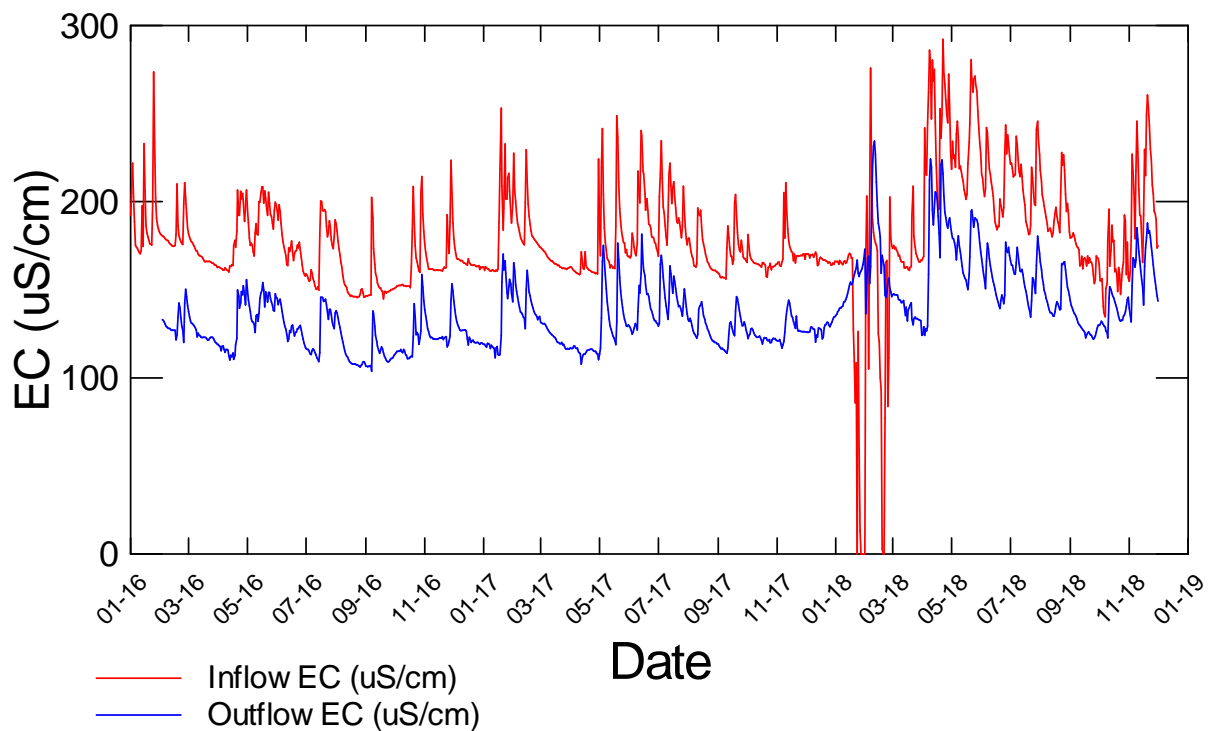


Figure 6-2: Comparison of hourly average inflow and outflow electrical conductivity. These values were derived from five-minute data.

One of the reasons for continuously measuring electrical conductivity was to assess whether it could be used to estimate nitrate-N concentrations and therefore evaluate treatment efficacy. The relationship between inflow electrical conductivity and nitrate-N concentration, and between electrical conductivity and inflow and outflow is summarised for various time periods in Appendix H. Although there is a positive relationship between these variables, it is complex, and prediction of nitrate-N concentrations in the N filter inflow or outflow using regression models was not improved using electrical conductivity as a covariate.

6.3 Turbidity

Turbidity is a proxy for suspended sediment and was measured in the inflow only to provide some measure of the load of particulate material transported into the filter via the tile drainage. Turbidity was generally low, exceptions being the winter of the 2016 calendar year, when animals were allowed to forage on the paddock draining to the N-filter⁴, and in the summer of 2017/18. Flows into the N-filter were very low during the latter period, and it is possible that these elevated measurements could reflect the accumulation of fine particulates in the chamber in which turbidity was measured.

The woodchip inflow structure contained a catch-pit, which trapped particulates through settling. This structure was cleaned several times during the assessment period, and moderate amounts of fine particulate material were removed. It was unlikely that substantial amounts of coarse particulate material were transferred into the woodchip filter, with the possible exception of the winter of 2016.

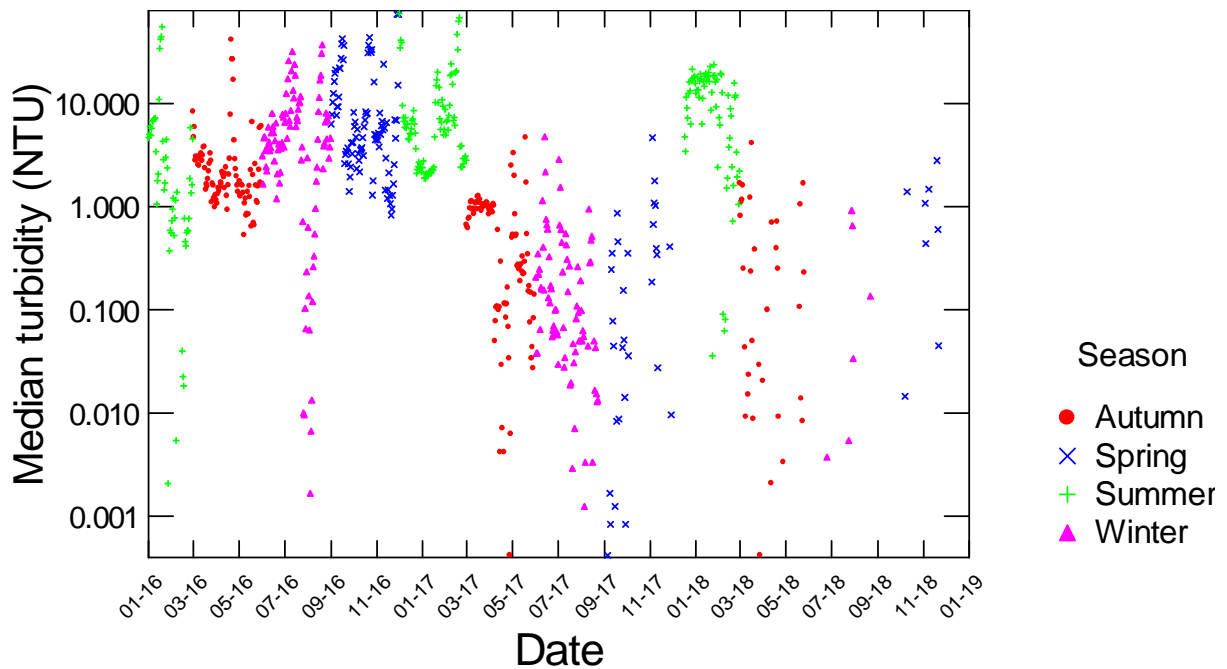


Figure 6-3: Time series of daily median turbidity values, woodchip filter inflow, classified according to season. These values were derived from five-minute data.

⁴ Dr Lucy McKergow NIWA Hamilton, pers. comm. February 2019.

7 Nitrate-N filter performance assessment

Woodchip filters are intended to reduce the concentration of nitrate-N from drainage water. The expectation is that under reasonably easy to achieve environmental conditions, the nitrate-N is converted largely into N_2 gas, which is lost to the atmosphere. Under less favourable conditions, nitrate-N may be converted in nitrous oxide (N_2O), a greenhouse gas, and/or ammoniacal-N. The latter is also bioavailable and able to promote growth of aquatic plants, as well as being toxic to aquatic organisms at low concentrations, with toxicity increasing as pH and temperature increase. Formation of ammoniacal-N in a denitrification filter is also undesirable because the ammoniacal-N may be converted back into nitrate following discharge into the receiving environment.

In this assessment, performance of the denitrification filter focused on:

- the reduction of the nitrate-N load using the procedures described in 2.6, and
- formation of ammoniacal-N (by comparing the load in the inflow and the outflow).
- Performance (efficacy of nitrate-N removal) accounted for factors such as temperature, retention time and the availability of organic carbon.

7.1 Estimation of mass loads

The woodchip filter was used under entirely uncontrolled conditions – it was subject to whatever hydraulic and mass load conditions arose from the combined effects of the weather and on-farm management decisions. These factors gave rise to a dynamic and highly variable system.

The hydrology of the woodchip filter was discussed in Section 4, and grab sample details are summarised in Appendix J. Graphical concentration-discharge relationships (Figure J-1) and summary statistics of inflow and outflow ammoniacal-N, nitrate-N and TN are included in Table J-1. Inflow and outflow concentration data are compared in box and whisker plots in Figure J-2.

It is challenging to quantify the mass load transported by surface and groundwater systems because mass load is estimated as the product of concentration and flow. It is relatively easy and cheap to measure flow continuously, whereas the cost of collecting and analysing grab samples for several chemical constituents is much higher. As a result, the number of water quality sample results was far smaller than estimates of flow. The usual response to this imbalance is reliance on modelling, where a relationship between flow and concentration is determined, and this relationship is applied to all flow measurements to provide estimates of concentrations for all flows. The product of these measured flow and estimated concentration values provides estimates of instantaneous load or flux, which may then be summed to provide estimates of load per unit time (e.g., unit mass per day, season or year). Other estimation techniques exist, such as directly comparing paired inflow and outflow concentrations and loads, or estimating these loads after applying concentration values to “bins” of similar flows, and adding these together. These approaches are relatively crude and do not account for seasonal factors.

The accuracy of the estimate of mass load is strongly dependent on the concentration-flow relationship. The relationship between concentration and flow for the three variables of concern is shown in Appendix H for all grab sample data. Several points should be noted:

- for the inflow
 - there is a concentration-flow relationship for all forms of N
 - it is positive and strong for nitrate-N and TN
 - it is negative and weak for ammoniacal-N.
- for the outflow
 - the relationship between TN and flow is weak, but remains positive
 - the relationship between nitrate-N and flow remains reasonably strong and positive, and
 - for ammoniacal-N, the relationship remains negative and is stronger than for the inflow.
- Ammoniacal-N concentrations are generally higher in the outflow than the inflow, indicating formation of ammoniacal-N from other forms of nitrogen.
- Total N concentrations are lower in the outflow than the inflow, but vary over a wide range.
- Nitrate-N concentrations are also lower in the outflow than the inflow (due to removal), but vary over a much wider range than in the inflow.

Based on these observations, it is expected that the nitrate filters will generally be a net source of ammoniacal-N (i.e., the outflow load is likely to be larger than the inflow) but will reduce the nitrate-N load (viz., be a net sink). The total N load is also likely to be smaller in the outflow, because nitrate-N is the dominant constituent of the TN load.

In order to characterise the performance of the nitrate filter at various timescales, models were developed to predict the concentrations of the nitrogen species as a function of flow, temperature, and other factors. These allowed nitrate removal to be quantified at monthly, seasonal and entire assessment period time scales. A process-based model was also developed to estimate nitrate-N removal as a function of reaction rate, inflow nitrate-N concentrations, availability of dissolved organic carbon, retention time, temperature and water depth.

7.2 Ammoniacal-N

Two approaches were used to estimate inflow and outflow ammoniacal-N loads – the LOADEST model suite, and a bootstrap regression model approach. The results are summarised in Figure 7-1 and Figure 7-2, where the instantaneous flux derived from grab sample concentrations are compared with the flux time series derived from the two model approaches. In Figure 7-3, the inflow and outflow flux estimates are compared. Points to note:

- Neither model perfectly predicts inflow or outflow grab sample flux estimates, but the trend over time is described tolerably well.
- Outflow model performance deteriorates in 2018 – it is not apparent whether this relates to reducing the water level in the woodchip filter bed, or whether it is a response to the drought in the preceding year and the lower soil moisture conditions.

The inflow model predicts the grab sample flux better than the outflow models, so it is most likely that the changed conditions in the wood chip filter bed following reduction in the water level is responsible for the decline in model performance.

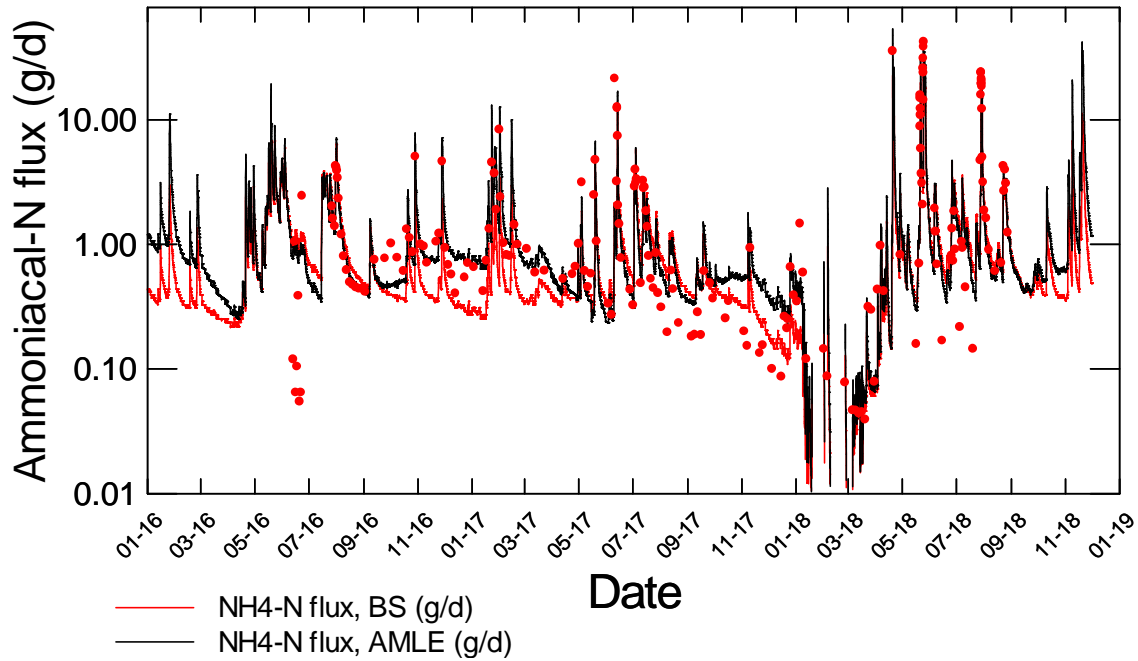


Figure 7-1: Ammoniacal-N inflow flux to woodchip filter, estimated using two models. The red dots indicate instantaneous flux estimated from grab samples used to calibrate the models. BS=bootstrap regression model (Rutherford, pers. comm.), AMLE = model from LOADEST modelling package (Runkel et al. 2013).

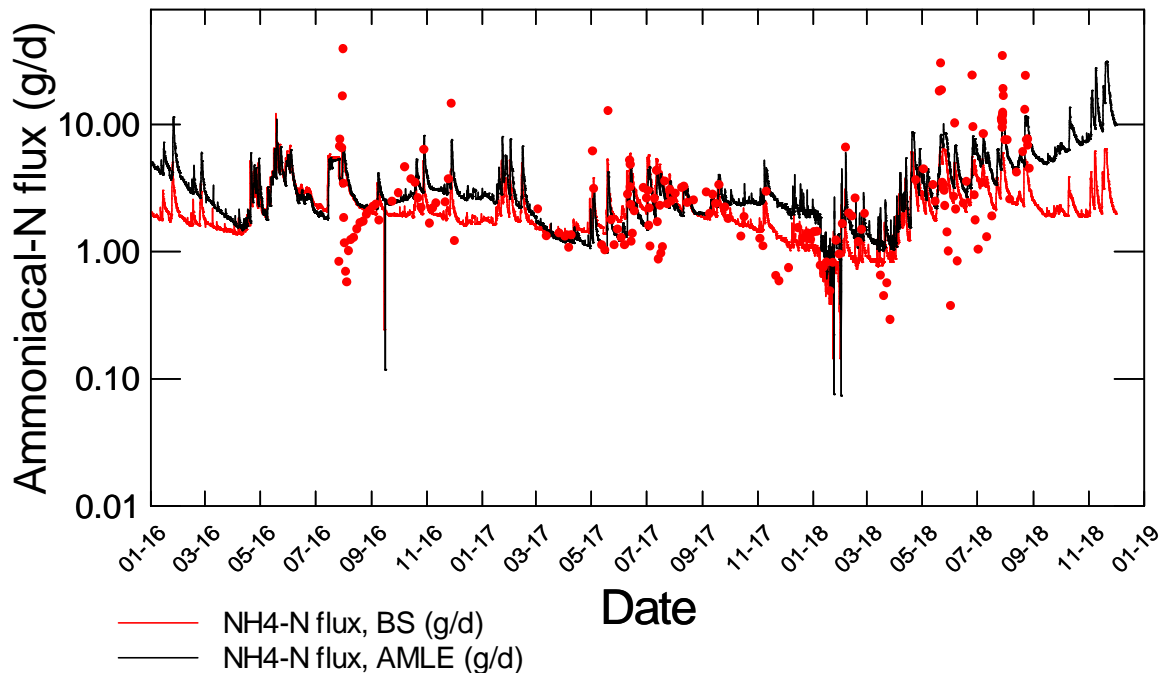


Figure 7-2: Ammoniacal-N outflow flux from woodchip filter, estimated using two models. The red dots indicate instantaneous flux estimated from grab samples used to calibrate the models. BS=bootstrap regression model, AMLE = model from LOADEST modelling package (Runkel et al. 2013).

The performance of the inflow model was assessed using a robust Least Median of Squares (LMS) regression technique, which indicated that the model accounted for more than 95% of the residuals ($R^2=0.955$) (text preceding Figure J-3). A similar assessment of the outflow model indicated that it accounted for almost 60% of the residuals ($R^2 = 0.583$) (text preceding Figure J-4).

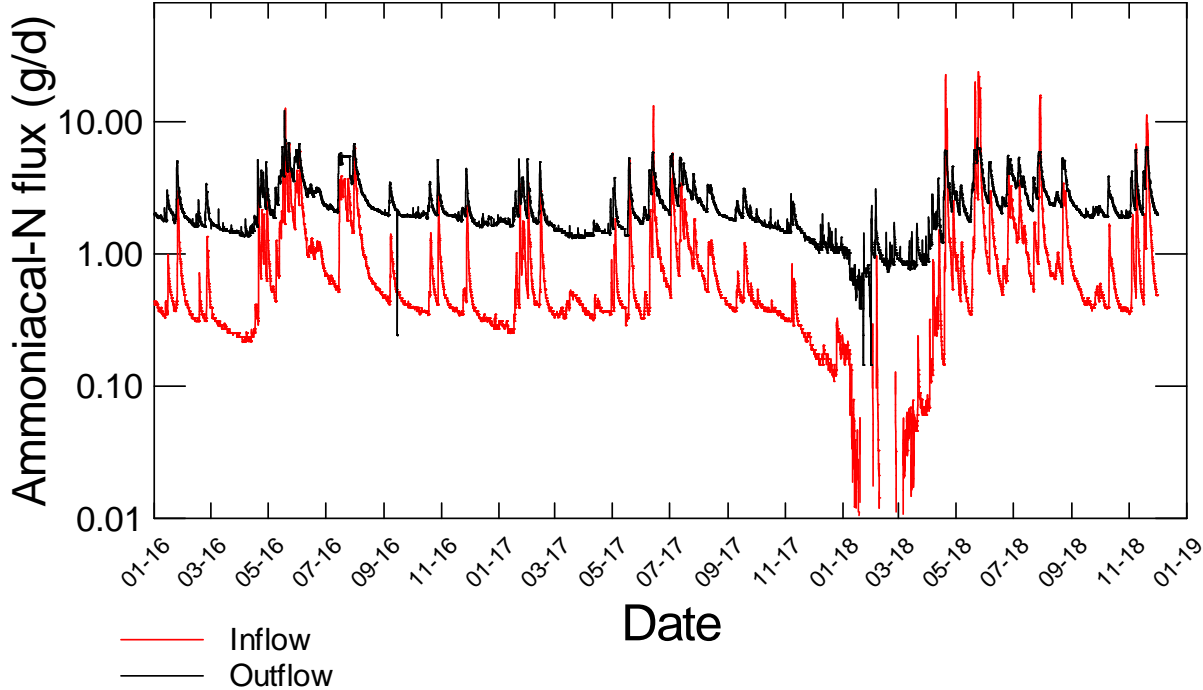


Figure 7-3: Comparison of woodchip filter inflow and outflow ammoniacal-N flux estimated using bootstrap regression models.

Ammoniacal-N removal performance

The performance of the woodchip filter in terms of ammoniacal-N removal is summarised as the mass removed per day (Figure J-10), and as the proportion of inflow load on a daily basis (Figure J-11), or according to month and season (Figure 7-4). Summary statistics of performance data are summarised in Table J-2. Over the entire assessment period average ammoniacal-N flux was 1.19 g/d, and the outflow flux was 3.48 g/d.

Table 7-1: Summary statistics for estimated ammoniacal-N inflow and outflow flux. Concentration and flux estimates were made using an LAD (inflow) and Bootstrap (outflow) regression model. Negative values indicate the filter was a net source of contaminant.

Statistic (Three-year assessment period)	AMLE predicted conc. (mg/L)		Predicted flux (g/d)		Mass removal (g/d)	Efficacy (%)
	Inflow	Outflow	Inflow	Outflow		
N of Cases	23328	23328	23328	23328	23328	23328
Minimum	0.00	0.02	0.1	0.1	-9.7	-2781.0
Maximum	12.15	0.51	53.6	31.1	43.8	74.7
Median	0.00	0.13	0.6	2.7	-1.2	-314.8
Arithmetic Mean	0.04	0.14	1.2	3.5	-1.1	-339.6
Std Error of Mean	0.00	0.00	0.0	0.0	0.0	1.5
95.0% LCL of Mean	0.03	0.14	1.1	3.5	-1.1	-342.5
95.0% UCL of Mean	0.04	0.14	1.2	3.5	-1.1	-336.6
Std Deviation	0.35	0.08	2.6	2.8	2.3	230.6
Cleveland percentiles						
0.01	0	0.03	0.1	1.1	-4.3	-1319.1
0.05	0	0.042	0.3	1.2	-2.7	-701.8
0.1	0.001	0.051	0.3	1.5	-2.0	-536.3
0.2	0.001	0.07	0.4	2.0	-1.7	-440.8
0.25	0.001	0.077	0.5	2.1	-1.7	-414.8
0.3	0.001	0.087	0.5	2.2	-1.6	-388.4
0.4	0.001	0.104	0.5	2.4	-1.4	-345.1
0.5	0.002	0.125	0.6	2.7	-1.2	-314.8
0.6	0.002	0.138	0.8	3.0	-1.1	-277.7
0.7	0.004	0.163	0.9	3.6	-1.0	-233.6
0.75	0.005	0.174	1.0	4.0	-0.9	-207.8
0.8	0.007	0.196	1.2	4.6	-0.9	-175.7
0.9	0.019	0.269	1.9	6.2	-0.7	-115.4
0.95	0.044	0.316	2.9	8.0	-0.2	-74.6
0.99	0.507	0.376	11.4	15.4	6.7	14.0

The woodchip filter is always a net source of ammoniacal-N (median outflow load typically 5 times larger than the inflow), but the absolute amount of ammoniacal N is small (typically 1-2 g/d). Ammoniacal-N is toxic to aquatic organisms, particularly fish, so it is important to ensure that the discharge does not impact adversely on receiving water quality. Flow and concentration data are available for the “Waituna Creek at Marshall Road” site, which is in the lower reaches of Waituna Creek. The median concentration of ammoniacal-N at this site over the period May 2011-December 2013 was 0.07 mg/L⁵, the average flow was 1,571 L/s⁶, and the calculated flux (average flow x average concentration) was 13,500 g/d. Over the three-year period of assessment, the woodchip

⁵ From the LAWA website

⁶ From the ES website, <http://envdata.es.govt.nz/index.aspx?c=flow&tab=hydro>

filter generated less than 10 g/d (typically 1-2 g/d), which is unlikely to have a measurable impact on the receiving water quality.

The ammoniacal-N concentration in the Waituna Creek at Waituna Road is lower (approximately 0.06 mg/L) than the outflow (measured average 0.105 mg/L and modelled average 0.151 mg/L). The average discharge from the woodchip filter was 0.45 L/s, and the average flux was therefore 5.8 g/d.

Flow data are not available for the “Waituna Creek at Waituna Road”, but assuming the flow is two-thirds that of the average at “Waituna Creek at Marshall Road”, then the flux at will be approximately 6,000 g/d. After mixing, the flux downstream of the woodchip filter will be increased by approximately 0.1%, which would probably be undetectable.

Even though the ammoniacal-N load discharged from the woodchip filter appears to be negligible and the likely impact on water quality less than minor, it would be prudent to assess the magnitude of this load under low flow conditions, when the dilution in the stream will be least. It would also be advisable to assess the cumulative effect of several of these devices in a single small catchment prior to implementing these mitigation tools in small, potentially sensitive stream catchments.

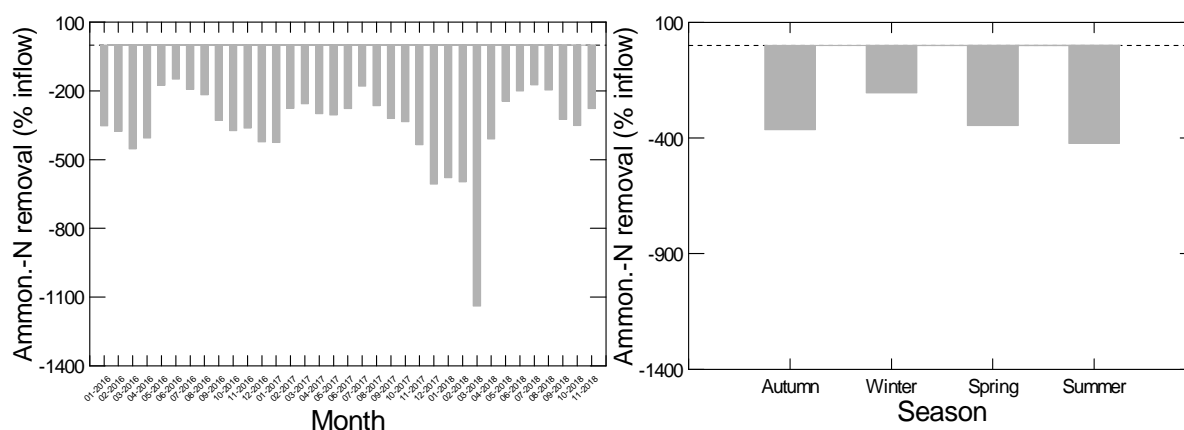


Figure 7-4: Performance of the woodchip filter in terms of ammoniacal-N removal, reported as proportion of inflow load by month (left) and season (right). Negative values indicate that the filter is a net source of ammoniacal-N. Very large negative values are artefacts of the modelling, timestep differences between the inflow and outflow, and very low outflow from the filter in summer 2017/2018.

7.3 Nitrate-N

Several approaches were trialled to assess the nitrate-N removal performance of the woodchip filter.

7.3.1 Regression models

First, models were developed to estimate continuous nitrate-N concentrations and fluxes from continuous flow and grab concentrations. Second, filter performance was calculated as the difference between estimated continuous inflow and outflow fluxes.

It was possible to model the inflow flux satisfactorily using several different techniques. Examples of the MLE approach of the LOADEST suite and a bootstrap regression model are shown in Figure 7-5, where good agreement between the predicted load and the flux derived from grab samples is evident. Either model captures baseflow and peak and extreme low flow loads satisfactorily. After adjusting for outliers, a robust Least Median of Squares (LMS) regression technique indicated an R^2 of 0.543.

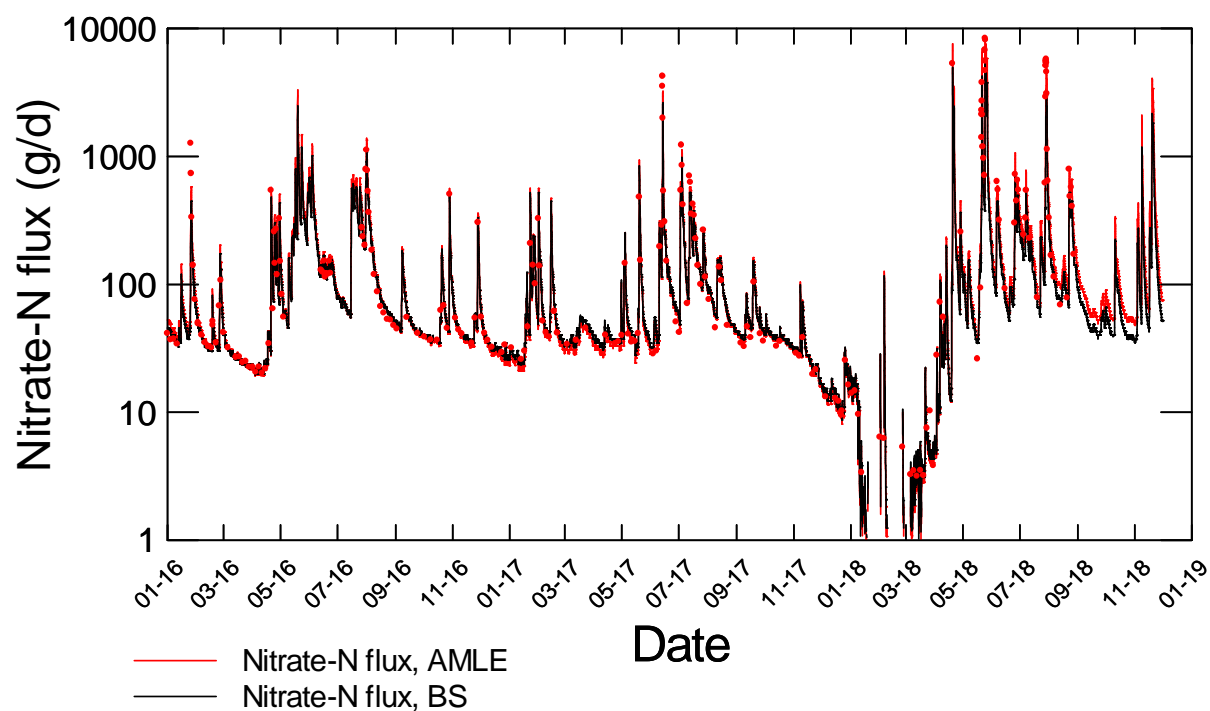


Figure 7-5: Nitrate-N inflow flux to woodchip filter, estimated using two models. The red dots indicate instantaneous flux estimated from grab samples used to calibrate the models. BS=bootstrap regression model, AMLE = model from LOADEST modelling package (Runkel et al. 2013).

Modelling the outflow flux was more challenging, as the two examples in Figure 7-6 indicate. Either model captures the general trend in nitrate-N flux during the assessment period, but both models fail to predict the nitrate flux adequately under baseflow conditions. This is not surprising – as indicated earlier, the denitrification process is biologically mediated, and neither of the models used incorporate reaction rate functions. Because they did not predict outflow concentration and flux adequately, when the difference between inflow and outflow flux was calculated both models under-estimated the nitrate-N removal efficacy. We found it was necessary to reflect the biologically-mediated processes whereby natural systems convert nitrate-N into other forms in order to estimate performance adequately. Examples illustrating the difference between inflow and outflow load estimated using two bootstrap models is shown in Appendix J, with Figure J-12 through Figure J-14 as examples.

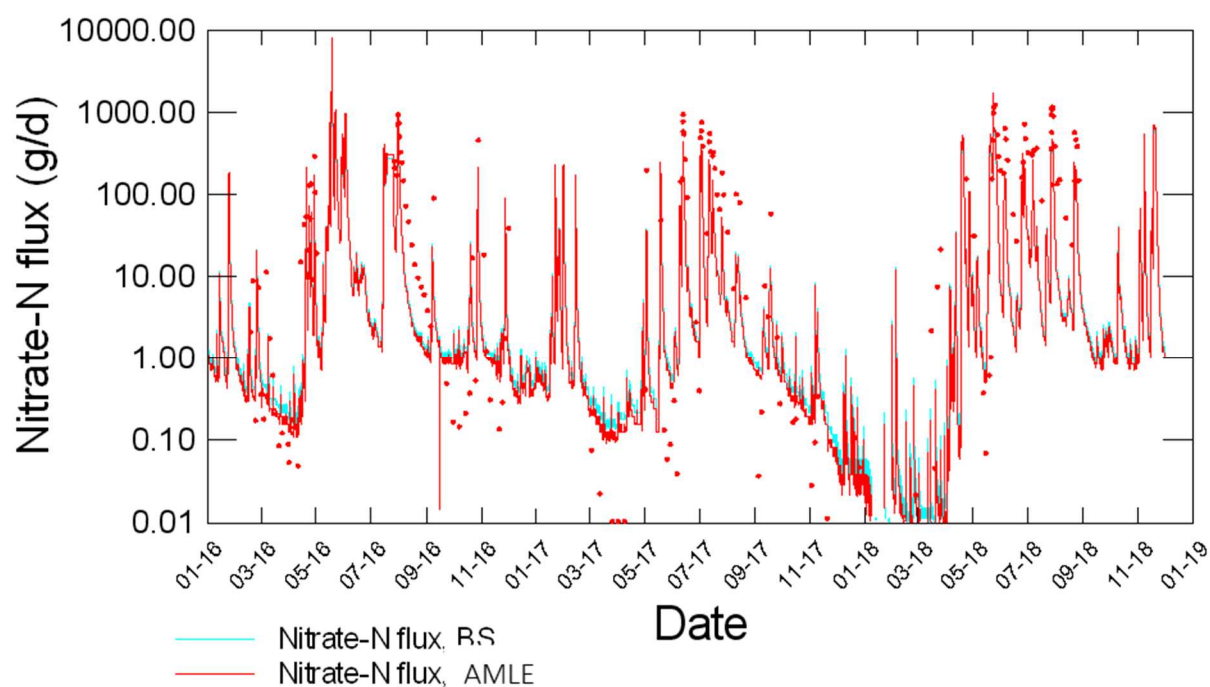


Figure 7-6: Nitrate-N outflow flux from woodchip filter, estimated using two models. The red dots indicate instantaneous flux estimated from grab samples used to calibrate the models. BS=bootstrap regression model, AMLE = model from LOADEST modelling package (Runkel et al. 2013).

7.3.2 Process-based models

Earlier, the development of a process-based identification model was described. The AMLE nitrate-N inflow model was shown to predict measured inflows well (Figure 7-5) and provides a reliable hourly flux inflow time-series. This time-series was converted into an hourly inflow nitrate-N concentration estimate by dividing the hourly flux estimate by the average flow for the hour (and adjusting for units of measure). This hourly inflow concentration estimate was then used to predict an hourly outflow concentration estimate using the process model described earlier (Equation 2-3). The outflow nitrate-N flux time series estimated through this process is compared with the mixed regression model and grab sample measurements in Figure 7-8 while the statistical relationship between measured and predicted concentrations is summarised in Appendix J.

The relationship between measured outflow nitrate-N concentrations and those predicted from inflow concentrations after accounting for the denitrification process is shown in Figure 7-7. The model accounts for 88% of the variance ($R^2 = 0.881$, Least Absolute Deviation regression model). The statistical relationship between measured and modelled values is described using different robust model in the text preceding Figure J-6 (Appendix J). Not all inflow samples were matched with an outflow sample (there were 108 pairs of samples). A time-series of all measured and predicted outflow concentrations is shown in Figure 7-8.

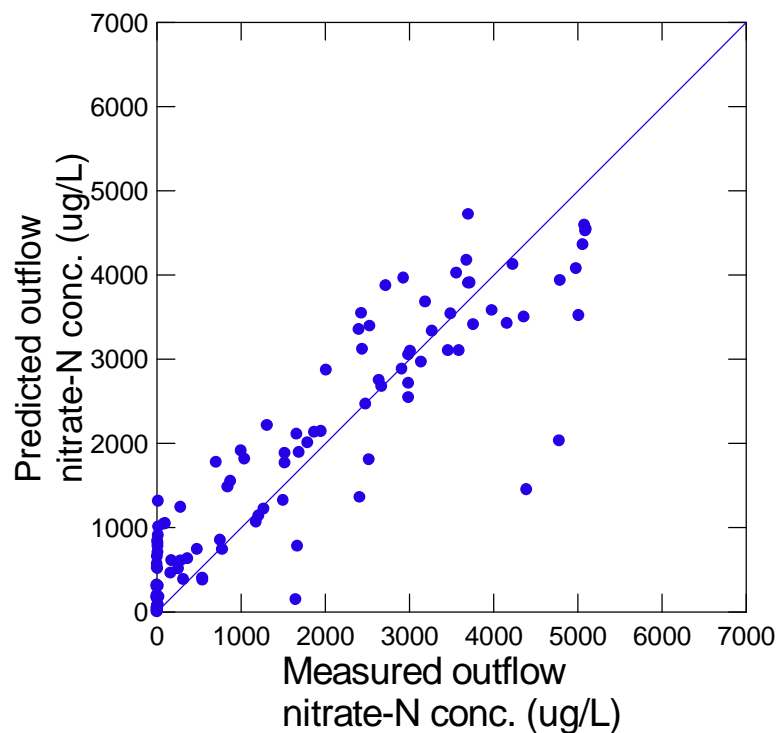


Figure 7-7: Comparison of woodchip filter measured and predicted nitrate-N outflow concentrations. The predicted concentrations were derived from measured inflow concentrations using Equation 2-3 described in section 2.5.2. The statistical relationship between measured and modelled values is described in Appendix J.

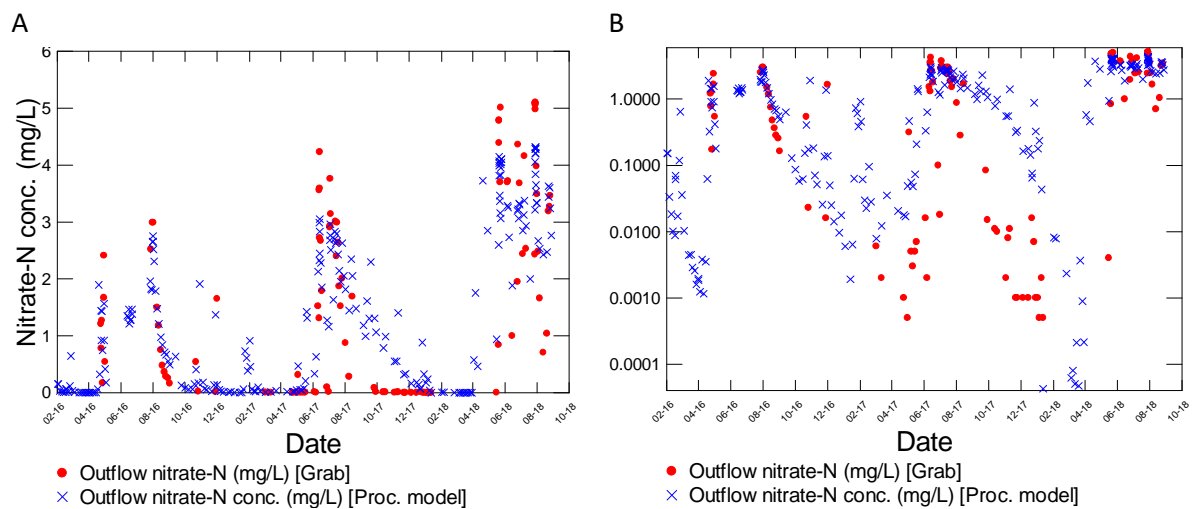


Figure 7-8: Time series of measured (red dots) and predicted (blue crosses) woodchip filter nitrate-N outflow concentrations at normal (A) and \log_{10} scale (B). The predicted concentrations were derived from the measured inflow concentrations using the process-based model (Equation 2-3) described in section 2.5.2. The statistical analysis of measured and modelled values is described more fully in Appendix J.

Figure 7-7, Figure 7-8 and the statistical relationship shown in Appendix J (material preceding Figure J-6) show a reasonable correspondence between measured and predicted outflow nitrate-N concentrations, particularly during high flow conditions. Under low flow conditions, however, the model predictions do not match observations closely (Figure 7-12). The likely reasons include larger capacity to remove nitrate-N than the load in the inflow, leading to almost quantitative removal – the model relies on a proportion of nitrate-N in the inflow, and as a result the model is unable to predict the low concentrations observed. Notwithstanding, the model appears to predict outflow nitrate-N adequately for this assessment. Points to note from Figure 7-8 and the figures in Appendix J:

- The match between observed and predicted values is good in the 2016 and 2018 calendar years, when rainfall was near-normal.
- The relationship was poor in 2017 during low-flow conditions, when the model overpredicts nitrate-N concentrations.
- The model appears to predict outflow nitrate-N concentrations well during high flow events, when the nitrate-N load is greatest.

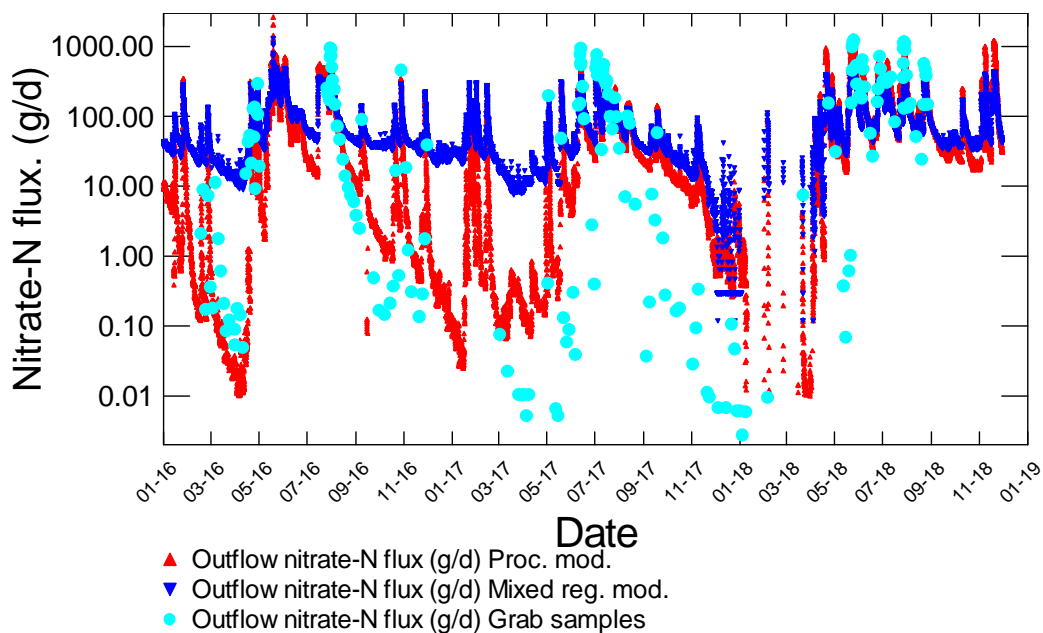


Figure 7-9: Time series of measured and predicted woodchip filter nitrate-N outflow flux. Note the y-axis has \log_{10} scale. The measured flux was derived from grab sample results. The predicted flux was derived from the measured inflow concentrations using the process model equation described in section 2.5.2 (Proc. Mod.), and from the mixed regression model previously described (Mixed reg. mod.).

Although neither of the models perfectly predicts the outflow nitrate-N flux, the process-based model better represents the flux during low flow conditions than does the mixed regression model. The periods of greatest discrepancy between the process-based model and the grab sample flux measurements occur during 2017, and correspond with very low inflow and outflow concentrations.

7.3.3 Nitrate-N removal efficacy

Statistics for several metrics associated with estimating nitrate-N removal and removal efficacy over the entire assessment period are summarised in Table 7-2. This table includes estimates of inflow and outflow nitrate-N concentrations and flux, as well as removal rates and removal efficacy, expressed as the proportion of inflow load that is removed. These data indicate that for 50% of the time, the woodchip filter nitrate-N removal efficacy is almost 70%. The relationship between nitrate-N load and removal efficacy is explored further in Section 7.3.4.

Table 7-2: Nitrate-N removal efficacy for the entire assessment period derived from hourly average values. The predicted flux was derived from the measured inflow concentrations using the process model equation described in section 2.5.2, and from the AMLE model in the LOADEST suite. Nitrate removal is expressed as the difference between the inflow and outflow nitrate-N loads, and as the proportion of nitrate-N removed from the inflow.

Statistic	Nitrate-N concentration (ug/L)		Nitrate-N flux (g/d)		Nitrate-N removal, inflow-outflow (g/d)	Nitrate-N removal eff. (% inflow)
	Inflow AMLE	Outflow Proc. mod.	Inflow AMLE	Outflow Proc. mod.		
N of Cases	24391	24391	24391	24391	24391	24391
Minimum	0.96	0.00	0.01	0.00	0.01	0.01
Maximum	5.27	4.75	8364.30	2628.04	6961.25	100.00
Median	2.25	0.68	51.32	15.32	32.74	71.94
Arithmetic Mean	2.42	0.99	146.11	72.85	73.26	66.15
SE Mean	0.00	0.01	2.77	0.97	2.09	0.20
95.0% LCL of Mean	2.41	0.97	140.68	70.95	69.16	65.76
95.0% UCL of Mean	2.42	1.00	151.55	74.76	77.37	66.54
Standard Deviation	0.50	1.02	432.77	151.94	327.11	31.01
Percentiles						
1%	1.69	0.00	2.57	0.00	2.37	6.69
5%	1.92	0.00	12.09	0.03	10.46	13.11
10%	1.95	0.01	21.58	0.10	15.90	19.97
20%	2.01	0.03	30.65	0.40	21.33	32.64
25%	2.07	0.05	33.19	0.75	23.23	39.32
30%	2.11	0.09	35.81	1.32	24.73	44.49
40%	2.17	0.28	41.55	5.40	28.38	57.52
50%	2.25	0.68	51.32	15.32	32.74	71.94
60%	2.38	1.11	65.80	28.03	36.54	86.90
70%	2.54	1.45	93.51	50.36	41.60	95.51
75%	2.70	1.69	116.78	69.15	46.11	97.65
80%	2.88	1.94	143.84	91.56	52.42	98.89
90%	3.08	2.54	285.25	201.08	88.61	99.63
95%	3.29	2.91	503.42	402.19	150.51	99.87
99%	4.03	3.61	1464.53	781.07	654.02	100.00

Seasonal performance data are summarised in Appendix K and results are summarised by year in Appendix L.

The removal performance is variable over time, as the time-series in Figure 7-10 indicates. The mass removal rate (g/d) is greatest when inflow loads are high (which counter-intuitively occurs when retention times are low), and smallest during summer periods when inflow loads are low (even though retention times are high – see Figure 7-11). This does not mean that performance efficacy follows the same trend. The largest proportion of the inflow load is removed during low flow periods, as indicated in Figure 7-11 and Figure 7-12.

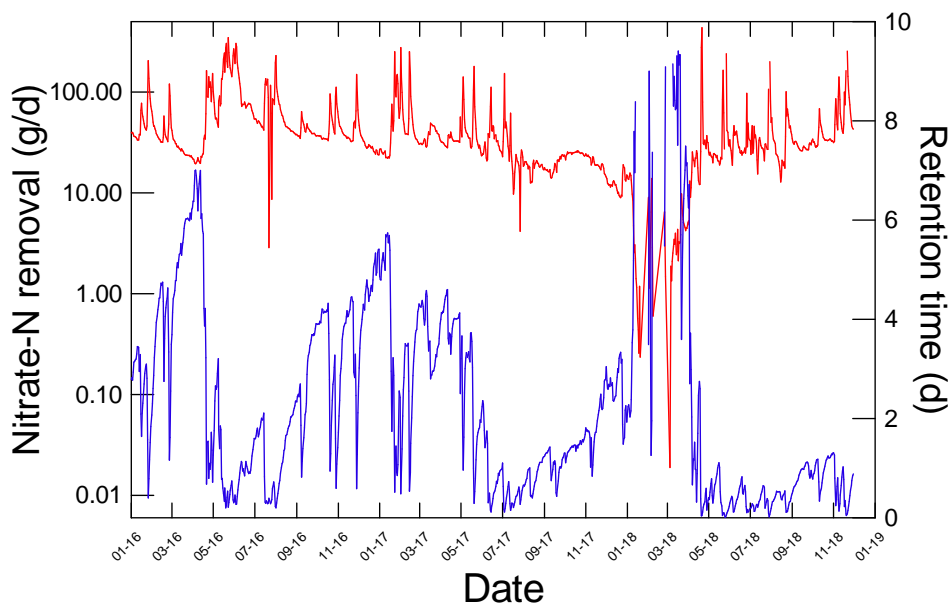


Figure 7-10: Relationship between nitrate-N removal (blue), estimated as the difference between inflow and outflow nitrate-N flux, and hydraulic retention time (grey). The inflow flux was estimated using the LOADEST AMLE model, and the outflow flux was estimated from inflow concentrations using the process described in section 2.5.2. These data are hourly average values.

Figure 7-12 shows the relationship over time between removal efficacy (expressed in terms of the proportion of inflow load removed) and hydraulic retention time. Periods of high removal efficacy (say greater than 80% of influent load) generally correspond with periods when retention time is greater than about four days. These results are presented in terms of mass removed in Figure K-1. The inverse relationship between nitrate-N removal and removal efficacy is shown in Figure 7-13 (B). The relationship in Figure 7-13 (A) may appear counterintuitive. It indicates that the mass removal of nitrate-N **increases** as retention time decreases. To explain this observation, it must be recalled that the flux of nitrate-N increases with flow, i.e., shorter retention times are related to higher nitrate inflow concentrations – there is more nitrate-N for the denitrifying bacteria to consume. The process model described by Equation 2-3 indicates that nitrate removal rate is positively related to the inflow nitrate concentration. The higher inflow (=shorter retention time) enables higher nitrate-N removal rates. The mass of nitrate-N removed during high flow events increases, but the efficacy of removal (expressed as the proportion of inflow load removed) decreases as retention time decreases. This is illustrated in Figure 7-11.

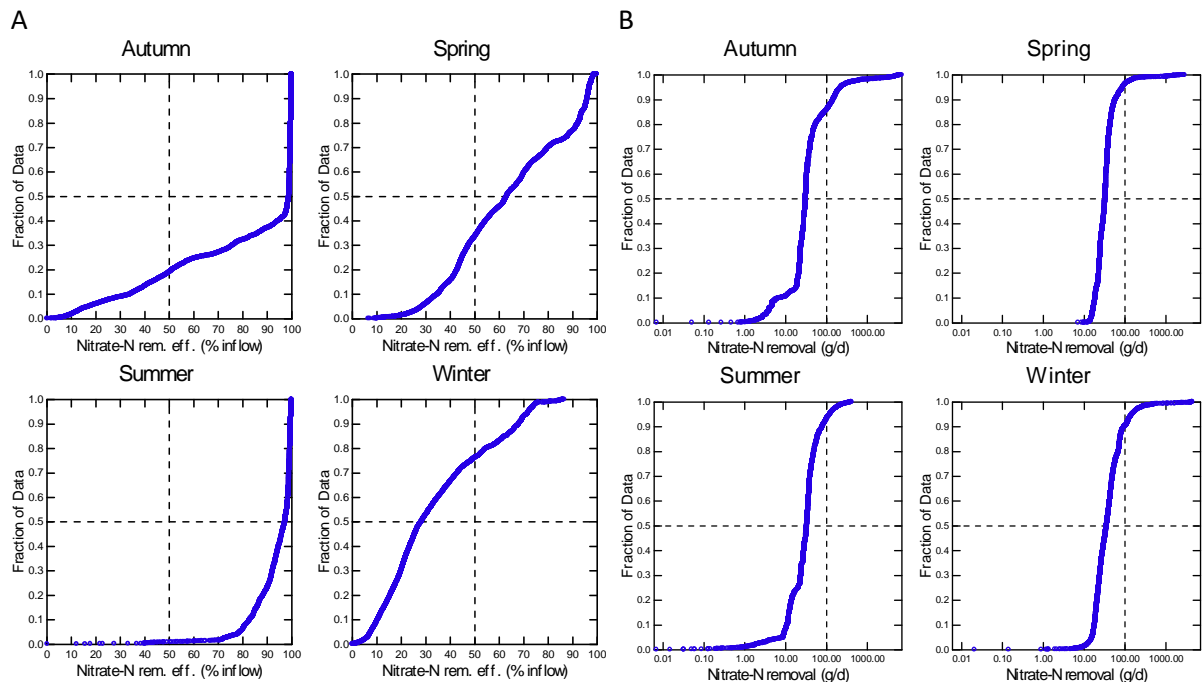


Figure 7-11: Seasonal variation in nitrate-N removal efficacy (A) and nitrate removal rate (B).

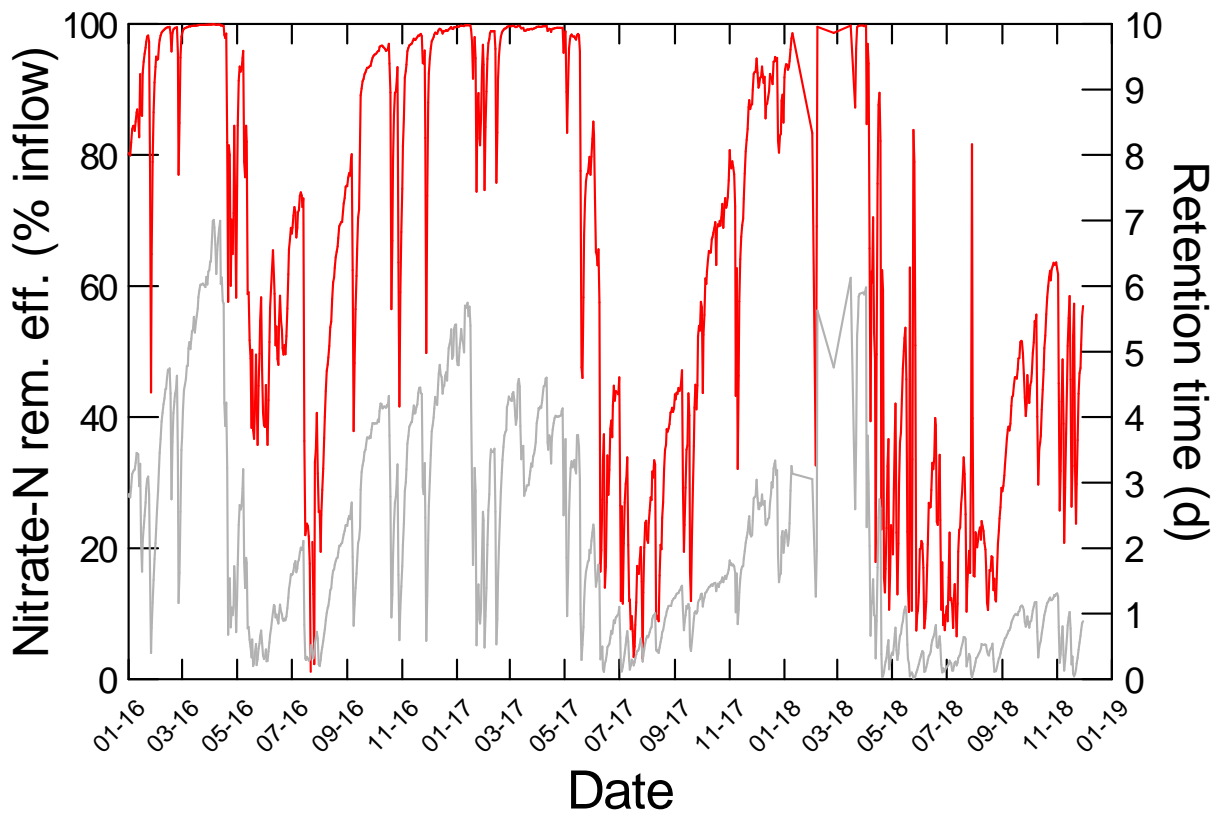


Figure 7-12: Relationship between nitrate-N removal efficacy (red) and hydraulic retention time (grey). Nitrate-N removal efficacy was estimated as the difference between inflow and outflow flux, expressed as a proportion of the inflow flux. Hydraulic retention time was estimated as the quotient of active biofilter volume and inflow, expressed in days after correcting for units. The relationship between water level and retention time was discussed in section 4. The inflow flux was estimated using the LOADEST AMLE model, and the outflow flux was estimated from inflow concentrations using the process described in section 2.5.2.

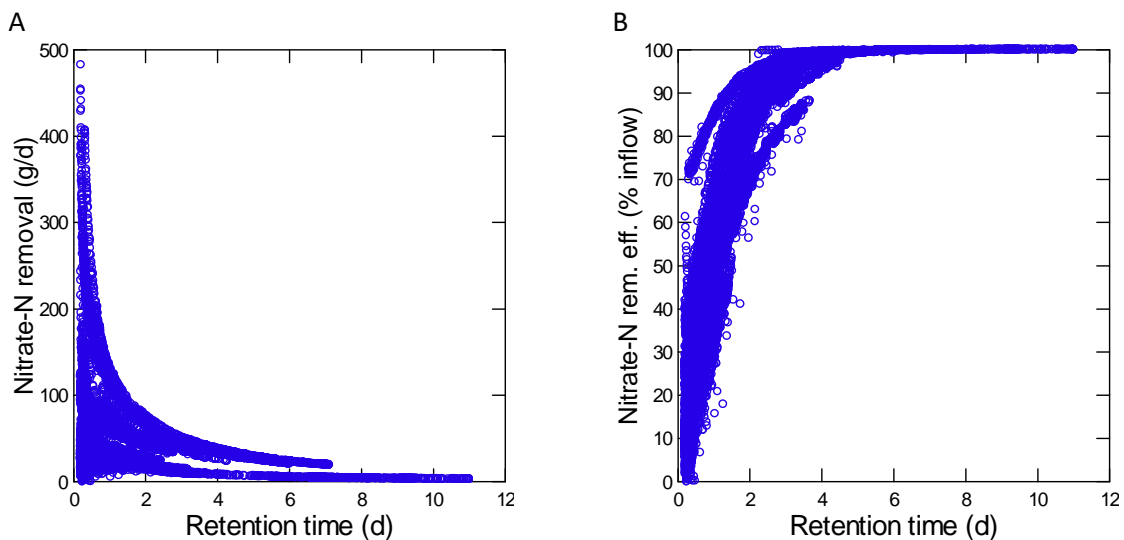


Figure 7-13: Relationship between nitrate-N removal and hydraulic retention time (A), and nitrate-N removal efficacy and hydraulic retention time (B). Nitrate-N removal efficacy was estimated as the difference between inflow and outflow flux, expressed as a proportion of the inflow flux. Hydraulic retention time was estimated as the quotient of active biofilter volume and inflow, expressed in days after correcting for units. The inflow flux was estimated using the LOADEST AMLE model, and the outflow flux was estimated from inflow concentrations using the process described in section 2.5.2.

Figure 7-14 shows how the mass of material delivered to the woodchip filter varies with time, and Figure 7-15 and Figure 7-16 show how the performance of the filter varies over time, while Figure 7-17 indicates the seasonal difference in influent load and treatment performance.

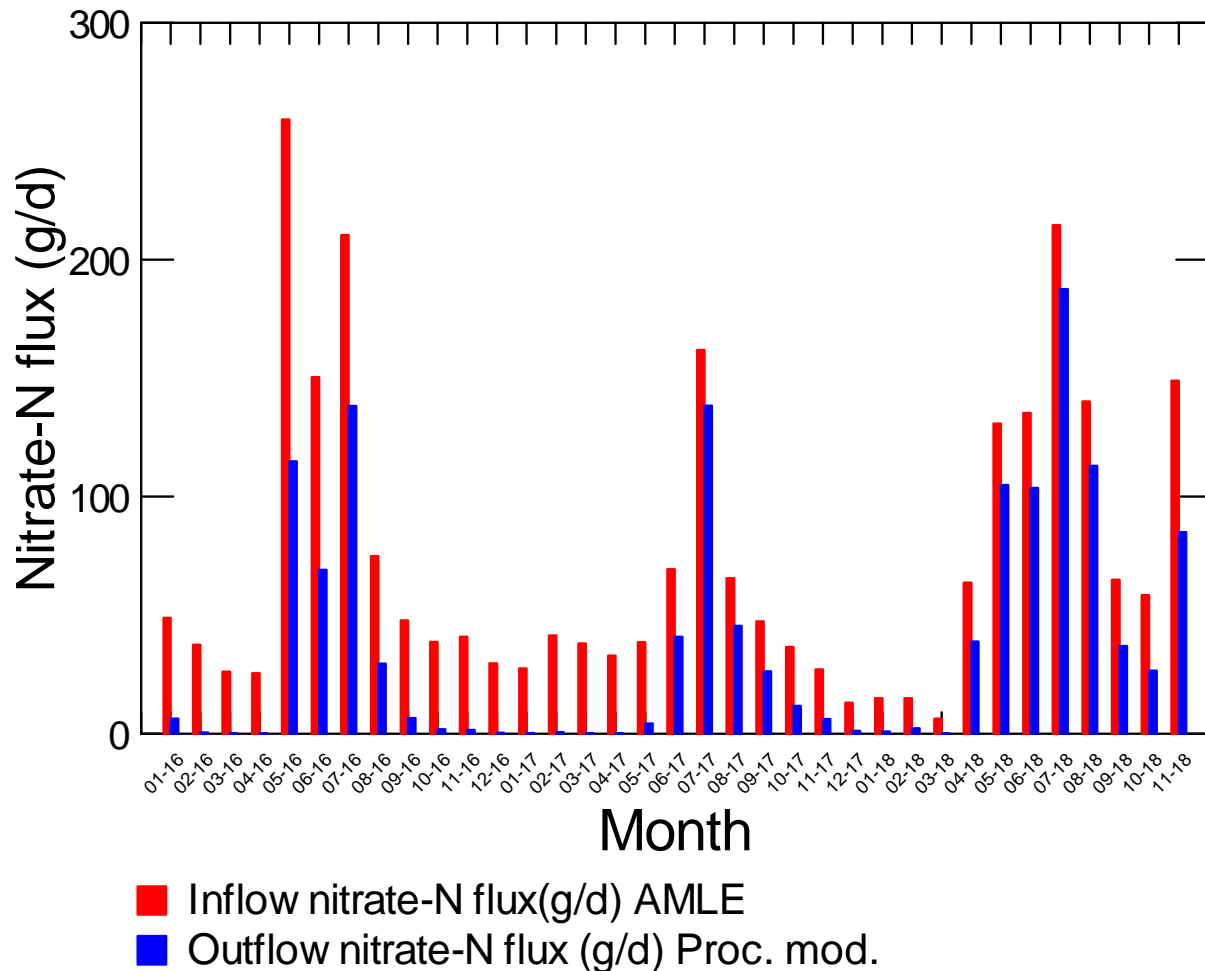


Figure 7-14: Comparison of median nitrate-N inflow and outflow flux by month. The inflow flux was estimated using the LOADEST AMLE model, and the outflow flux was estimated from inflow concentrations using the process described in section 2.5.2.

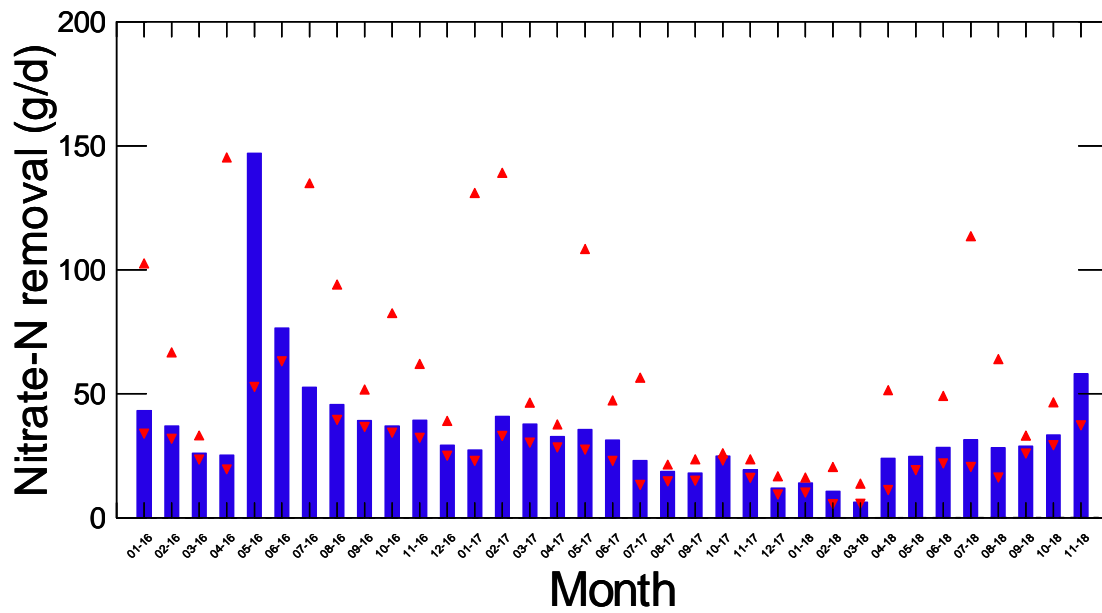


Figure 7-15: Median nitrate-N removal, estimated as the difference between inflow and outflow flux by month. The inflow flux was estimated using the LOADEST AMLE model, and the outflow flux was estimated from inflow concentrations using the process model described in section 2.5.2. These data were derived from hourly estimates. The red triangles indicate the 10th and 90th percentile values.

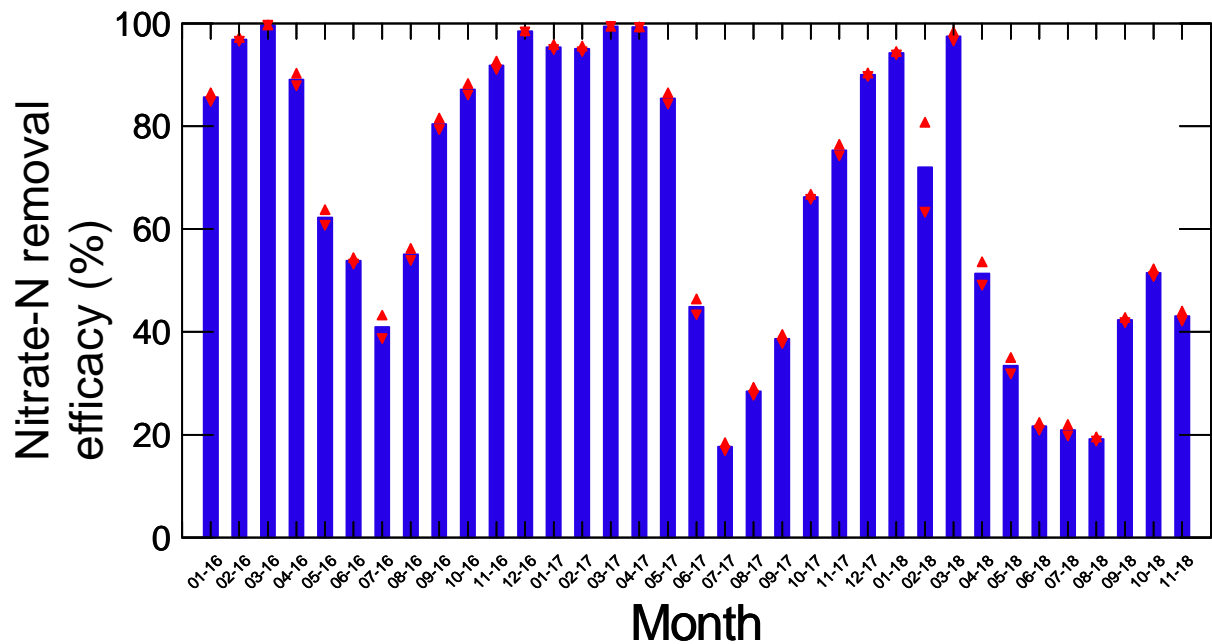


Figure 7-16: Average nitrate-N removal efficacy, estimated as the percent of inflow flux removed by the filter by month. The inflow flux was estimated using the LOADEST AMLE model, and the outflow flux was estimated from inflow concentrations using the process model described in section 2.5.2. These data were derived from hourly estimates. The red triangles indicate the 95% lower and upper confidence intervals of the monthly mean values.

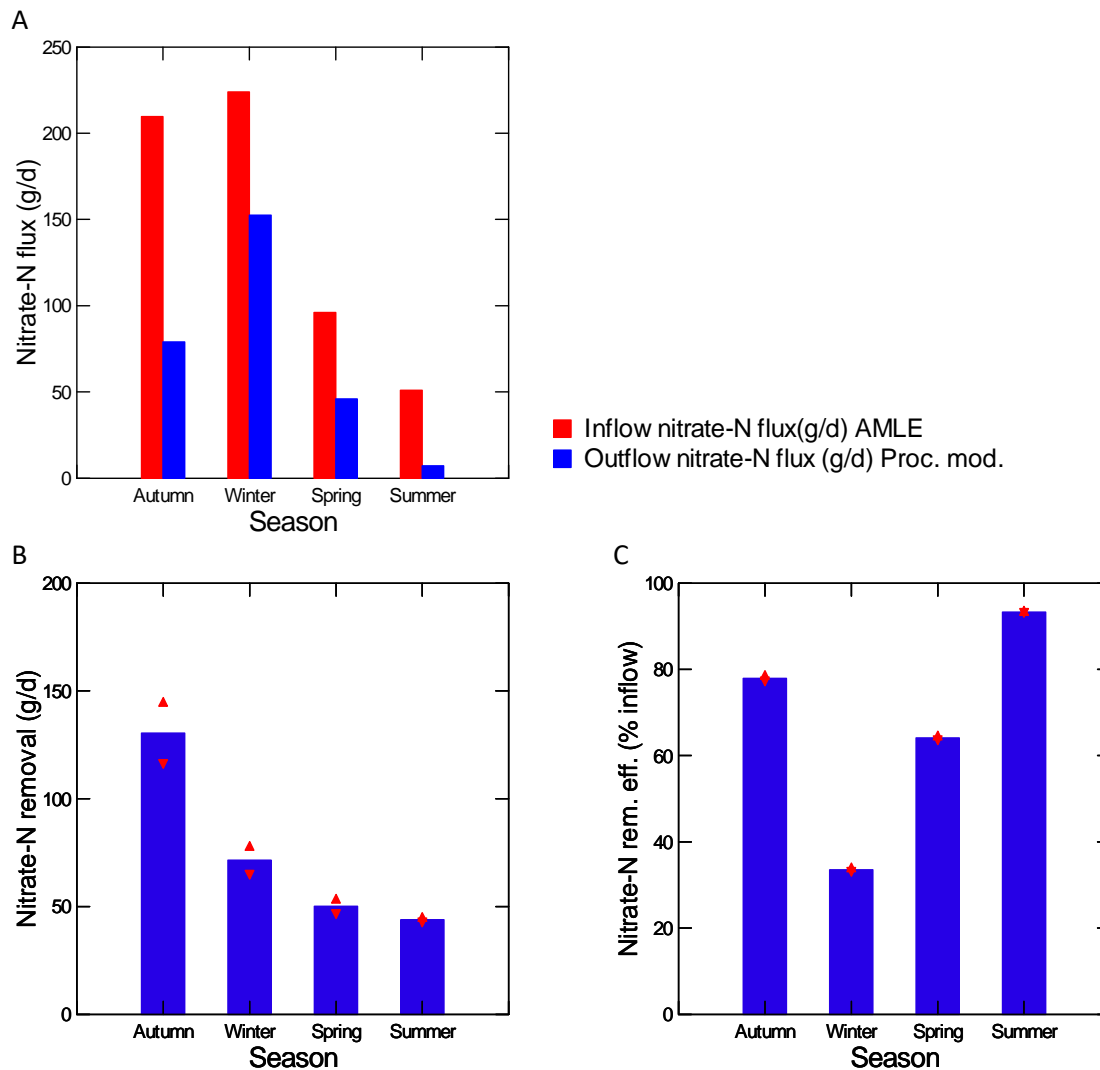


Figure 7-17: Seasonal nitrate-N flux (A), removal (B) and efficacy (C). The inflow flux was estimated using the LOADEST AMLE model, and the outflow flux was estimated from inflow concentrations using the process model described in section 2.5.2. Nitrate-N removal is the difference between inflow and outflow nitrate-N flux, and removal efficacy is the difference between inflow and outflow flux expressed as a percentage of the inflow. These data were derived from hourly estimates. The red triangles indicate the 95% lower and upper confidence intervals of the seasonal mean.

Points to note regarding treatment performance:

- The woodchip filter always removes some of the influent nitrate-N load, irrespective of the retention time.
- Increasing retention time when inflow flux remains constant increases the proportion of inflow nitrate-N load that is removed.
- Reducing the bed depth in May 2017 may have provided the potential for buffering higher inflows and creating longer retention times, but it did not achieve the expected increase in retention times or removal because of the way it was done.

The likely consequences of reducing the bed depth is discussed in section 7.5 – the performance data discussed above indicates that decreasing the bed depth did not improve performance efficacy, either in terms of mass of nitrate removed, or proportion of influent load removed.

Increasing the retention time would increase filter performance. Achieving increased retention times will require additional engineering design and additional infrastructure. The latter could still be relatively simple and require little additional management. Inclusion of an up-gradient detention system (which would temporarily store the tile drainage in a pond or tank, from which it could subsequently be discharged into the filter), and/or an outlet weir and orifice plate in the outlet structure are options for increasing retention time, while not necessarily adding complexity or greatly increasing the construction or operating expense.

Treatment performance may also be expressed in terms of mass removed per unit time per treatment volume (e.g., g N removed/m³/day), discussed in 2.6. When expressed in this way, it is possible to directly compare treatment performance with results reported in other trials. Treatment performance data are provided in this form in Appendix L. Selected statistics are presented in Table 7-3. These results are placed in context by comparison with other recent studies in Section 9.

Table 7-3: Nitrate-N removal performance over the three-year assessment period. Complete statistics for the three-year period, as well as results for each calendar year, are provide in Appendix L.

Statistics (Three year assessment period)	Nitrate-N removal (g/d)	Nitrate-N removal rate (g/m ³ /d)
N of Cases	24391	24391
Minimum	0.0	0.0
Maximum	6961.2	305.5
Median	32.7	0.9
Arithmetic Mean	73.3	2.4
Standard Error of Arithmetic Mean	2.1	0.1
95.0% LCL of Arithmetic Mean	69.2	2.2
95.0% UCL of Arithmetic Mean	77.4	2.6
Standard Deviation	327.1	14.7

7.3.4 Other information provided by treatment performance data

The distribution of retention times is informative. Figure K-4 shows how retention times have altered (generally decreased) since the trial started, and how reducing the bed depth has impacted on retention times in 2018 specifically. The very long retention times in 2018 relate to the drought during summer 2017/2018; once normal rainfall resumed retention times were generally less than two days. The effect on treatment performance is shown in Figure K-5A and Figure K-6. Treatment performance (removal efficacy) can be ranked 2016 > 2017 > 2018 which is the same as the ranking of retention time indicating that removal efficacy decreased as retention times decreased. This is confirmed in Figure K-5B.

Figure K-6 shows how retention times decreased over the assessment period, and the deleterious effect this has had on treatment performance. The proportion of time when nitrate-N reduction exceeded 100 g/d is much greater in 2016 than in the following years, and the longer retention times anticipated following reduction in water levels in 2017 have either not materialised, or have failed to deliver the improved treatment anticipated.

These data may also be used for woodchip filter design. A model was fitted to the removal efficacy data of the form:

$$\text{Nitrate - N removal efficacy} = \frac{a}{Q_{in}^b} \quad \text{Equation 7-1}$$

where: Q_{in} = inflow (L/s)

$a = 54.77$ and $b = 0.327$

When fitted to the 2016 data (see Figure 7-23 B) $R^2 = 0.84$.

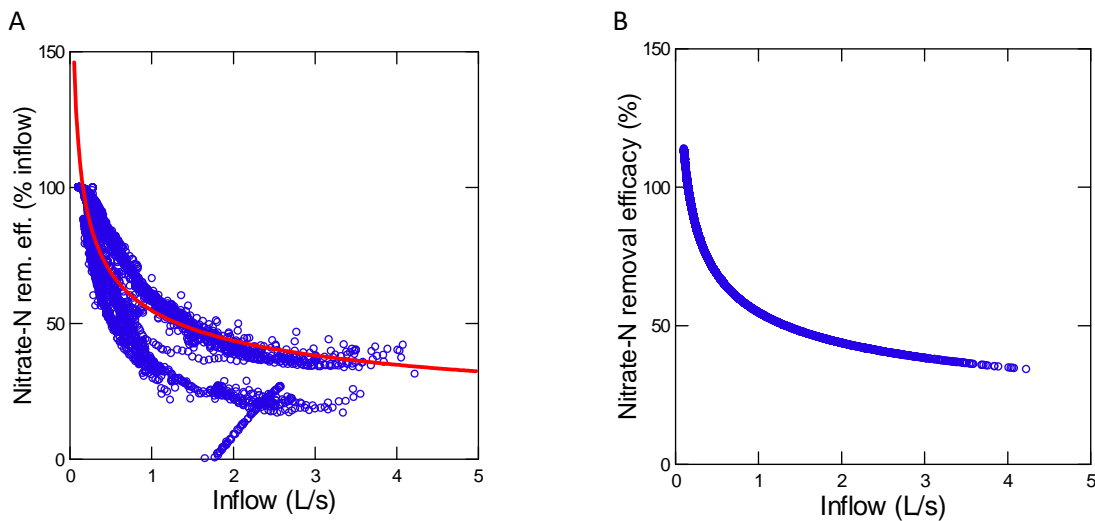


Figure 7-18: Relationship between nitrate-N removal performance and inflow, 2016 data only. Left) model fitted to data, and Right) model that could be used to guide design.

The influence of temperature was accounted for in the process model. The effect of temperature on treatment performance is indicated in Figure 7-19, where the results of two different performance assessment approaches are compared. Both show that nitrate-N removal efficacy is positively correlated with temperature, with the process-based model demonstrating this effect more clearly.

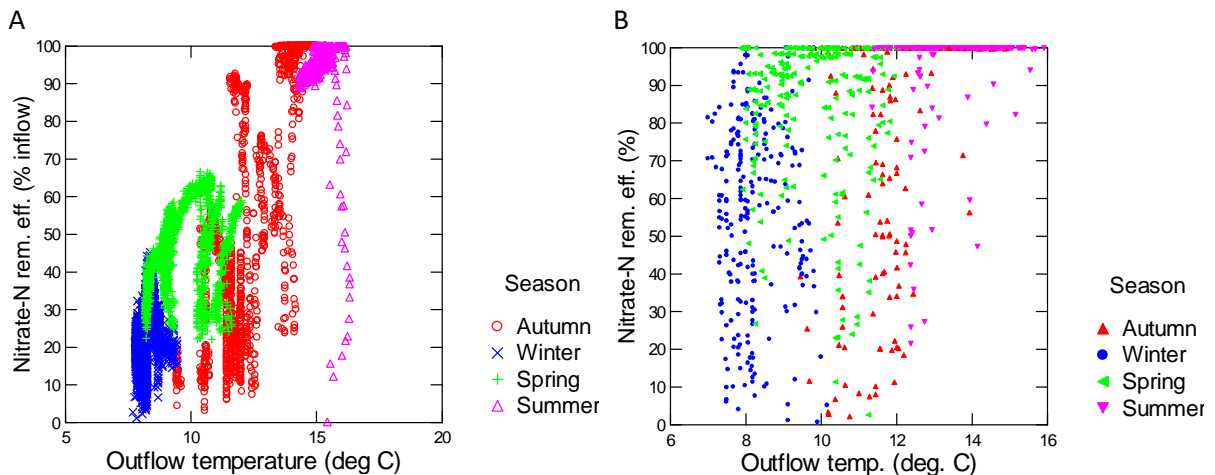


Figure 7-19: Influence of temperature on nitrate-N removal performance. A) Performance data derived from the process model, B) performance data derived from the regression model.

7.4 Total nitrogen

As Figure 7-20 and Figure 7-21 indicate, the regression models are able to predict TN flux into and out of the filter tolerably well. Other model predictions are summarised in Figure J-15 and Figure J-16. The results from the AMLE models are summarised in Appendix H.

Treatment performance was estimated in terms of TN removal using bootstrap regression models.

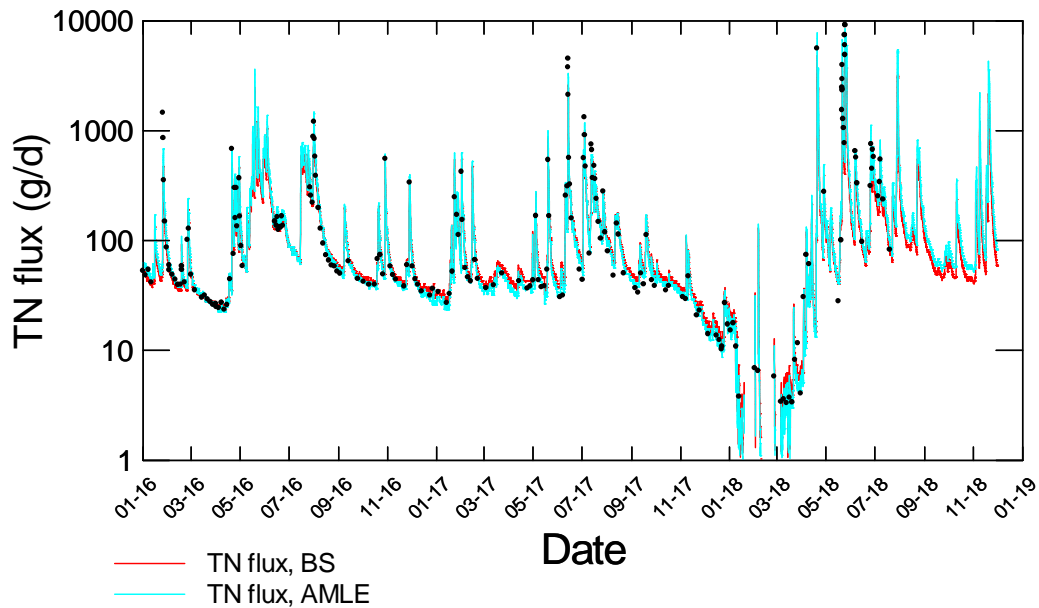


Figure 7-20: TN inflow flux to the woodchip filter, estimated using two models. The black dots indicate instantaneous flux estimated from grab samples used to calibrate the models. BS=bootstrap regression model, AMLE = model from LOADEST modelling package (Runkel et al. 2013).

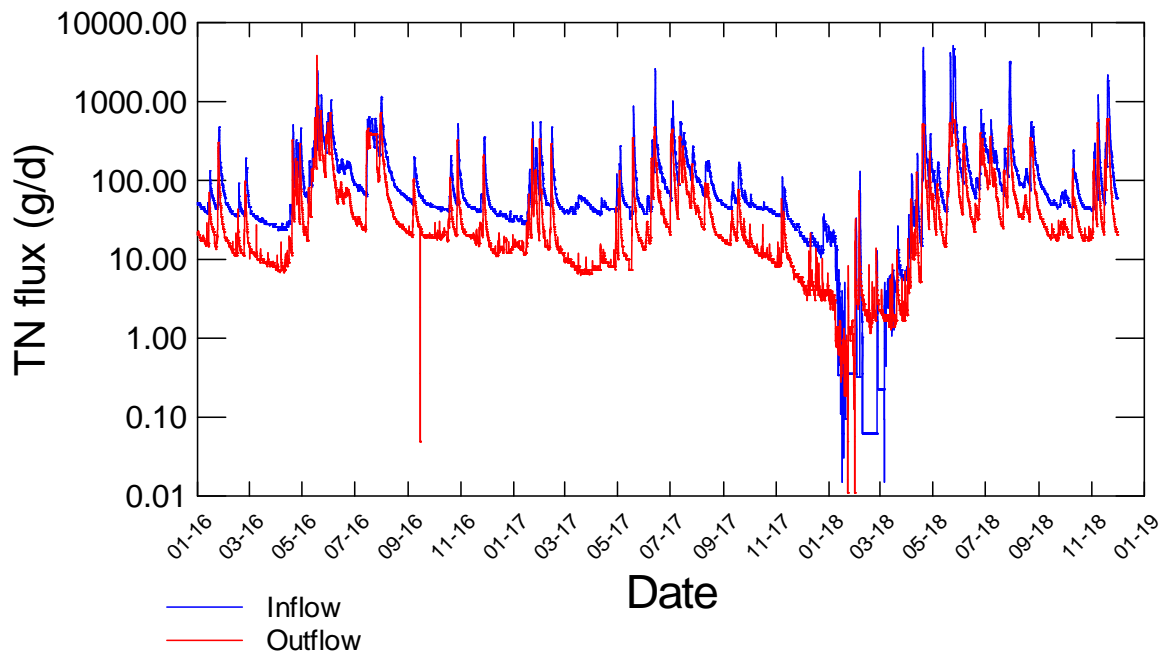


Figure 7-21: Comparison of woodchip filter inflow and outflow TN flux estimated using bootstrap regression models.

Treatment performance is summarised in Figure J-17 and Figure J-18 as mass removed per day and proportion of inflow removed per day. These data indicate that TN removal performance is variable, subject to input load and retention time in the same manner as nitrate-N removal. Selected performance data are summarised in Table 7-4. Additional performance data are summarised in Table J-6.

Table 7-4: Woodchip filter performance in terms of TN removal and removal efficacy. Concentration and flux estimates were made using an AMLE regression model.

Statistic (Three-year assessment period)	AMLE predicted conc. (mg/L)		Predicted flux (g/d)		Mass removal (g/d)	Efficacy (%)
	Inflow	Outflow	Inflow	Outflow		
N of Cases	23328	23328	23328	23328	23328	23328
Minimum	0.0	0.7	2.2	1.3	0.0	0.0
Maximum	2031.2	8.3	8486.2	3064.0	6764.1	97.8
Median	0.2	1.1	56.1	24.0	32.1	54.4
Arithmetic Mean	6.5	1.3	140.8	72.2	68.6	54.1
Std Error of Mean	0.5	0.0	2.9	1.1	2.0	0.1
95.0% LCL of Mean	5.6	1.3	135.1	70.0	64.6	53.9
95.0% UCL of Mean	7.4	1.3	146.5	74.3	72.6	54.3
Std Deviation	70.0	0.8	440.5	166.5	310.5	15.5
Cleveland percentiles						
0.01	0.0	0.7	4.7	3.6	0.9	6.1
0.05	0.0	0.7	15.6	5.0	9.4	21.8
0.1	0.0	0.7	25.8	7.5	14.5	34.7
0.2	0.1	0.8	34.1	10.8	21.3	46.1
0.25	0.1	0.8	37.3	12.0	23.3	48.1
0.3	0.1	0.9	39.4	14.0	25.1	49.5
0.4	0.1	1.0	45.9	18.9	28.3	52.0
0.5	0.2	1.1	56.1	24.0	32.1	54.4
0.6	0.2	1.2	69.8	32.1	38.6	57.3
0.7	0.4	1.4	97.0	44.9	49.1	60.2
0.75	0.7	1.5	117.6	56.0	56.9	63.3
0.8	1.0	1.6	145.8	72.3	66.9	66.8
0.9	2.8	2.1	252.6	155.7	85.7	73.3
0.95	6.4	2.8	396.9	301.2	101.9	76.5
0.99	71.1	4.5	1517.4	942.4	429.8	84.5

Table J-6 indicates that overall TN removal for the three-year assessment period was approximately 33% (inflow flux reduced from approximately 150 g/d to approximately 100 g/d). The mean removal rate shown in Table 7-4 is slightly larger, but it excludes values less than 0.1 g/d (approximately 2,200 values).

The bulk of the influent TN is nitrate-N – the performance characteristics for TN mirror those estimated for nitrate-N closely – median nitrate-N removal rate (Table 7-3) was approximately 33 g/d, and that is close to that estimated for TN over the entire assessment period (32 g/d).

7.5 Effect of water level adjustment on woodchip filter

As indicated in Section 4, NIWA was directed to lower the water table by approximately 500 mm, with an expectation that this would allow the bed to fill and more gradually empty, thereby lengthening retention times.

Figure 4-1 and Figure 4-2 both suggest that the longer retention times anticipated were not realised. Peak inflows were buffered to some extent (the magnitude of the outflow was lower, but conversion of the flashy inflow to a gradual outflow does not appear to have been achieved. The tails (extreme high or low flows) are less obvious in the outflow data in, but these appear to not have been translated into longer-term changes in the flow duration for the outflow.

The observed inflow attenuation (viz., difference between peak inflow and outflow) depends on the nature of the woodchip matrix. The woodchip selected for the bed was screened and of uniform size. Within three years of establishment, the characteristics of the bed are unlikely to have changed, and would comprise a substantial proportion of rigid, largely impermeable woodchip, plus pore or void space. The material would be free draining. Consequently, a rainfall event generating inflow would most likely cause the following series of events, leading to one of two outcomes.

Outcome 1 - assuming:

- the inflow was uniformly distributed across the bed
- the bed material was relatively uniform
- the horizontal dispersion of water was to some extent hindered by the bed material
- a temporary mound of water would be created along the inlet distribution manifold.

As a result, the mound of water would gradually propagate across the bed, with the rate and extent of travel determined by the inflow rate, the head difference between the inflow and outflow, and the available volume within the bed. These factors would determine how the inflow would gradually raise the water level across the bed until a new level was formed. The water would subsequently drain from the bed over a long period of time giving a lower peak outflow than the flashy inflow.

Outcome 2 – assuming

- the inflow was uniformly distributed across the bed
- the bed material was relatively uniform
- the horizontal dispersion of water hindered very little by the bed material

- mounding of water at the inflow (or anywhere else in the bed) would be minimal and transient.

Given these circumstances, the increased inflow would travel through the bed of the filter, raising the level appreciably only if some factor restricted drainage from the outflow. If there was no restriction in the outflow, the bed level would hardly change and there would be very little additional retention of water in the bed.

Results for two rainfall events are shown in Figure 7-22. The event was too small to cause a substantial change in water level – although there is some indication of a small increase in water level at the inlet well at the time of the event, extending over the following week, and in the outflow well approximately one week after the event, extending over the following week. These changes appear to be within the error of measurement and daily fluctuation in water level (hourly average data are plotted in Appendix G). For an event of this size, the lowering the water level (viz decreasing bed depth) did not result in measurable flow attenuation (viz., inflow and outflow were similar). This indicates that lowering the water level provided no additional storage and did not produce a measurable increase in retention time.

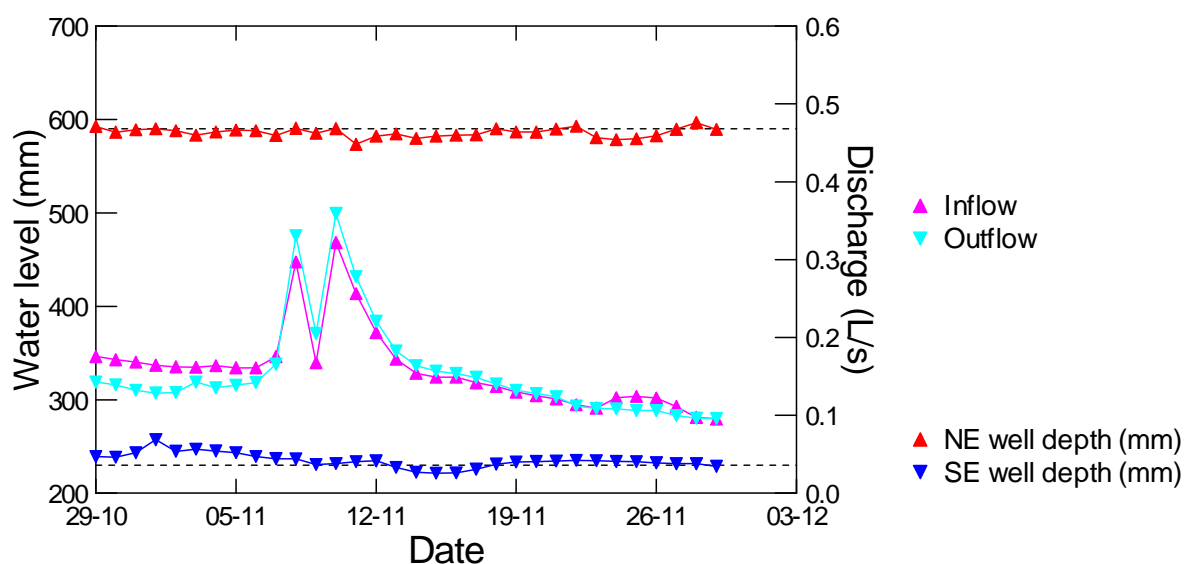


Figure 7-22: Time-series of daily average inflows and outflows, and water levels in the woodchip filter, recorded in the NE (inlet) SE (outlet) corner of the bed. Results for two closely spaced minor inflow events during November 2017 are shown. These are daily average flows derived from five-minute data. The broken horizontal lines are for visual reference purposes.

Section 7.3.3 described the effect of retention time on treatment efficacy, where it was shown that nitrate-N removal efficacy is positively related to retention time. This suggests that unless the drainage water arising from larger events is retained in the system for additional time, the additional storage capacity is likely to be unused, or will be used inefficiently. These findings suggest that additional infrastructure is required to maintain the water in the bed for an extended period. This could be achieved relatively simply by including an orifice plate in the outlet structure. During periods of low flow, the orifice plate would be oversized for the inflow, and water entering the system would leave the system unhindered, analogous to the current situation. During the larger events, however, the orifice plate would restrict the discharge rate to a value substantially smaller than the peak inflow. This would allow the filter bed to fill to a predetermined maximum depth. A

weir structure could be included in the outflow, which would allow discharge greater than the orifice plate capacity to leave the filter bed unhindered (and relatively untreated). This discharge via the weir would only occur once the storage depth defined by the weir was exceeded. This would be similar to operation of the filter bed prior to May 2017. During and after peak inflow conditions, the excess water stored in the bed would continue to slowly drain via the orifice plate. The inflow data derived from this project could be used to size the plate to provide a suitable retention time. This would allow the treatment efficacy to be optimised.

Caution is required before adopting this approach. Periodic wetting and drying of the woodchip material could have undesirable effects on filter performance arising from an increase in the rate of degradation of the woodchip material (Rivas et al. 2019). Aerobic conditions encourage “aerobic composting”, a combination of hydrolysis, aerobic microbially-mediated decomposition, assisted by fungi and moulds. Fungi and actinomycetes are the most active organisms in low-temperature composting. In the woodchip filter, temperatures were always close to ambient, favouring colonisation of the woodchip by fungi and actinomycetes. These organisms play an important role in the decomposition of cellulose, lignins and more resistant plant materials – these dominate in wood chip.⁷ Periodic wetting and drying is therefore likely to encourage degradation of the woodchip, generation of fine material more likely to cause clogging of the filter medium, and generally shorten the life of the woodchip filter.

The periodic inundation of the woodchip is unlikely to benefit the denitrifying performance of the bacteria that undertake most of the denitrification. Although they are not strict anaerobes, in the presence of oxygen the genes encoding denitrifying enzymes are repressed. In addition, nitrous oxide reductase is sensitive to the presence of molecular oxygen, which causes inactivation of the enzyme (Lu et al. 2014; Ward 2015). In addition to slowing denitrification, periodic wetting and drying is likely to increase production of nitrous oxide (N₂O) over N₂, which is a very undesirable outcome. N₂O is a potent greenhouse gas.

Denitrifying organisms are also relatively slow-growing. Although they have been associated with bulk liquid in wastewater treatment plant, they tend to dominate biofilms (Lu et al. 2014). It is therefore likely that maintaining a relatively stable water level will provide the largest possible surface area for an attached microbial population, which will favour high denitrification rates.

⁷ E.g., <https://web.extension.illinois.edu/homecompost/science.cfm> and <https://aggie-horticulture.tamu.edu/earthkind/landscape/dont-bag-it/chapter-1-the-decomposition-process/>

8 Treatment performance – opportunities for optimisation

From the assessment of performance data, several factors have been identified that determine or influence nitrate-N removal performance, including:

1. The concentration of nitrate-N in the inflow.
2. The availability of organic carbon.
3. Retention time within the biofilter.
4. Temperature.

There is little opportunity to influence 1) and 4). Opportunity does exist to influence 2) and 3), and these factors are in some way inter-related. In the woodchip filter, the release of organic carbon is likely to be diffusion-related, as materials are gradually released from the woodchip matrix into the surrounding liquid. When the water level was maintained at approximately 700 mm depth, most of the filter bed was covered with water, and the upper layer was likely to have been very damp. As the water level was lowered, an increasing proportion of the bed was not covered with water. This could have several consequences:

- A. Wood chip not constantly exposed to liquid is unlikely to release organic material following transient exposure – overall, this would reduce the amount of organic carbon available, particularly in those periods when the influent nitrate-N load is elevated (the autumn-winter period). This is likely to reduce overall performance, but particularly impair removal during the peak inflow events. Although insufficient data exists to prove that organic carbon supply may be limiting denitrification at times, the concentrations of DOC in the outflow were lower in the winter period.
- B. The denitrifying organisms are likely to be attached to the bed matrix, as opposed to floating freely in the liquid surrounding the matrix. These organisms are unlikely to thrive on damp woodchip, because the supply of nutrient would be limiting, and it is possible that the void space surrounding damp woodchip may be aerobic – neither of these circumstances would favour the denitrifiers. Reducing the bed liquid level would therefore limit the volume (and surface area) of woodchip available to a viable population of denitrifying bacteria, and this in turn is likely to reduce the performance of the filter bed.
- C. Periodic inundation of the woodchip may accelerate degradation of the bed material – information presented recently (Rivas et al. 2019) suggested that the bed life may be substantially decreased by failing to maintain sufficient water level to keep the bed matrix covered.

Maintaining a higher water level in the bed would therefore probably:

- increase the working life of the bed material by limiting aerobic decomposition
- improve the delivery of organic carbon from woodchip to the surrounding liquid
- create a larger volume of woodchip bed that favours denitrifying organisms, and

- the larger volume (and surface area) of woodchip material would maximise the population of denitrifying organisms, which would increase treatment performance.

Although treatment performance in winter high-flow conditions is greater than in summer, this is largely a function of the influent mass of nitrate-N. It would be desirable to increase treatment efficacy by improving bed retention time. Inclusion of additional control in the outflow structure has been discussed. Previously it was suggested that a storage tank be installed at the inlet of the filter bed, to prevent high flows through the woodchip filter, but to retain drainage for subsequent treatment. A small solar-powered pump could be used for this purpose. Ninety percent of the flow is less than 1 L/s, so a modest (say 50 m³ structure) would provide temporary storage for much of the peak flow. Were this buffer pond equipped with a bypass as well, flows that exceeded the immediately available storage could be directed around the filter bed to the outlet structure. This would minimise the potential to flush organic carbon or denitrifying bacteria from the filter bed, while maintaining a less variable flow through the filter bed generally.

The data derived from this project (including the process model) could be used to refine the design of these mitigation devices.

9 Summary

The efficacy of a woodchip denitrification filter was assessed over a three-year period. The performance was similar to that reported in the earlier assessment summary but is likely to better represent performance because of improvements made to the estimation techniques. The results of the assessment are summarised in Table 9-1.

Table 9-1: Summary of median measured and predicted concentrations and performance metrics.

Negative values indicate net increase in concentration between inflow and outflow. N/A indicates value not calculated.

Nitrogen form	Estimation method	Median concentration (mg/L)		Mass removal (g/d)	Specific removal (g/m ³ /d)	Efficacy (%)
		Inflow	Outflow			
Ammoniacal-N	Model	0.02	0.125	-2.0	N/A	-314
	Grab	0.019	0.078	N/A	N/A	N/A
Nitrate-N	Model	2.3	0.7	32.7	0.9	72
	Grab	2.2	0.78	N/A	N/A	N/A
Total N	Model	2.41	1.094	32.1	N/A	54.4
	Grab	2.45	1.12	N/A	N/A	N/A

Previously, regression-based models (viz., flow v concentration regressions fitted to grab samples) were used to estimate the flux of material flowing into and out of the woodchip filter. Several inflow models were shown to adequately estimate inflow loads of ammoniacal-N, nitrate-N and total N. Using the same approaches, the outflow loads of ammoniacal-N and total N were estimated tolerably well. In the case of ammoniacal-N, the relatively small mass outflows (typically in a range from 1-2 g/d) made accurate estimation less critical – it was found that although the woodchip filter was a net source of ammoniacal-N, the loads generated in the filter bed were not likely to have measurable effect on the receiving stream (Waituna Creek).

In the case of total nitrogen, the regression model approach provided credible estimates of outflow flux except during periods of low outflow, when the models predicted higher fluxes than those measured using grab samples. Using flux estimates derived from regression models is therefore conservative – the actual mass loads leaving the woodchip filter are likely to be smaller than those predicted. Removal of TN was variable over time, determined principally by influent load and retention time, and temperature. Over the full trial period, approximately 33% of the TN was removed, reducing the influent flux from approximately 150 g/d to 100 g/d.

Determination of nitrate-N treatment performance was more difficult than for ammoniacal-N or TN. None of the regression model approaches trialled provided acceptable estimates of outflow nitrate-N concentrations or flux, particularly under low-flow conditions. The likely reason is time variable removal by denitrification. Denitrification is a microbially mediated process, and the rate of reaction is determined by inflow nitrate-N concentrations as well as organic carbon supply, temperature and retention time. All the regression model approaches (which were based on correlations between concentration and flow) under-predicted nitrate removal performance. A process-based model was developed that allowed outflow nitrate-N concentration and flux to be predicted from influent nitrate-N concentrations, temperature, retention time and organic carbon supply. The process-based model predicted outflow concentrations and fluxes significantly better than the regression

models. Using results from the process-based model, mean and median nitrate-N removal rates were estimated to be 75 g/d and 33 g/d respectively, and mean and median removal efficacy over the entire period 65% and 70% respectively (calculated as the proportion of influent load removed). Although the removal efficacy was lower in winter than summer, the mass of material removed was greater in the winter or high flow conditions – this reflected the larger mass of nitrate-N in the inflow during these periods.

Treatment efficacy is influenced strongly by retention time – greater time allows the fixed microbial biomass to utilise the influent nitrate-N load. This is evident from Figure 9-1, where the effect of lowering the level of water twice during 2017 is evident. Reducing the bed water depth reduces the effective treatment volume – the volume of wood chip colonised by denitrifying bacteria. This gives rise to two outcomes:

- the nitrate-N removal rate expressed in g/d decreases as bed depth decreases, and
- the treatment efficiency expressed as g/m³/d also decreases.

Reducing the bed depth increases potential storage, but does not increase active bed volume, treatment capacity or efficiency – the population of denitrifying bacteria in the ‘dry’ part of the filter (which only fills when inflows are high) is not able to increase quickly enough to utilise the additional nitrate-N load. Reducing the bed depth therefore increases the cost of treatment – much of the capacity is un- or underutilised much of the time. Reducing the bed depth when the wood chip medium has high permeability reduces the retention time which also acts to reduce nitrate-N removal.

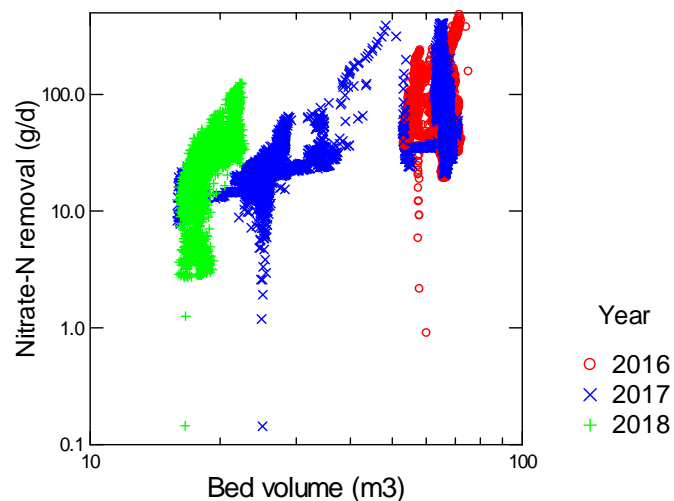


Figure 9-1: Relationship between nitrate-N removal rate and active bed volume by year. The active bed volume is the volume of bed submerged in water, as opposed to the total volume of woodchips.

The performance of the woodchip filter is similar to published nitrate-N removal rates – several are provided in Table 9-2.

Table 9-2: Comparison of measured nitrate-N removal with other published performance data.

Indicative nitrate-N removal rates (g/m ³ /d)	Factor dominating treatment efficacy or performance	Reference
5 - 10	Nitrate-N load	Schipper et al. (2010)
16 – 6.4	Filter medium age	Robertson (2010)
6.4	Nitrate-N non-limiting	Woli et al. (2010)
23 – 44	Degradable carbon (medium age), ambient temperature	David et al. (2016)
1.2 - 11		
7.6	Not identified	Warnecke et al. (2011)
0.38 – 1.06	Ambient temperature, hydraulic load	Christianson et al. (2013)
0 – 72	Ambient temperature	Hassanpour et al. (2017)
0.7 – 22	Not identified	Halaburka et al. ((2017))
~2.0 (0.5 – 2.8)	Hydraulic load, ambient temperature, water level, influent load	This study

During the second assessment period, several additional water quality variables and novel measurement techniques were investigated to determine their usefulness for treatment assessment purposes. We demonstrated that:

- Loads of suspended sediment in the inflow were generally low, and indicated that clogging of the woodchip filter was unlikely.
- Electrical conductivity was related to inflow and outflow nitrate-N flux, but unsuitable as a surrogate for predicting nitrate flux.
- The inflow was generally anoxic, and the small mass of oxygen introduced during inflow events was unlikely to impair denitrification. The outflow was always anoxic.
- Dissolved organic carbon concentrations in the inflow and outflow were reasonably constant and appeared to meet denitrification requirements at all times.
- The TriOS continuous hyperspectral analyser provided very robust nitrate concentration data at five-minute frequency. It was not measurably influenced by the changes in dissolved organics in the inflow or outflow. It has great potential to provide inflow and outflow flux data more efficiently than through traditional grab sampling techniques. These devices provide data in near-real time, thereby reducing the potential to lose key data. They are well-suited for moderate duration deployments (weeks to months), creating the potential to provide very detailed flow-treatment efficacy information.

The data and information that has been derived from this assessment will allow the design and operation of future woodchip denitrification filters to be further refined and optimised.

10 Acknowledgements

We acknowledge the following:

- Roger Hodson from Environment Southland for water quality data.
- Kathy Walters (NIWA Christchurch) for provision of climate data.
- John Scandrett, Evan Sanderson and Quenton Scandrett for carefully managing the collection and dispatch of water quality samples, as well as assisting in many other ways.
- Stephan Heubeck and George Payne for preparing equipment for the Spectra::lyser deployment.
- Eike Breitbarth or REZO (Dunedin) for making the TriOS sensors available for the second deployment period.
- The NIWA Dunedin field team for ongoing support.
- Mr Ewen Pirie for allowing the trial to take place on his property.
- NIWA (through SSIF grant FWWQ1909) and MBIE for funding deployment and use of the nitrate sensors.
- DairyNZ for funding the bulk of the project.

11 Glossary of abbreviations and terms

Anaerobic	In wastewater treatment, the term anaerobic is used to indicate the absence of any common electron acceptor such as nitrate, sulfate or oxygen.
Anoxic	In wastewater treatment, the absence of oxygen alone is termed anoxic.
Effectiveness	To be effective is when results accomplish their purposes, thus giving an effective outcome.
Efficacy	<p>the power or capacity to produce a desired effect.</p> <p>To be efficacious involves possession of a quality that gives the produced results the potential to lead to an effective outcome.</p> <p>Efficacy has to do with the ability or capacity to do something, but not about how something is done.</p> <p>Efficacy may be expressed as the difference between inflow and outflow mass load, or flux.</p> <p>Efficacy may also be expressed in terms of mass removed/volume of treatment material/unit of time, e.g., “g N/m³/day”.</p>
Efficiency	<p>Efficiency is the quality or property of being efficient.</p> <p>To be efficient is to produce an output in a competent and qualified way.</p> <p>Efficient means acting or producing with a minimum or waste, expense, or unnecessary effort.</p>
Flux	<p>This is the product of concentration and discharge or flow. It is reported as mass/unit of time, and may be expressed as g/s, g/d or any other suitable equivalent unit.</p> <p>These units are interchangeable (with unit conversion).</p>
Load	This is the product of concentration and discharge or flow integrated over a period of interest. It has units of mass, but the period of time over which the flux is integrated must be specified. For example, if the flux is integrated over a day, the load is reported as g/d or similar.
Yield	This is the mass load derived per unit area of land. Yield is often expressed as kg/ha/year or similar.

12 References

- Appelboom, T.W., Chescheir, G.M., Birgand, F., Skaggs, R.W., Gilliam, J.W., Amatya, D. (2010) Temperature coefficient for modeling denitrification In surface water sediments using The mass transfer coefficient *American Society of Agricultural and Biological Engineers*, 53(2): 465-474.
- Arenas Amado, A., Schilling, K.E., Jones, C.S., Thomas, N., Weber, L.J. (2017) Estimation of tile drainage contribution to streamflow and nutrient loads at the watershed scale based on continuously monitored data. *Environmental Monitoring and Assessment*, 189(9): 426. 10.1007/s10661-017-6139-4.
- Ballantine, D.J., Tanner, C.C. (2010) Substrate and filter materials to enhance phosphorus removal in constructed wetlands treating diffuse farm runoff: a review. *New Zealand Journal of Agricultural Research*, 53(1): 71-95. DOI: 10.1080/00288231003685843.
- Birgand, F. (2000) Quantification and Modeling of In-Stream Processes in Agricultural Canals of the Lower Coastal Plain. *Biological and Agricultural Engineering*. North Carolina State University: 469.
- Burkitt, L.L., Jordan, P., Singh, R., Elwan, A. (2017) High resolution monitoring of nitrate in agricultural catchments - a case study on the Manawatu River, New Zealand. *EnviroLink report prepared for Horizons Regional Council*. Report No. pp.
- Christianson, L. (2011) Woodchip Bioreactors for Nitrate in Agricultural Drainage. Report No. PMR 1008: 4.
- Christianson, L.E., Bhandari, A., Helmers, M.J. (2012a) A practice-oriented review of woodchip bioreactors for subsurface agricultural drainage. *Applied Engineering in Agriculture*, 28(6): 861.
- Christianson, L.E., Bhandari, A., Helmers, M.J., Kult, K.J., Sutphin, T., Wolf, R. (2012b) Performance evaluation of four field-scale agricultural drainage denitrification bioreactors in Iowa. *Transactions of the ASABE*, 55(6): 2163.
- Christianson, L.E., J. Frankenberger, C. Hay, M.J. Helmers, G. Sands (2016) Ten Ways to Reduce Nitrogen Loads from Drained Cropland in the Midwest. Report No. Pub. C1400: 46.
- Heinen, M. (2006) Simplified denitrification models: Overview and properties. *Geoderma*, 133: 444-463.
- Hudson, N., Baddock, E. (2019) Review of high frequency water quality data. Advice regarding collection, management and use of nitrate-nitrogen data. Draft NIWA client report prepared for Environment Southland, Otago Regional Council and Environment Canterbury as deliverable for MBIE-funded projects ELF18203 and FWWQ1909. Report No. 184 pp.

- Hudson, N., McKergow, L., Baddock, E., Scandrett, J., Burger, D. (2017) Waituna catchment - evaluation of nutrient mitigation options: Nitrogen and Phosphorus filters. Prepared for DairyNZ, Living Water - Department of Conservation - Fonterra Partnership Report No. 2017184HN: 66.
- Hudson, N., McKergow, L., Tanner, C., Baddock, E., Burger, D., Scandrett, J. (2018) Results from a 15-month trial of a woodchip denitrification filter, Waituna Lagoon catchment, Southland. *New Zealand Land Treatment Collective Annual Conference: Benefits and risks*, Rotorua Energy Events Centre, Rotorua, New Zealand.
- Kelly, C.A., Rudd, J.W.M., Hesslein, R.H., Schindler, D.W., Dillon, P.J., Driscoll, C.T., Gherini, S.A., Hecky, R.E. (1987) Prediction of biological acid neutralization in acid-sensitive lakes. *Biogeochemistry*, 3(1): 129-140. 10.1007/bf02185189.
- Lu, H., Chandran, K., Stensel, D. (2014) Microbial ecology of denitrification in biological wastewater treatment. *Water Research*, 64: 237-254. <https://doi.org/10.1016/j.watres.2014.06.042>.
- Maalim, F.K., Melesse, A.M. (2013) Modelling the impacts of subsurface drainage on surface runoff and sediment yield in the Le Sueur Watershed, Minnesota, USA. *Hydrological Sciences Journal*, 58(3): 570-586. 10.1080/02626667.2013.774088.
- May, D., Hodson, R., Elliotte, D., Rissman, C. (2015) Real-time optical nitrate and DOC monitoring in a lowland gravel bed river (poster). *New Zealand Freshwater Sciences Society Conference*, Silverstream, Lower Hutt.
- McKergow, L., Tanner, C., Baddock, E., Pattinson, P., Scandrett, J. (2015) The 'Nitrate Catcher' design and installation of a bioreactor to monitor nitrate-N removal from drainage water. *NIWA Client Report*. Report No. HAM2015-044: 26.
- McKergow, L., Tanner, C., Hickey, C., Payne, G., Baddock, E., de Lima, S., Burger, D., Scandrett, J. (2016) The phosphorus filter: Design and installation of a phosphorus filter for tile drainage water. NIWA client report prepared for DairyNZ and the Living Water DoC-Fonterra Partnership. Report No.: 21.
- McKergow, L.A., Tanner, C., Monaghan, R., Anderson, G.C. (2008) Stocktake of diffuse pollution attenuation tools for New Zealand pastoral farming systems. *NIWA Client Report* HAM2007-161. Report No. pp.
- Miller, M.P., Tesoriero, A.J., Capel, P.D., Pellerin, B.A., Hyer, K.E., Burns, D.A. (2016) Quantifying watershed-scale groundwater loading and in-stream fate of nitrate using high-frequency water quality data. *Water Resources Research*, 52(1): 330-347. doi:10.1002/2015WR017753.
- Neitsch, S.L., Arnold, J.G., Kiniry, J.R., Williams, J.R. (2011) Soil and Water Assessment Tool - Theoretical Documentation, v2009. Report No. TR-406: 647.
- Pellerin, B.A., Bergamaschi, B.A., Gilliom, R.J., Crawford, C.G., Saraceno, J., Frederick, C.P., Downing, B.D., Murphy, J.C. (2014) Mississippi River nitrate loads from high frequency sensor measurements and regression-based load estimation. *Environmental Science & Technology*, 48(21): 12612-12619. 10.1021/es504029c.

- Pons, M.-N., Assaad, A., Oucacha, C., Pontvianne, S., Pollier, B., Wagner, P., Legout, A., Guérol, F. (2017) Nitrates monitoring by UV–vis spectral analysis. *Ecohydrology & Hydrobiology*, 17(1): 46-52. <https://doi.org/10.1016/j.ecohyd.2016.12.001>.
- Rivas, A., Barkle, G., Moorhead, B., Clague, J., Stenger, R. (2019) Nitrate removal efficiency and secondary effects of a woodchip bioreactor for the treatment of agricultural drainage. *Nutrient Loss Mitigations for Compliance in Agriculture, 32nd Annual FLRC Workshop*, Massey University, Palmerston North, February 2019.
- Runkel, R.L., Crawford, C.G., Cohn, T.A. (2004) Load Estimator (LOADEST): A FORTRAN Program for Estimating Constituent Loads in Streams and Rivers: U.S. Geological Survey Techniques and Methods Book 4, Chapter A5. Report No.: 69.
- Schipper, L., Vojvodic-Vukovic, M. (1998) Nitrate removal from groundwater using a denitrification wall amended with sawdust: Field trial. *Journal of Environmental Quality*, 27(3): 664-668.
- Schipper, L.A., Robertson, W.D., Gold, A.J., Jaynes, D.B., Cameron, S.C. (2010) Denitrifying bioreactors--An approach for reducing nitrate loads to receiving waters. *Ecological Engineering*, 36(11): 1532-1543. DOI: 10.1016/j.ecoleng.2010.04.008.
- Schwab, M.P., Klaus, J., Pfister, L., Weiler, M. (2017) How runoff components affect the export of DOC and nitrate: a long-term and high-frequency analysis. *Hydrology and Earth System Sciences Discussions*: 1-21. 10.5194/hess-2017-416.
- Šlmeč, M., Cooper, J.E. (2002) The influence of soil pH on denitrification: progress towards the understanding of this interaction over the last 50 years. *European Journal of Soil Science*, 53(3): 345-354. doi:10.1046/j.1365-2389.2002.00461.x.
- Sukias, J.P.S., Tanner, C.C., McKergow, L.A. (2005) Management of Dairy Farm Drainage Pollution-2005. *NIWA Client Report HAM2005-102 for Dairy Insight*. Report No. pp.
- Sukias, J.P.S., Tanner, C.C., McKergow, L.A. (2006) Dairy farm drainage nitrate attenuation wetlands and filters. *19th Annual Fertilizer and Lime Research Centre Workshop: Implementing Sustainable Nutrient Management Strategies in Agriculture*, Palmerston North, NZ, 8-9 February 2006.
- Tan, J., Cherkauer, K.A., Chaubey, I. (2015) Using hyperspectral data to quantify water-quality parameters in the Wabash River and its tributaries, Indiana. *International Journal of Remote Sensing*, 36(21): 5466-5484. 10.1080/01431161.2015.1101654.
- Tanner, C., Hughes, A., Sukias, J. (2013) Assessment of potential constructed wetland sites within the Waituna Lagoon catchment. *NIWA Client Report*. Report No. HAM2013-071: 70.
- Villeneuve, J. (2017) Water Quality Considerations for Surface and Subsurface Agricultural Drainage. Water Quality Section, Alberta Agriculture and Forestry.
- Ward, B. (2015) *Molecular Medical Microbiology*.

Appendix A Instrumentation deployed at nitrate-N woodchip filter

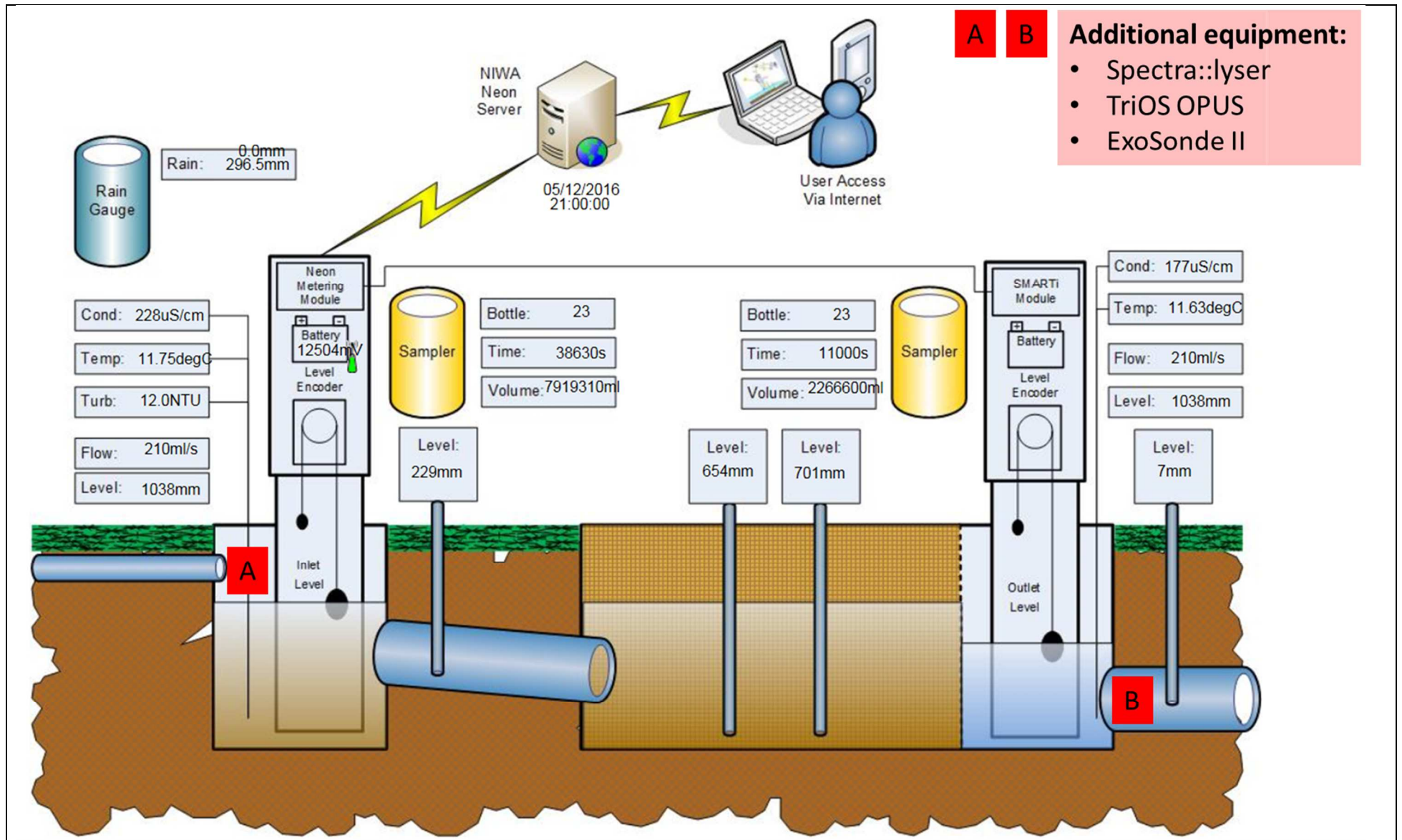


Figure A-1: Schematic from NEON logger schema indicating location and type of measurement equipment. A and B indicate location and type of additional equipment.

Appendix B Hyperspectral measurement devices

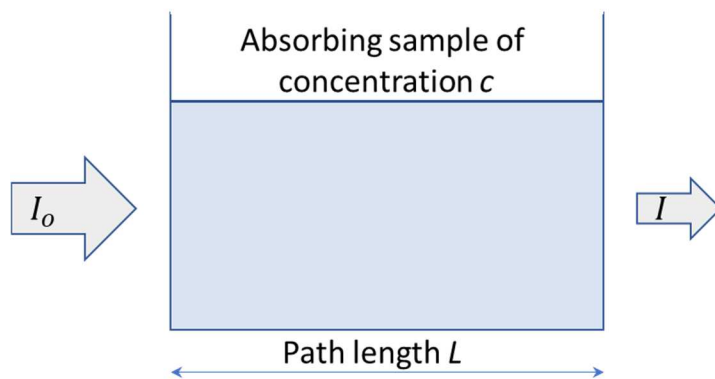
The measurement principle

The measurement principle of these instruments is based on the Beer-Lambert Law, which describes the relationship between light absorbance and the concentration of an absorbing species. The general Beer-Lambert law is usually written as:

$$A = \varepsilon(\lambda) \times L \times c$$

where A is the measured absorbance, $\varepsilon(\lambda)$ is a wavelength-dependent absorptivity coefficient, L is the path length, and c is the analyte concentration.

Consider a solution receiving a beam of light:



where I_0 is the **initial light intensity** and I is the **light intensity** after it passes through the sample.

Measurements are usually made in terms of **transmittance (T)**, which is defined as:

$$T = \frac{I}{I_0}$$

The relationship between A and T is:

$$A = -\log T = -\log \frac{I}{I_0}$$

The concentration of an absorbing substance may be obtained by rearranging the previous equations:

$$c = \frac{A_\lambda}{\varepsilon_\lambda \times L}$$

Where c is the concentration of absorbing material, A_λ is the absorbance at a specific wavelength (λ), ε_λ is a constant (the molar absorptivity of the absorbing substance at a specific wavelength λ), and L is the path length. The unknown concentration of a substance of interest can be determined using a working curve that defines the relationship between absorbance and concentration, derived from a series of standards of known concentration.

- If no substances in the solution absorb light of the wavelength of interest, I_0 and I will be equal, absorbance will be 0 absorbance units and transmittance will be 100% (i.e., the concentration of the analyte will be zero).

- Varying amounts of the material of interest in the sample will create solutions that absorb the incident light to smaller or greater extent, and this absorbance may be related to concentration.
- If high concentrations of other substances that absorb light at the same wavelength occur in solution (interferents), absorbance will be significant, and transmittance will be less than 100%, In which case concentrations of analyte would be overestimated.
- If a substantial amount of particulate or suspended material is in solution, considerable light scattering and attenuation of the incident light intensity may occur. Absorbance may still be low, but transmittance may be reduced substantially, also potentially causing over-estimation of analyte concentration.

The latter two points present challenges to the use of absorbance measurement of any material – there is no guarantee that the absorbance is entirely due to analyte, and any suspensoid will reduce or attenuate the light intensity. Both of these factors must be accounted for when quantifying an analyte, including nitrate-N.

At user-selectable frequency (maximum measurement frequency is generally around two minutes), the instruments record absorbance spectra over a wavelength range. The width of this range and the spectral resolution varies according to the instrument manufacturer, the measurement capability and the specificity of measurement. The Spectra:lyser instrument measures from 190 nm to 750 nm, covering the ultraviolet, visible and near-infrared spectrum. This 560 nm wide spectrum is resolved into 256 wavelength slices of approximately 2.2 nm bandwidth. Each wavelength slice effectively represents a discrete signal. The TriOS instrument measures from 190 nm to 350 nm, but at finer resolution (approximately 0.9 nm bandwidth).

In operation, proprietary software performs a “data mining” operation, and uses the relative intensity of several spectral bands and a specially developed algorithm to calculate the nitrate-N concentration. The algorithm compensates for possible interferences (the principal ones being dissolved organic matter and suspended sediment) – after compensation, the resulting value is reported as an equivalent nitrate-N concentration. Other water quality variables may also be measured in this manner, including turbidity and dissolved organic matter. All calculated values are reported as equivalent concentrations or values.

It is essential that grab samples of the water being measured are collected periodically and submitted to the laboratory for conventional water quality analysis – this allows the results reported by the hyperspectral device to be verified. If necessary, post-processing may be applied to the data using the raw spectral data to adjust the record so that it better represents the measured water quality. This process is similar to corrections applied to other continuous data, such as pH and dissolved oxygen.

The instrument selected for deployment should be matched to the typical water quality. If low concentrations are anticipated, a longer pathlength is desirable to improve sensitivity, but this will need to be balanced against the amount of dissolved organic matter or suspended sediment. The latter will attenuate the light, and there may be insufficient light to measure the compound of interest (in this case nitrate-N). In this circumstance, it may be necessary to use an instrument with a shorter pathlength – a compromise between high sensitivity and ability to measure nitrate-N at all may have to be achieved. Instrument manufacturers have anticipated this compromise by providing instruments with varying path lengths.

Issues associated with use of the Spectra::lyser device

During the autumn of the third year of operation, two Spectra::lyser® hyperspectral water quality analysers were shipped to the woodchip filter site. The objective was to measure nitrate concentrations in the inflow and outflow every xxx minutes in order to quantify short-term variations in nitrate concentration and better estimation of removal. Considerable ancillary equipment was required to make these instruments (intended primarily for laboratory operation) capable of deployment in the field. This included solar panel arrays, high capacity 12 v batteries and associated electrical supply and control equipment. Remote operation of the Spectra::lyser is a complex operation, requiring flawless operation of several electronic components.

Shortly after powering up the instrument and peripheral devices, the miniature computer that controlled the Spectra::lyser deployed at the inlet site malfunctioned and became completely inoperable. No measurement of water quality was possible at this site using this equipment. The device deployed at the outlet site operated successfully, and recorded data until approximately midnight on the first day of operation. At this time, the software and computer attempted to connect to the internet via cellphone communication equipment. The cellphone signal was known to be weak prior to deployment, but proved inadequate for the instrument software to check the time and transfer data. After several attempts, the instrument went into standby mode, and no additional data were captured. It proved impossible to acquire a similar miniature computer to repair the device deployed at the inlet sites, and it was necessary to conclude that the available equipment was not suited for real-time measurement in rural Southland. Further measurement with Spectra::lyser devices was not possible.

Appendix C Derivation of a process-based denitrification model

Following a critical review of 50 soil denitrification models, Heinen (2006) generalised these models in the form indicated in Equation C-1:

$$D_a = \alpha \int N \int S \int T \int pH \quad \text{Equation C-1}$$

Where

D_a = actual denitrification rate

α = a parameter used to account for (as required) organic carbon and depth of the denitrifying medium etc., and

$\int N \int S \int T \int pH$ = dimensionless reduction functions related to nitrate-N concentration, soil moisture content, soil temperature and pH respectively.

Actual denitrification has a range of units, determined by the application of the model to a point, layer or loss of nitrate-N from soil solution.

The Theoretical Documentation for the SWAT model describes bacterial reduction of nitrate-N in soils as a function of water content, temperature, the presence of a carbon source and nitrate (p195, Neitsch et al. 2011), which is described using Equation C-2:

$$N_{denit,ly} = NO_{3ly} \cdot (1 - \exp[-\beta_{denit} \cdot \gamma_{tmp,ly} \cdot orgC_{ly}]) \quad \text{Equation C-2}$$

where:

$N_{denit,ly}$ is the amount of nitrogen lost to denitrification (kg N/ha)

NO_{3ly} is nitrate-N concentration in layer ly (kg/ha)

β_{denit} is the rate coefficient for denitrification (1/d)

$\gamma_{tmp,ly}$ is a nutrient cycling temperature factor (unitless, always greater than 0.1)

$orgC_{ly}$ is the amount of organic carbon (%).

The SWAT model includes factors to account for soil moisture which are not necessary for the woodchip filter because the active carbon source is always saturated with water.

Appelboom et al. (2010) refined a mass transfer coefficient approach to describing sediment denitrification by accounting for water column nitrate-N concentration and flow depth. This was expanded to incorporate a relationship between temperature and denitrification rate. This effectively combined Equation C-3, Equation C-4 and Equation C-5:

$$[C_1] = [C_0] \cdot e^{(-kt)} \quad \text{Equation C-3}$$

where

$[C_0]$ is the initial concentration

$[C_1]$ is the concentration at time t , and

k is the decay coefficient (t^{-1}).

Kelly (1987) proposed a mass transfer coefficient to predict nitrate removal rates based on water column nitrate-N concentrations:

$$\rho = \frac{RR}{[C]} \quad \text{Equation C-4}$$

Where

ρ = mass transfer coefficient (m/d)

RR = measured nitrate removal rate (mass/area/d)

$[C]$ = water column nitrate-N concentration (mass/volume)

The approach above does not account for several factors, including time step, water depth, labile carbon, temperature and pH - Birgand (2000) partly addressed these limitations using

$$[C_1] = [C_0]. e^{(-\rho \frac{t}{D})} \quad \text{Equation C-5}$$

where

$[C_0]$ is the initial concentration,

$[C_1]$ is the concentration at time t ,

t is the time step (day)

D is water column depth (/m), and

ρ is the mass transfer coefficient (m/d).

The mass transfer coefficient (ρ above) approach was incorporated by Appelboom et al. (2010) when estimating nitrate-N removal in sediments; it allows for dynamic prediction of water column nitrate-N concentrations over time, rather than being restricted to estimating a removal rate at a single concentration.

Equation C-4 was modified to account for temperature

$$C_{10} = \left(\frac{RR_2}{RR_1} \right)^{\frac{10}{(T_2-T_1)}} \quad \text{Equation C-6}$$

where and

RR_1 and RR_2 are reaction rates at temperatures T_1 and T_2 respectively, and

C_{10} is Q_{10} , the temperature coefficient.

The latter is a factor that accounts for the increase in reaction rate following a temperature increase of 10° C. It has an effective temperature range from 0 °C to 40 °C.

Equation C-4, Equation C-5 and Equation C-6 were combined by Appelboom et al. (2010) to describe denitrification:

$$[C_1] = [C_0] * \exp(-\rho_{T_1} * t * C_{T_1-T_2} / D) \quad \text{Equation C-7}$$

where

$[C_1]$ and $[C_0]$ are as defined previously,

ρ_{T_1} is the mass transfer coefficient at temperature T_1 (m/d),

D is the depth of the water column (m).

$C_{T_1-T_2}$ = correction factor for the change in temperature (unitless).

Appelboom et al. (2010) used Equation C-5 to determine site-specific mass transfer coefficients for a series of tanks, as well as an average value of ρ . Equation C-7 provided model estimates that closely matched measured values.

For the current work, the average mass transfer coefficient identified by Appelboom et al. (2010) was applied to the woodchip denitrification filter. Credible estimates of woodchip filter outflow nitrate-N concentrations were obtained from a model of the form:

$$[NO_{3_{out}}] = [NO_{3_{in}}] \times (\exp(-0.016 \times RT \times T_{out}) / D \times [DOC]) \quad \text{Equation C-8}$$

where

0.016 is the average mass transfer coefficient from Appelboom et al. (2010) (m/d)

RT is estimated retention time (days), estimated from inflow rate (L/s), real-time woodchip filter water level (m) (D below), and nominal 100 m² filter area.

T_{out} is the outflow temperature (°C)

D is the water depth in the wood chip filter bed (m), and

$[DOC]$ is the concentration of dissolved organic carbon (g/m³).

Prediction of nitrate-N removal rates were assessed using seasonally varying inflow DOC concentrations, but these provided no advantage over use of an average value derived from measurements made over the assessment period, based on goodness of fit.

Appendix D Climate data

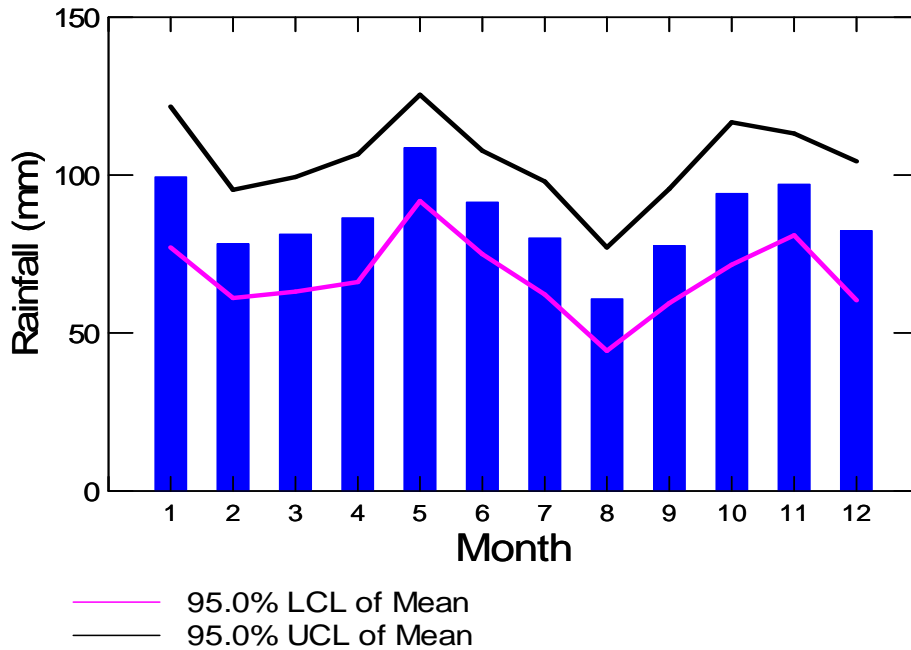


Figure D-1: Monthly average rainfall, 2001-2018 inclusive. Data sourced from “Invercargill Aero AWS”, Site 684305.

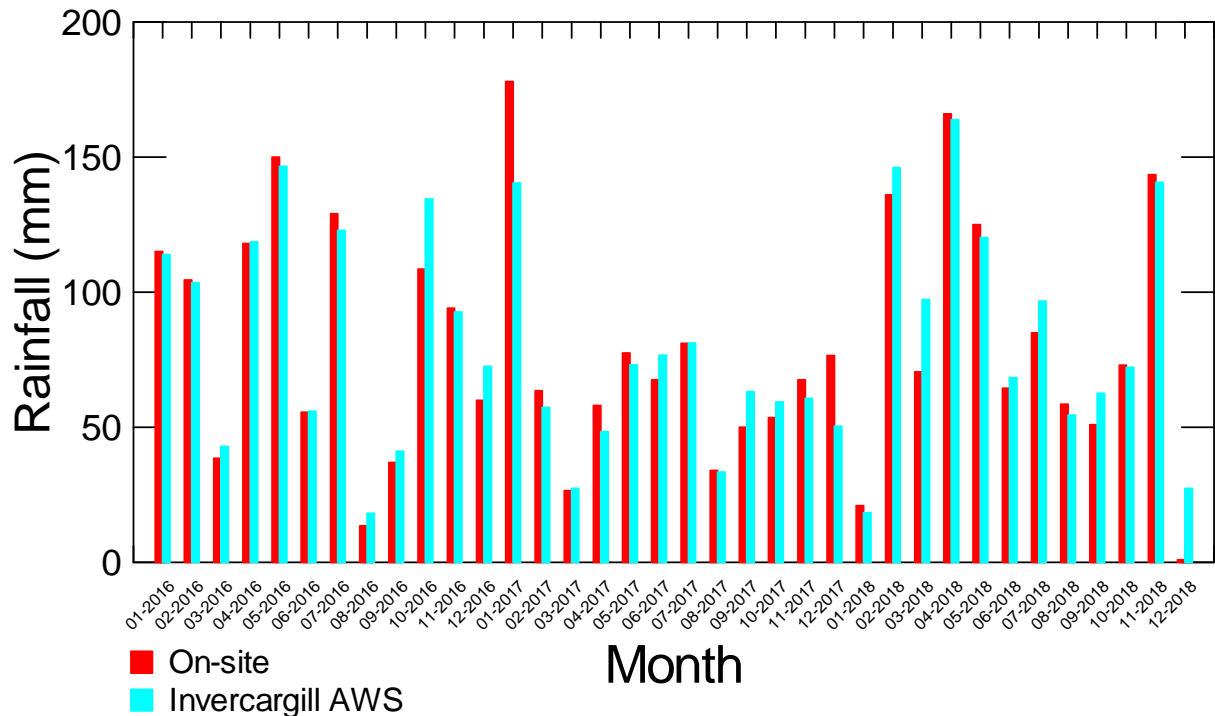


Figure D-2: Comparison of on-site monthly total rainfall, 2016-2018 inclusive, with rainfall recorded at Invercargill airport. Data sourced from “Invercargill Aero AWS”, Site 684305.

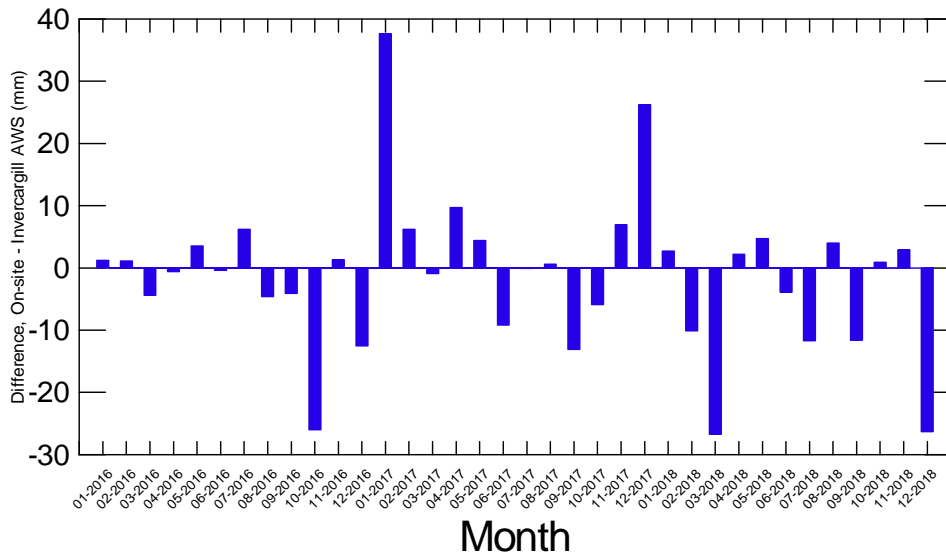


Figure D-3: Difference between monthly total rainfall measured on site with rainfall measured at Invercargill airport. Data sourced from “Invercargill Aero AWS”, Site 684305.

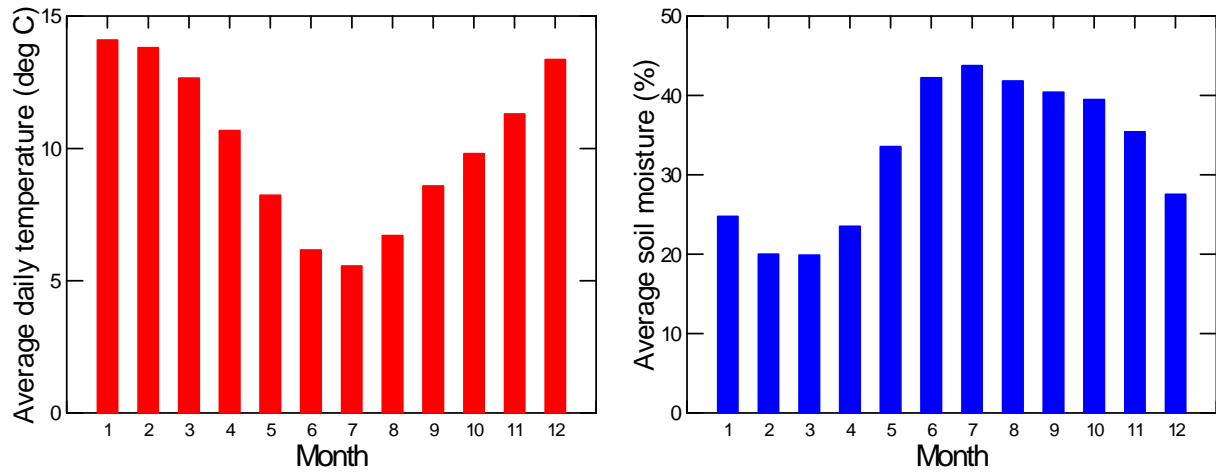


Figure D-4: Long-term average daily temperature and soil moisture recorded at Invercargill airport for the period 2001-2018. Data sourced from “Invercargill Aero AWS”, Site 684305.

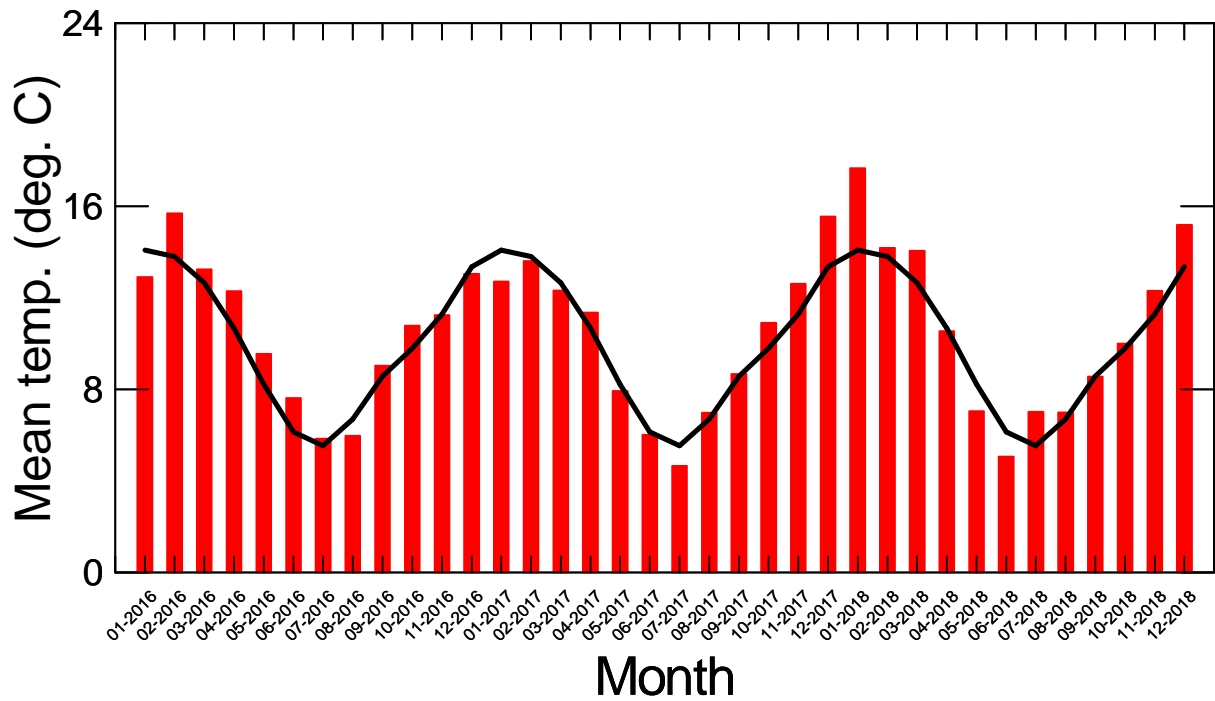


Figure D-5: Comparison of monthly average temperatures recorded at Invercargill airport between January 20016 and December 2018, and the long-term average value (black line). Data sourced from “Invercargill Aero AWS”, Site 684305.a.

Appendix E Woodchip filter hydrology

Table E-1: Summary statistics for woodchip filter inflow and outflow.

Statistic	Inflow (L/s)	Outflow (L/s)
N of Cases	25560	25560
Minimum	0.000	0.001
Maximum	20.7	11.7
Median	0.2	0.3
Arithmetic Mean	0.5	0.4
Standard Error of Arithmetic Mean	0.0	0.0
95.0% LCL of Arithmetic Mean	0.5	0.4
95.0% UCL of Arithmetic Mean	0.6	0.5
Standard Deviation	1.2	0.6
Cleveland percentiles		
1.000%	0.0	0.0
5.000%	0.0	0.0
10.000%	0.1	0.1
20.000%	0.2	0.1
25.000%	0.2	0.2
30.000%	0.2	0.2
40.000%	0.2	0.2
50.000%	0.2	0.3
60.000%	0.3	0.3
70.000%	0.4	0.4
75.000%	0.5	0.5
80.000%	0.6	0.6
90.000%	1.1	1.0
95.000%	1.8	1.8
99.000%	4.6	2.8

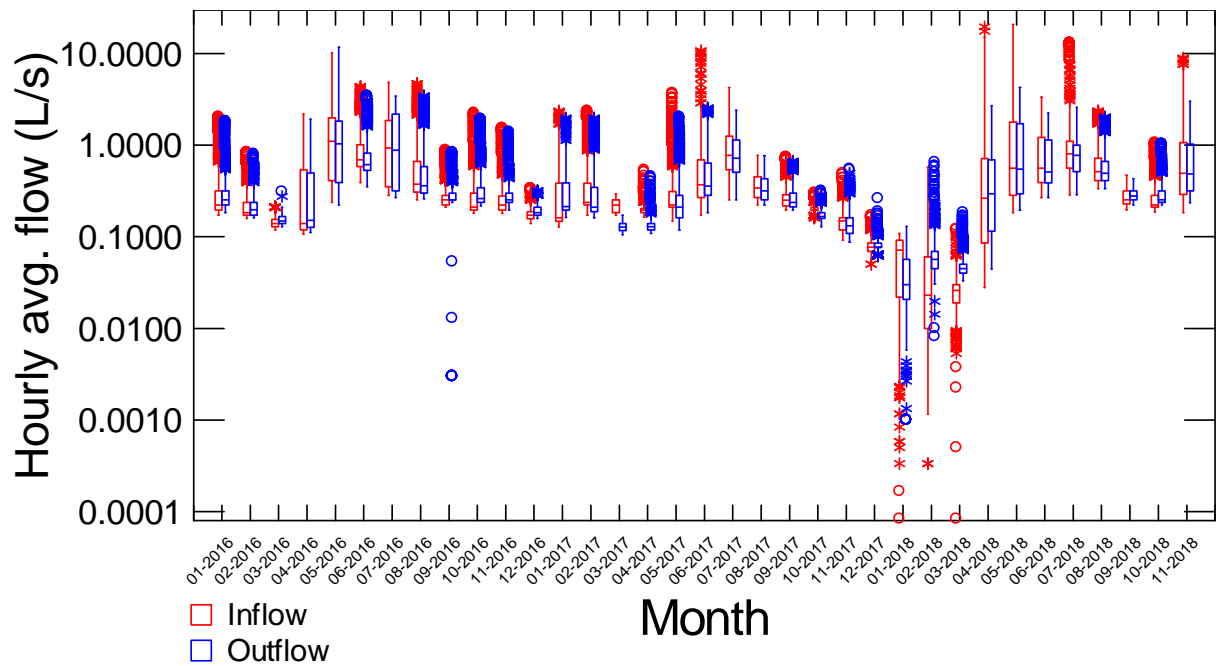


Figure E-1: Hourly average flow recorded for woodchip inflow and outflow. Data derived from five-minute data.

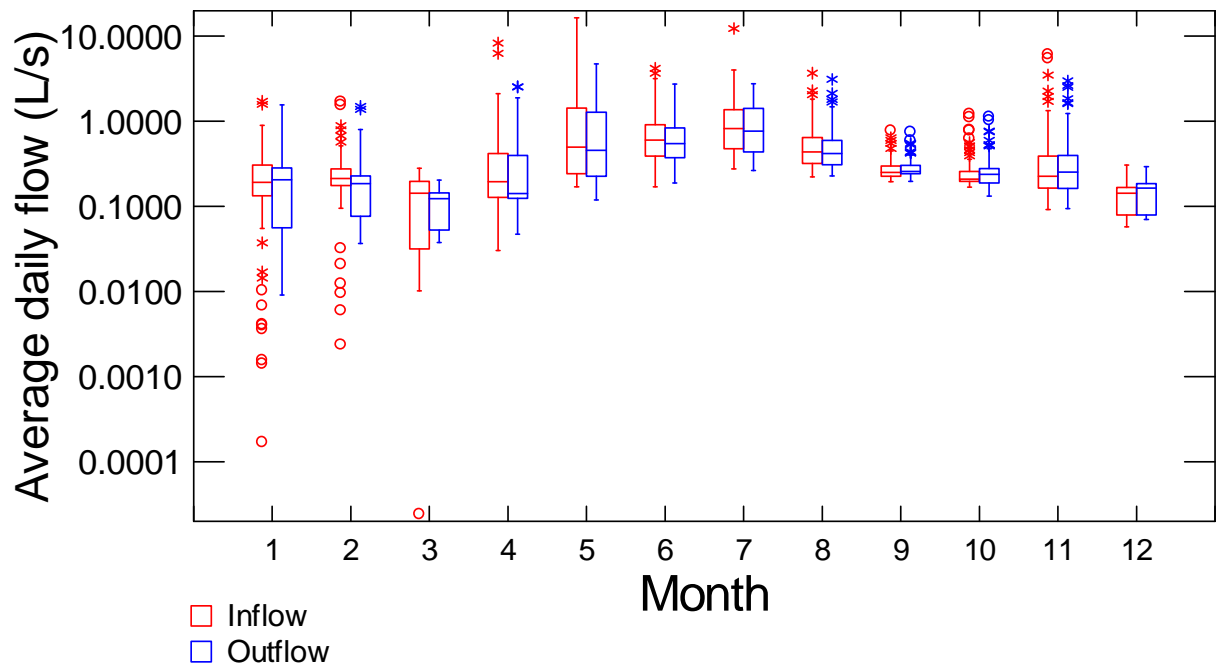


Figure E-2: Daily average flow recorded for woodchip inflow and outflow. Data derived from five-minute data.

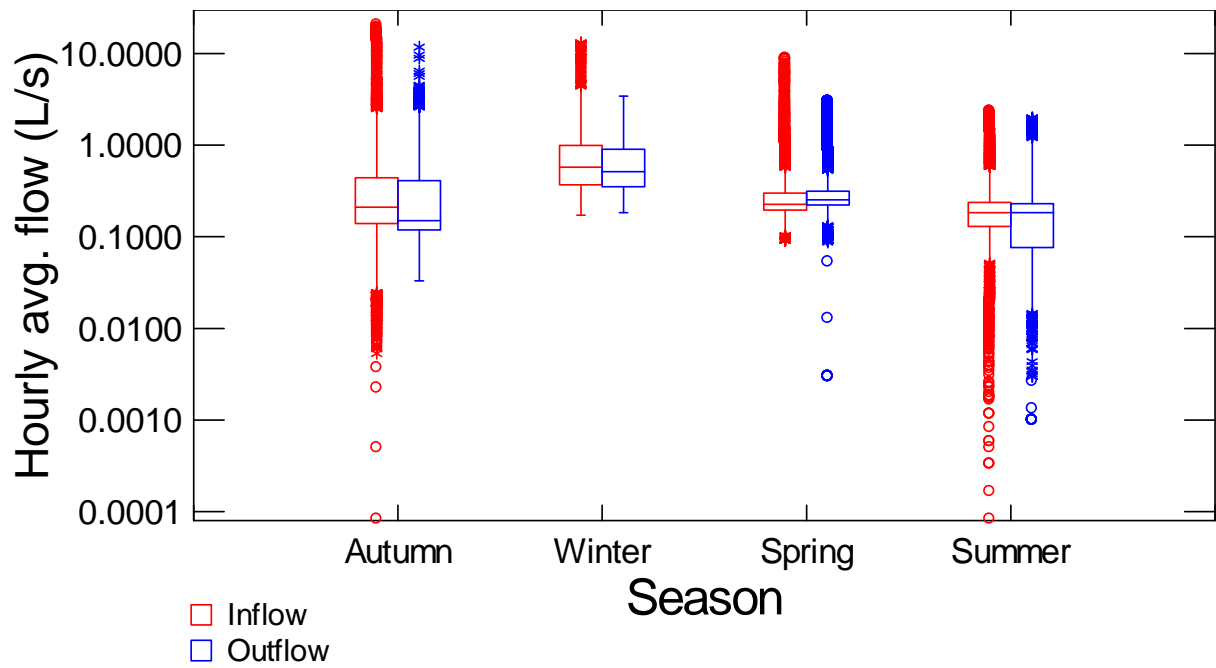


Figure E-3: Seasonal average flow recorded for woodchip inflow and outflow. Data derived from five-minute data.

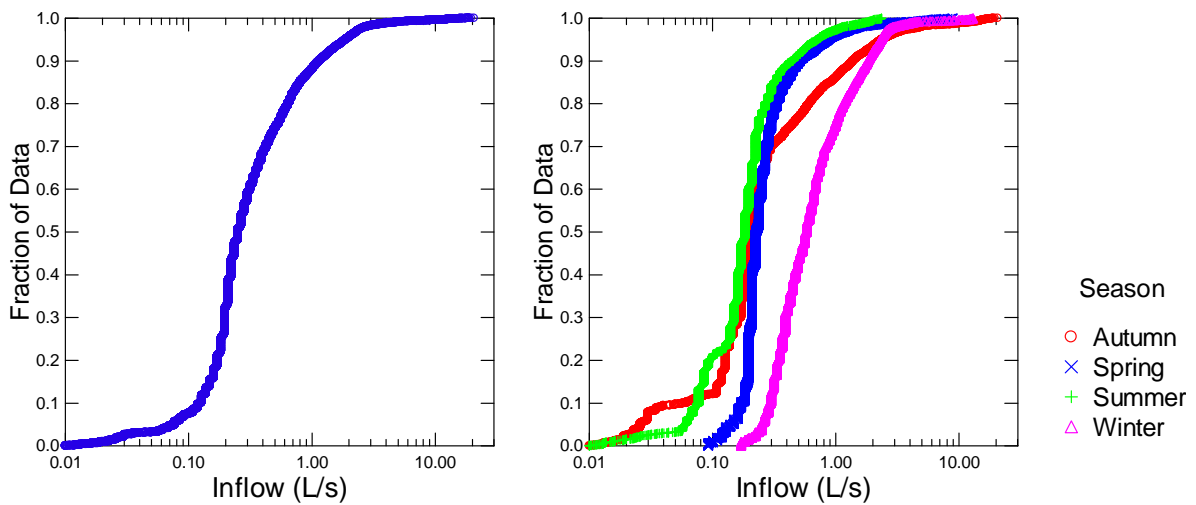


Figure E-4: Distribution of inflow values for the entire assessment period (left) and by season (right). Note the x-axis has \log_{10} scale.

Appendix F Explanation of box and whisker plot

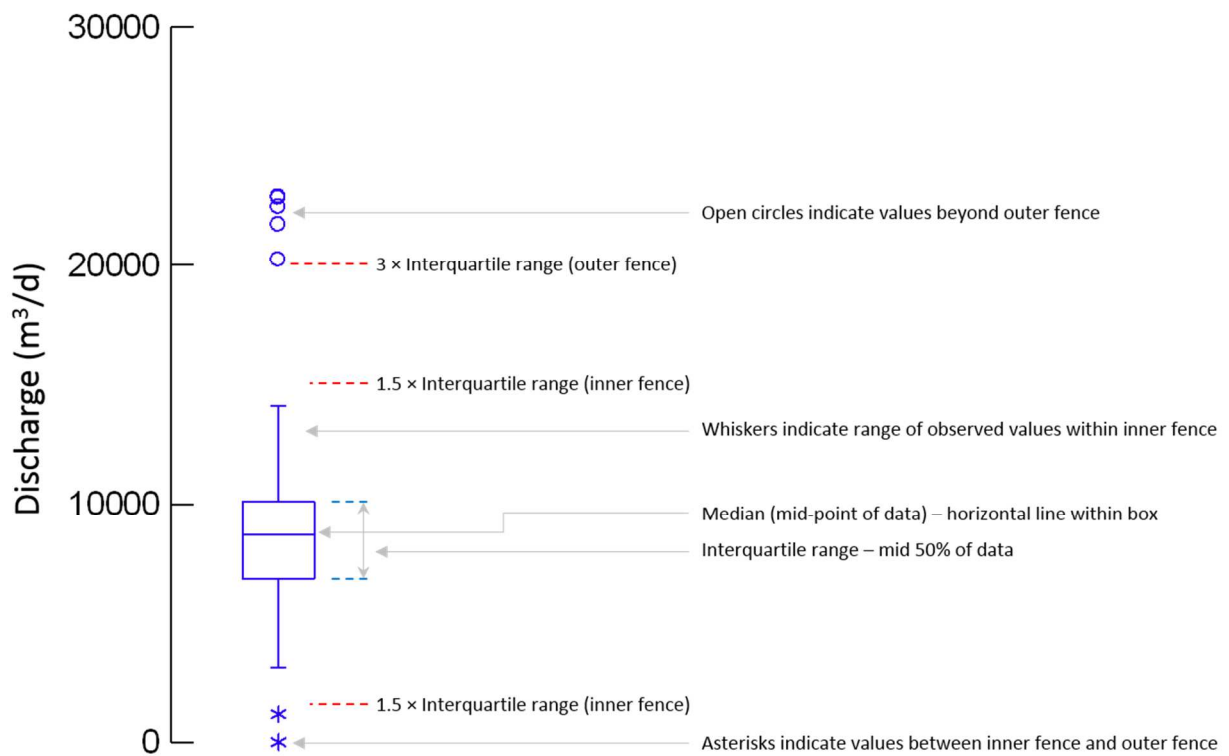


Figure F-1: Explanation of a box-and-whisker plot. This explanation applies to box and whisker plots generated by Systat for Windows, and may differ from those generated by other software.

Appendix G Woodchip filter bed water level changes in response to rainfall events

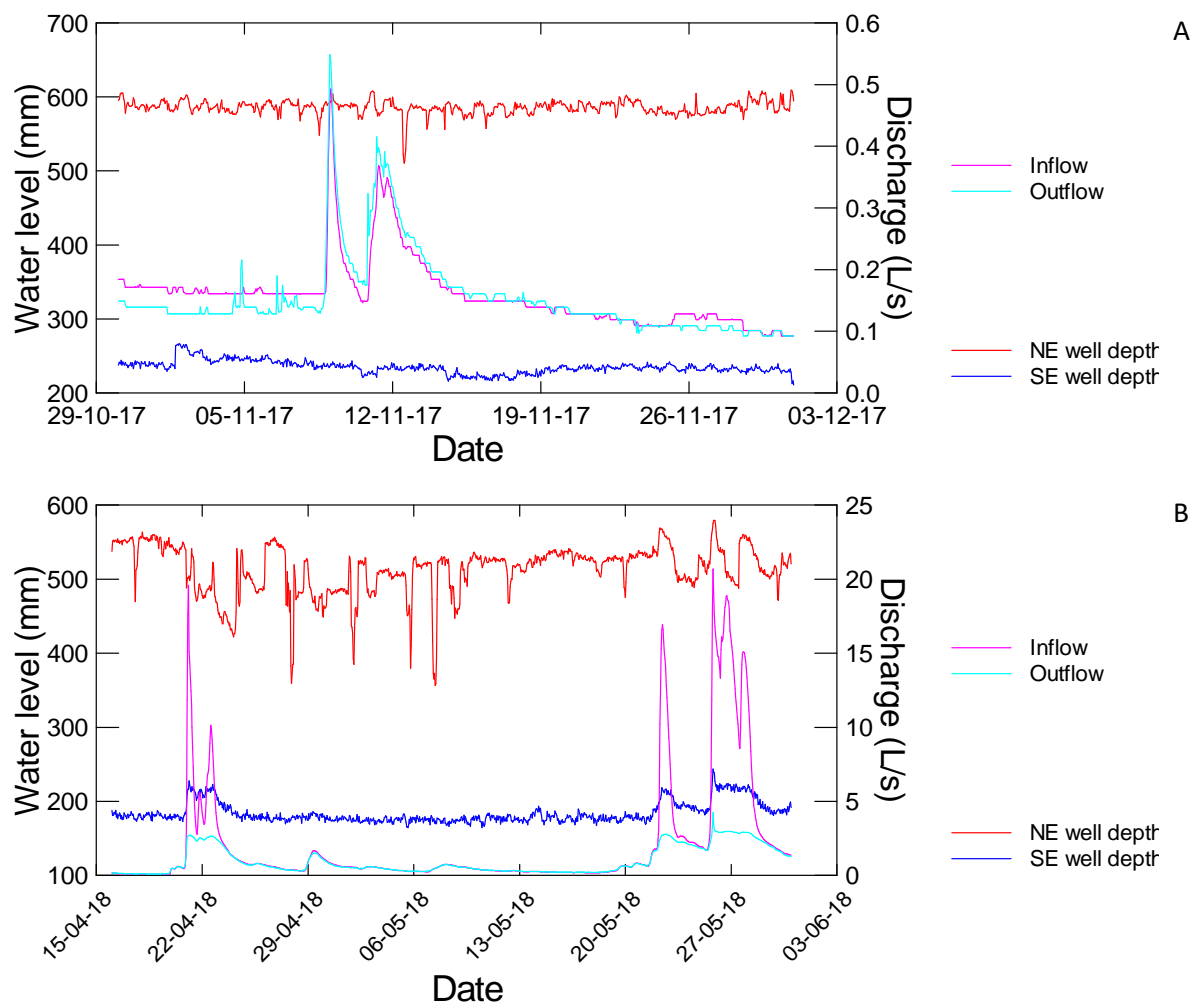


Figure G-1: Time-series of hourly average inflows and outflows, and water levels in the woodchip filter, recorded in the NE (inlet) SE (outlet) corner of the bed. A) shows results for two closely spaced minor inflow events (November 2017), and B) shows the results for a series of much larger events in autumn 2018. These are hourly average values derived from five-minute data.

Appendix H Electrical conductivity measurements

The correlation between daily average inflow and outflow electrical conductivity according to season is summarised in Figure H-1 and Figure H-2, and between electrical conductivity and nitrate-N concentration in Figure H-3. These data are separated according to month in Figure H-4 and Figure H-5.

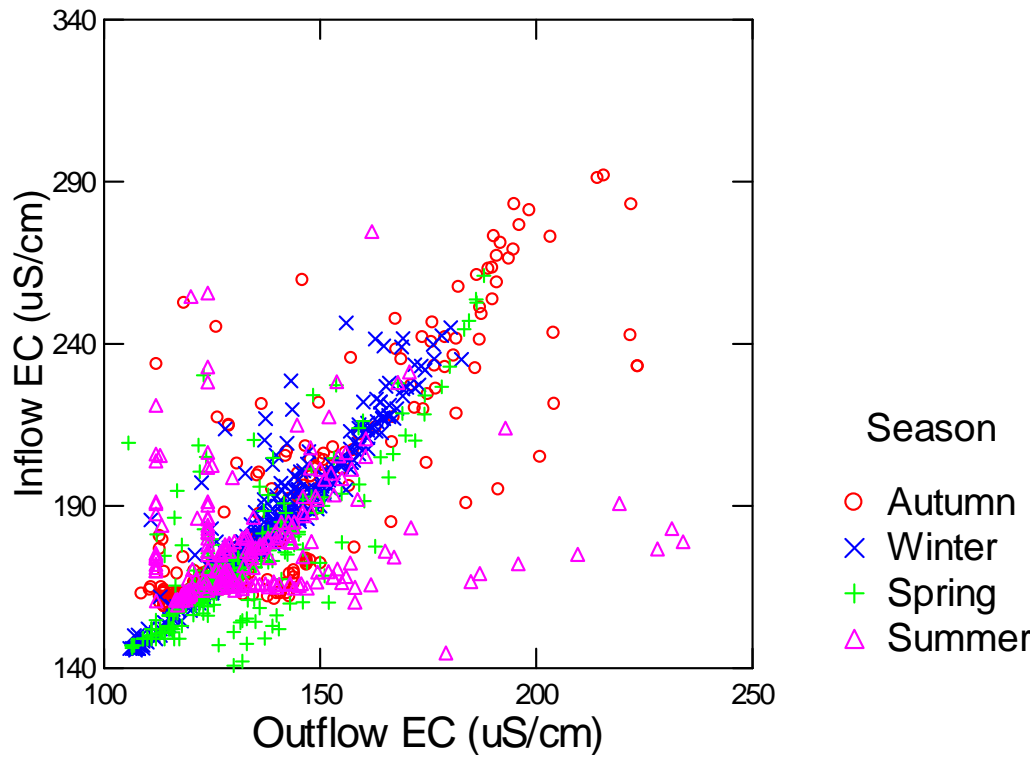


Figure H-1: Relationship between daily average inflow and outflow electrical conductivity according to season. These values were derived from five-minute data.

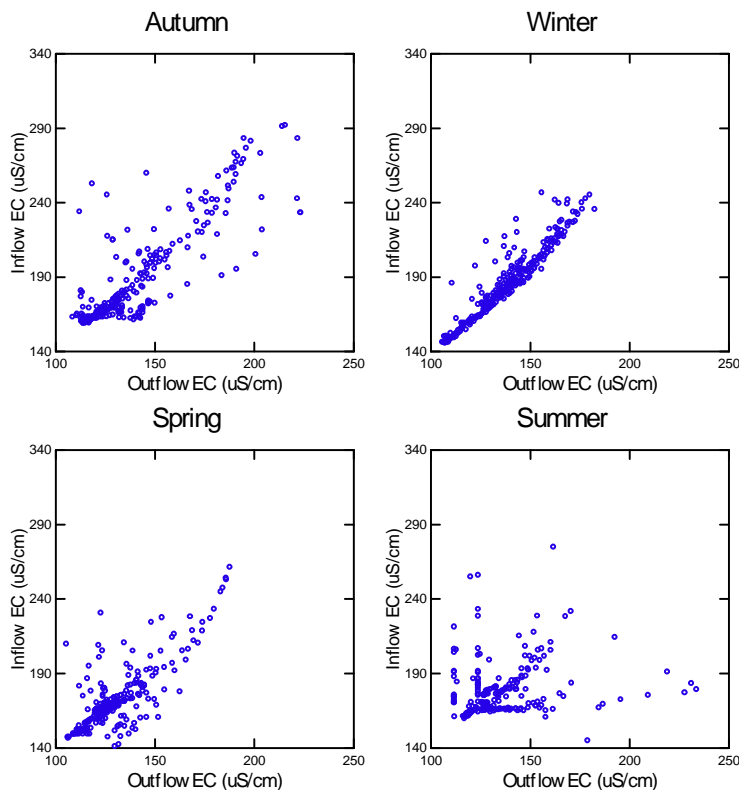


Figure H-2: Relationship between daily average inflow and outflow electrical conductivity according to season. These values were derived from five-minute data.

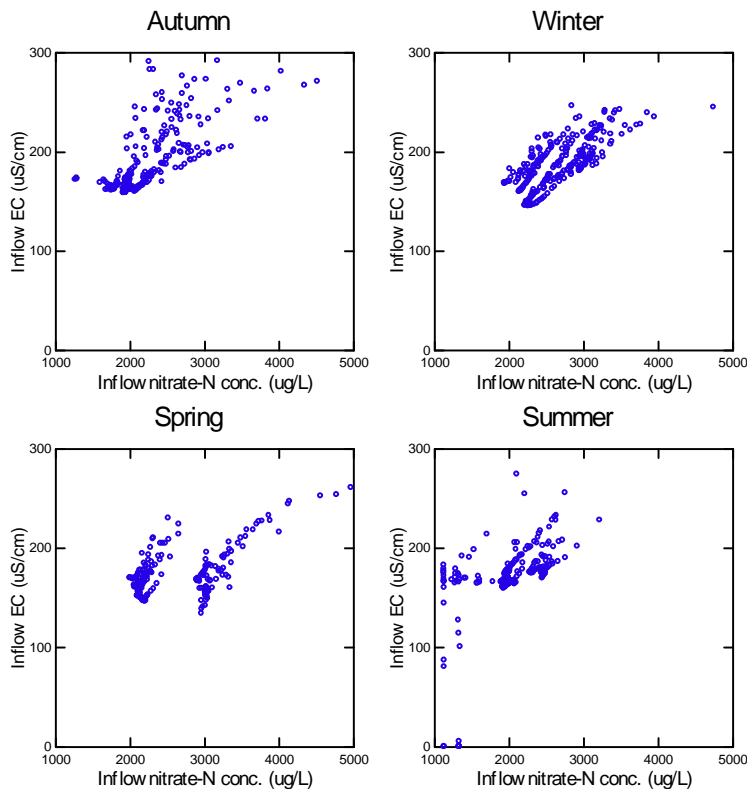


Figure H-3: Relationship between daily average inflow and outflow nitrate-N according to season. These values were derived from five-minute data.

EC vs flow – Inflow

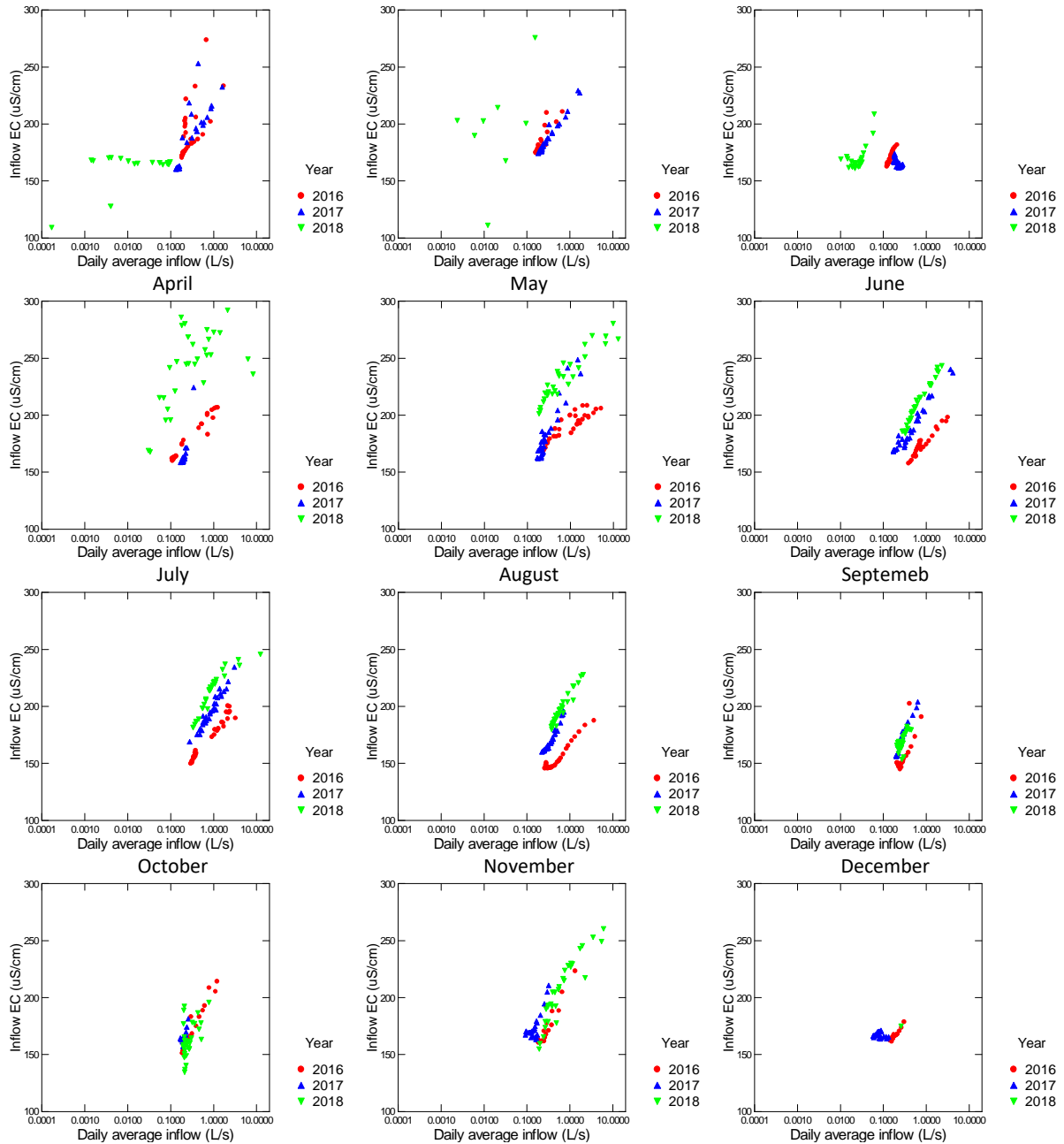


Figure H-4: Relationship between daily average inflow and electrical conductivity according to month and year. These values were derived from five-minute data.

EC vs Flow - Outflow

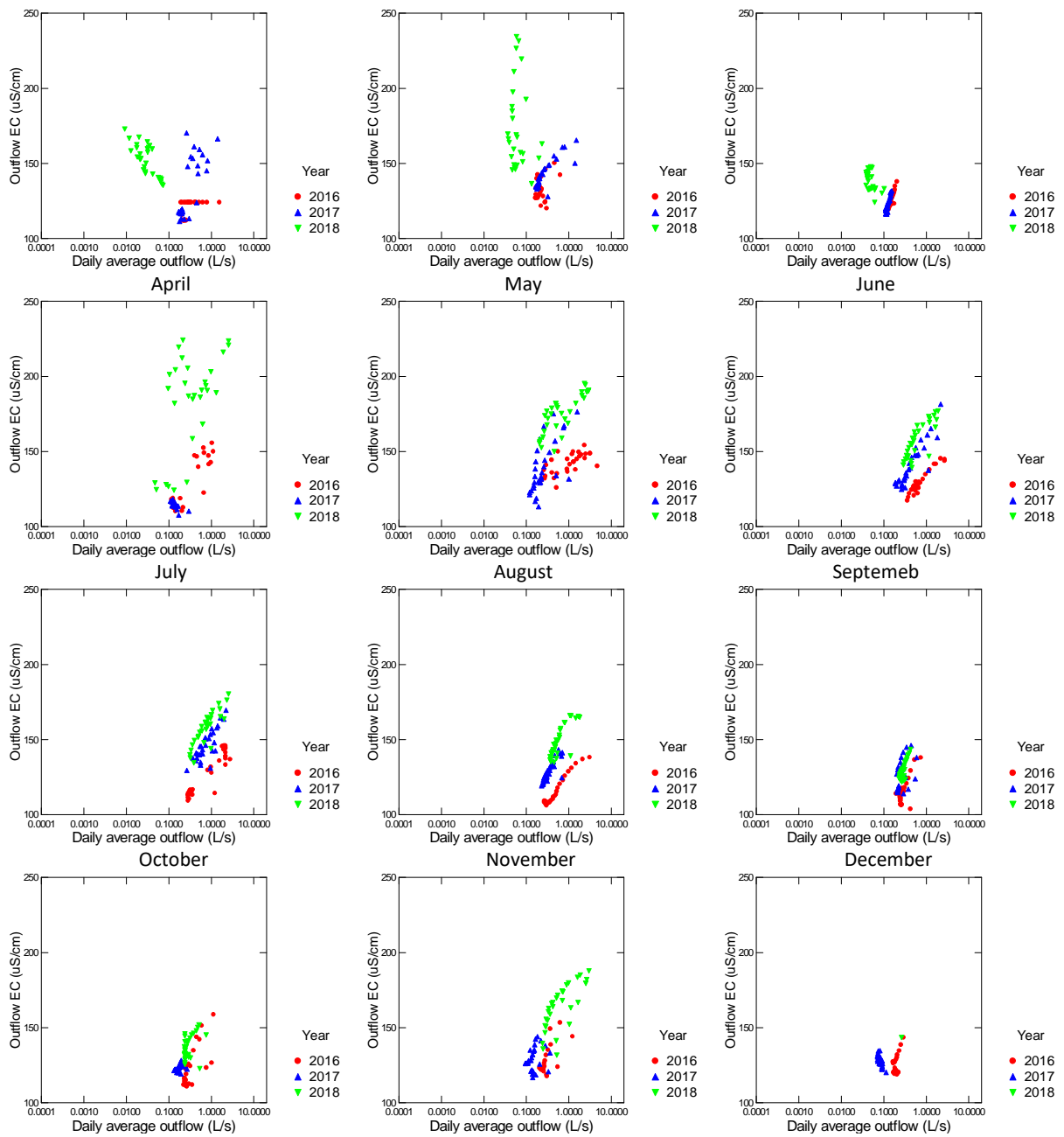


Figure H-5: Relationship between daily average outflow and electrical conductivity according to month and year. These values were derived from five-minute data.

Appendix I Turbidity-flow relationships

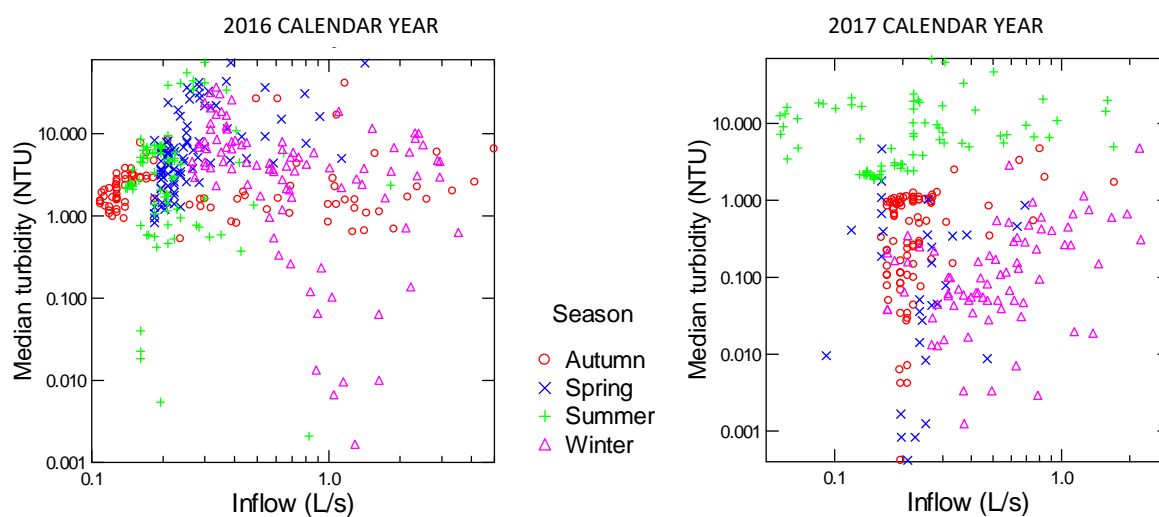
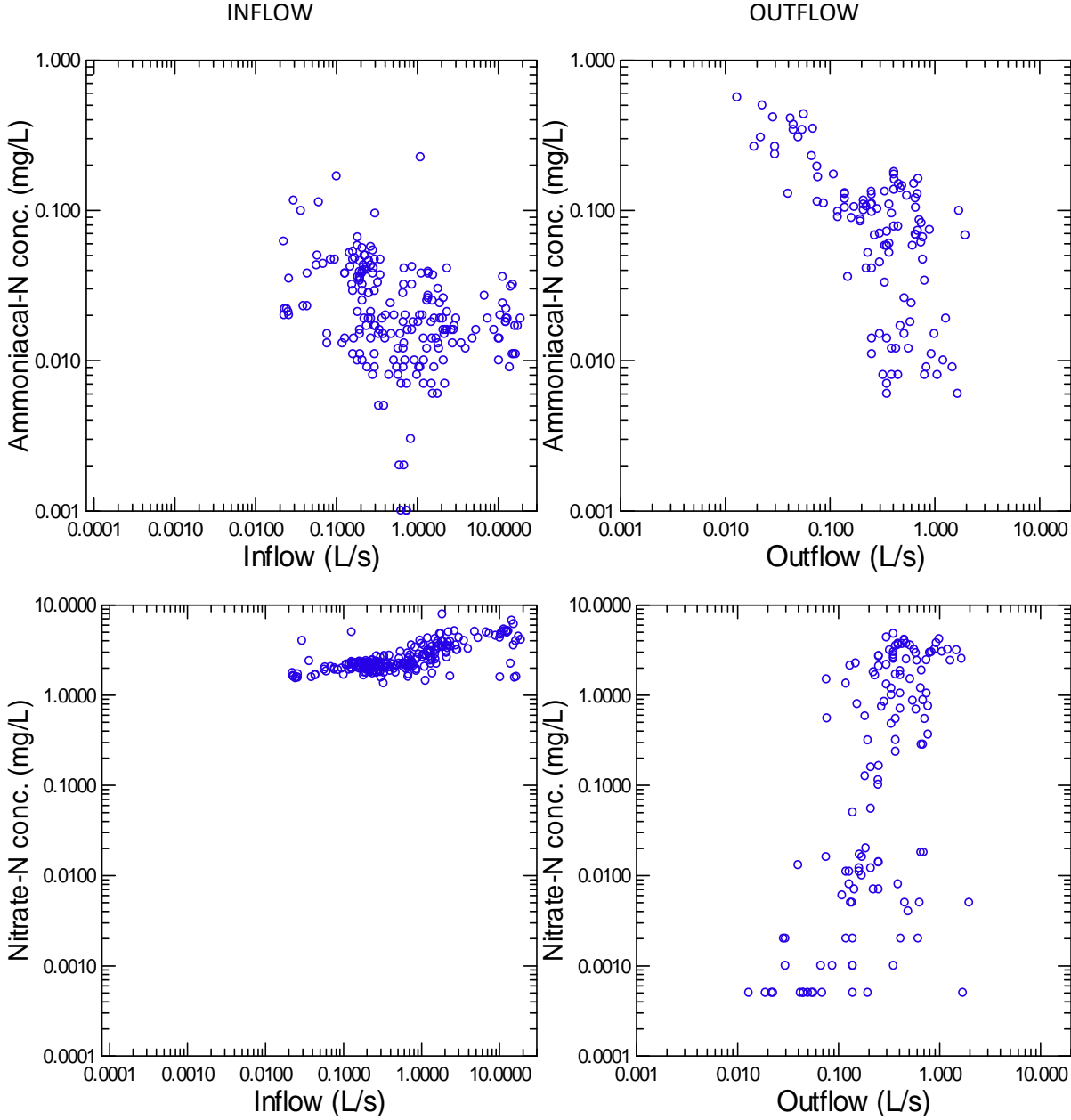


Figure I-1: Relationship between daily median turbidity and woodchip inflow classified according to season. These values were derived from five-minute data. Note x axis scales are different. Both x- and y- axes have log₁₀ scale.

Appendix J N-filter load estimation – concentration data

Concentration vs flow relationships



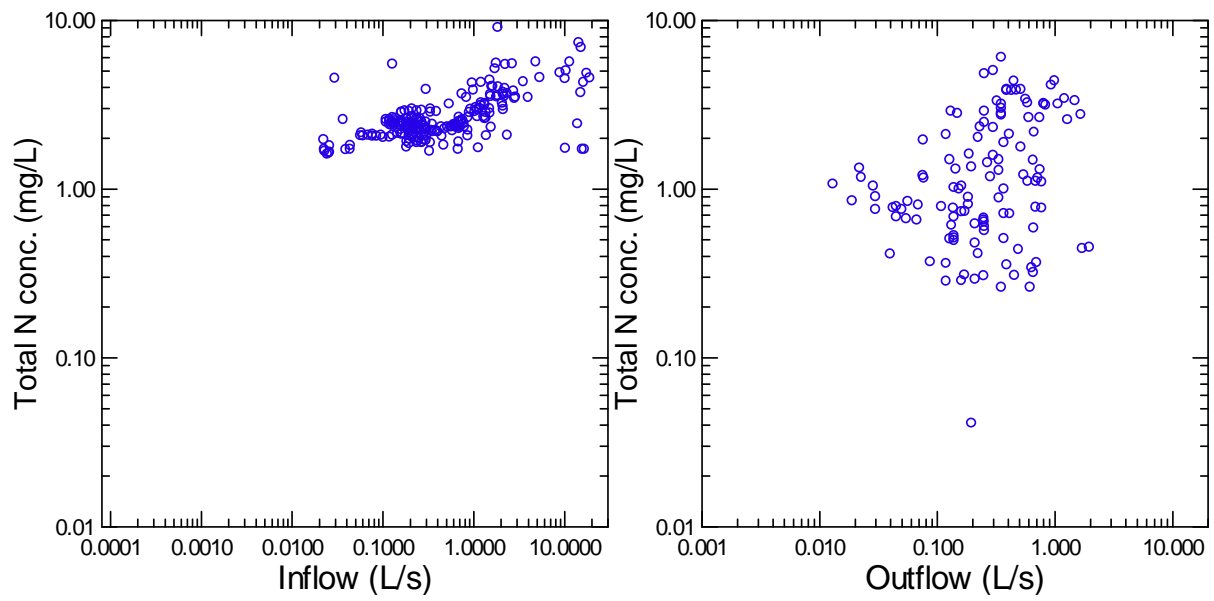
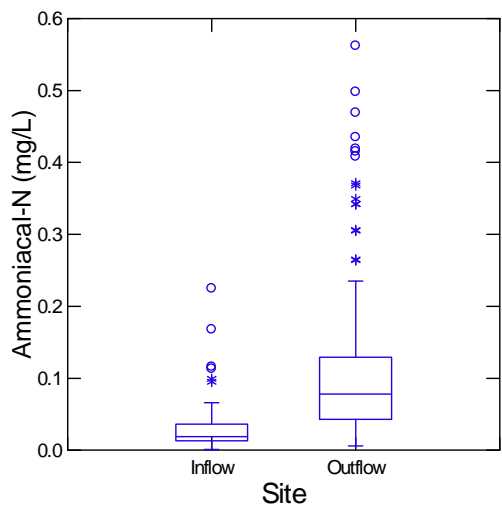


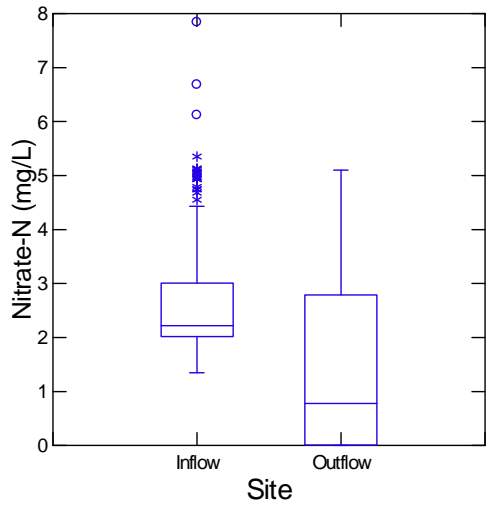
Figure J-1: Comparison of measured concentration and flow values for three forms of nitrogen. Note that x and y axes have a \log_{10} scale.

Table J-1: Summary statistics for all grab sample concentration data for woodchip filter inflow and outflow.

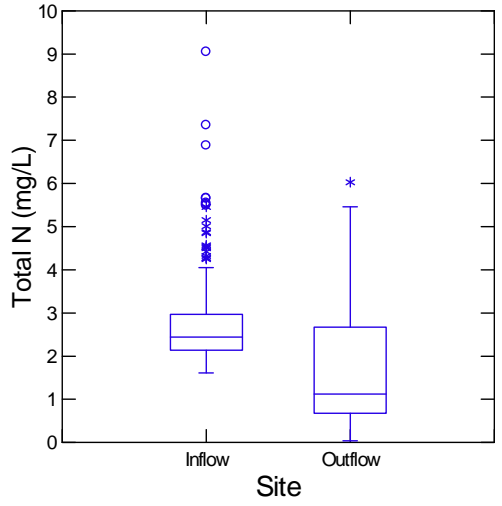
Statistic	Ammoniacal-N (mg/L)		Nitrate-N (mg/L)		Total N (mg/L)	
	Inflow	Outflow	Inflow	Outflow	Inflow	Outflow
N of Cases	200	177	264	205	242	183
Minimum	0.001	0.006	1.35	0.001	1.61	0.041
Maximum	0.225	0.562	7.84	5.1	9.05	6.03
Median	0.019	0.078	2.205	0.777	2.45	1.12
Arithmetic Mean	0.027	0.105	2.606	1.468	2.772	1.691
Std Err. of Mean	0.002	0.008	0.064	0.113	0.066	0.1
95.0% LCL of Mean	0.023	0.089	2.481	1.245	2.642	1.493
95.0% UCL of Mean	0.03	0.12	2.731	1.691	2.902	1.889
Std Deviation	0.025	0.104	1.032	1.619	1.028	1.357
Cleveland percentiles						
1.00%	0.001	0.006	1.543	0.001	1.648	0.262
5.00%	0.007	0.009	1.624	0.001	1.746	0.308
10.00%	0.009	0.012	1.77	0.001	1.917	0.373
20.00%	0.011	0.024	1.913	0.007	2.08	0.599
25.00%	0.013	0.042	1.975	0.01	2.18	0.674
30.00%	0.014	0.051	2.03	0.014	2.25	0.702
40.00%	0.017	0.06	2.12	0.169	2.34	0.846
50.00%	0.019	0.078	2.205	0.777	2.45	1.12
60.00%	0.023	0.098	2.29	1.655	2.58	1.538
70.00%	0.032	0.114	2.613	2.45	2.849	2.294
75.00%	0.036	0.129	2.96	2.793	2.98	2.675
80.00%	0.039	0.14	3.355	3.13	3.211	2.944
90.00%	0.047	0.228	4.262	3.78	4.05	3.834
95.00%	0.056	0.361	4.956	4.78	4.926	4.468
99.00%	0.142	0.49	6.012	5.085	6.918	5.335



A



B



C

Figure J-2: Comparison of inflow and outflow concentrations for all grab samples (mg/L).
 A= Ammoniacal- N, B= Nitrate-N C= Total N.

Measured vs Model estimated concentrations Ammoniacal-N

Ammoniacal-N Inflow models – Observed vs. predicted concentrations

▼ Robust Regression

Dependent Variable	LOG_IN_AMLE_NH4_MGL
No. of cases	200
No. of Regressors	1

Least Median of Squares (LMS) Regression

Method of Estimation	Quick Search
----------------------	--------------

Number of Subsamples	995
----------------------	-----

LMS Parameter Estimates	
Effect	Coefficient
CONSTANT	-0.066
LOG_GRAB_IN_NH4_MGL	0.956

Scale Estimates	0.202
-----------------	-------

Cutoff Point	3.000
Number of Outliers Detected	9

Robust R-Square	0.971
-----------------	-------

Ordinary Least Squares (OLS) Regression for Outlier Free Data

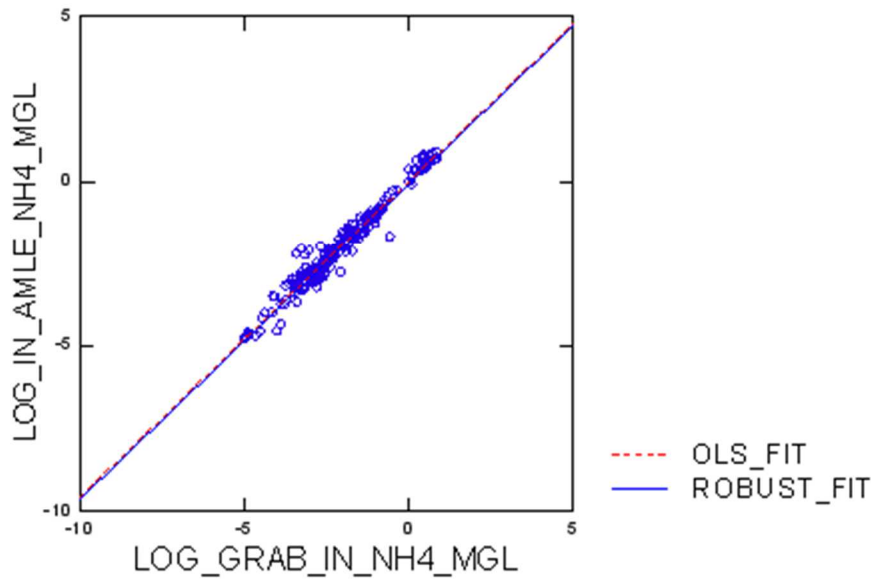
Multiple R	0.978
Squared Multiple R	0.956
Adjusted Squared Multiple R	0.955
Standard Error	0.278

OLS Parameter Estimates				
Effect	Coefficient	Standard Error	95.00% Confidence Interval	
			Lower	Upper
CONSTANT	0.004	0.038	-0.071	0.079
LOG_GRAB_IN_NH4_MGL	0.956	0.015	0.927	0.986

Analysis of Variance					
Source	SS	df	Mean Squares	F-Ratio	p-Value
Regression	314.044	1	314.044	4065.227	0.000
Residual	14.600	189	0.077		

Durbin-Watson D Statistic	0.881
First Order Autocorrelation	0.538

OLS and ROBUST Lines Plot



Plot of Residuals vs. Predicted Values

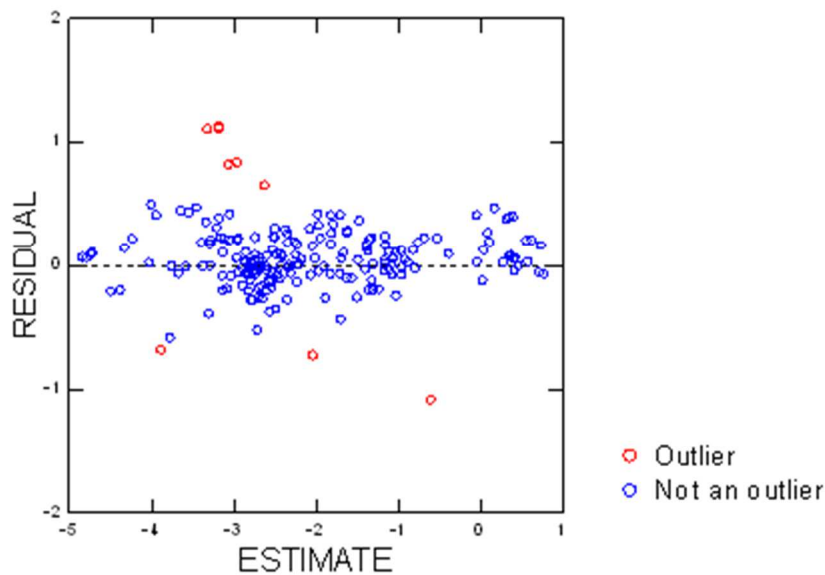


Figure J-3: Comparison of measured and predicted inflow ammoniacal-N concentration. Note that concentrations are expressed as \log_{10} values.

Ammoniacal-N Outflow models - Observed vs. predicted concentrations

ROBREG

> MODEL LOG_GRAB_OUT_NH4_MGL = CONSTANT + LOG_OUT_AMLE_NH4_MGL

> LMS / QS

> ESTIMATE / CUTOFF = 3 CONFI = 0.95 TOL = 1e-012

▼ Robust Regression

Dependent Variable	LOG_GRAB_OUT_NH4_MGL
No. of cases	177
No. of Regressors	1

Least Median of Squares (LMS) Regression

Method of Estimation	Quick Search
----------------------	--------------

Number of Subsamples	778
----------------------	-----

LMS Parameter Estimates	
Effect	Coefficient
CONSTANT	-0.181
LOG_OUT_AMLE_NH4_MGL	0.818

Scale Estimates	0.236
-----------------	-------

Cutoff Point	3.000
Number of Outliers Detected	9

Robust R-Square	0.688
-----------------	-------

Ordinary Least Squares (OLS) Regression for Outlier Free Data

Multiple R	0.765
Squared Multiple R	0.585
Adjusted Squared Multiple R	0.583
Standard Error	0.304

OLS Parameter Estimates				
Effect	Coefficient	Standard Error	95.00% Confidence Interval	
			Lower	Upper
CONSTANT	-0.102	0.075	-0.250	0.046
LOG_OUT_AMLE_NH4_MGL	1.002	0.065	0.873	1.131

Analysis of Variance					
Source	SS	df	Mean Squares	F-Ratio	p-Value
Regression	21.613	1	21.613	234.064	0.000

Analysis of Variance					
Source	SS	df	Mean Squares	F-Ratio	p-Value
Residual	15.328	166	0.092		

Durbin-Watson D Statistic	0.865
First Order Autocorrelation	0.556

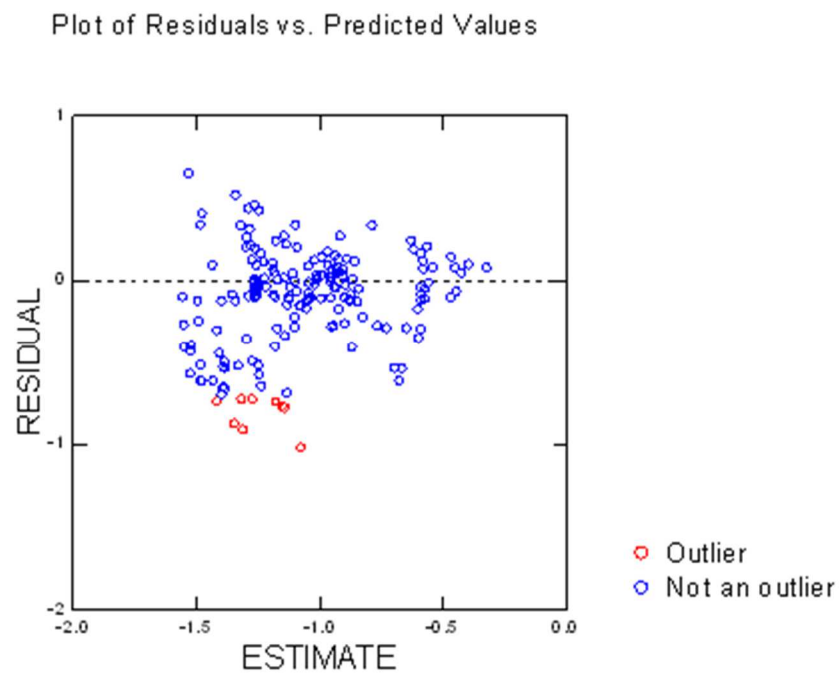
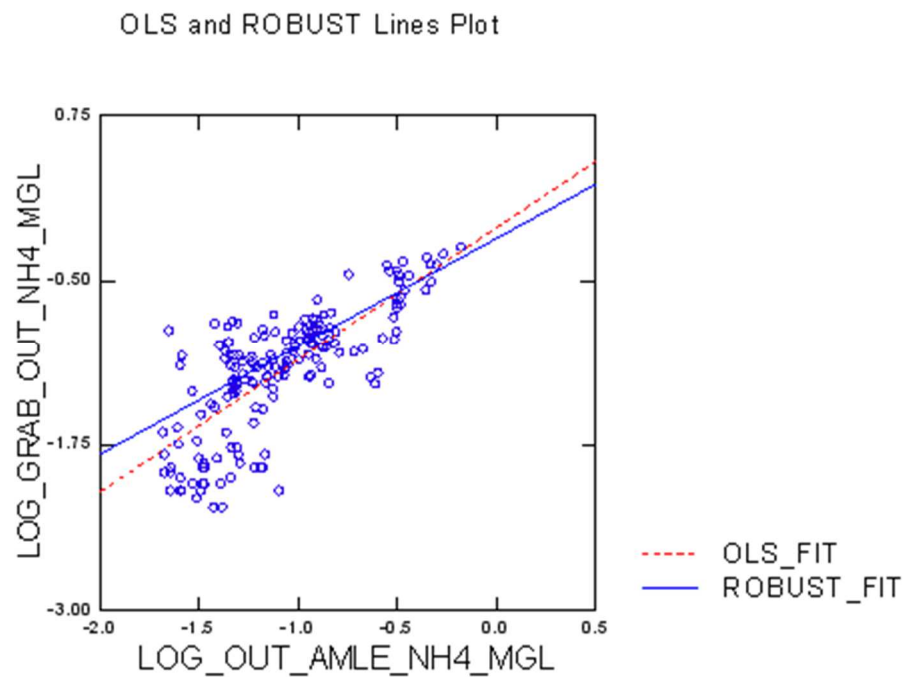


Figure J-4: Comparison of measured and predicted outflow ammoniacal-N concentration. Note that concentrations are expressed as \log_{10} values.

Nitrate-N

Nitrate-N Inflow models - Observed vs. predicted concentrations

> REM -- Following commands were produced by the LMSREG dialog:
 > REM ROBREG
 > MODEL LOG_IN_MLE_NO3_MGL = CONSTANT + LOG_GRAB_IN_NO3_MGL
 > LMS / QS
 > ESTIMATE / CUTOFF = 3 CONF1 = 0.95 TOL = 1e-012

▼ Robust Regression

Dependent Variable	LOG_IN_MLE_NO3_MGL
No. of cases	244
No. of Regressors	1

Least Median of Squares (LMS) Regression

Method of Estimation	Quick Search
----------------------	--------------

Number of Subsamples	1482
----------------------	------

LMS Parameter Estimates	
Effect	Coefficient
CONSTANT	0.157
LOG_GRAB_IN_NO3_MGL	0.559

Scale Estimates	0.054
-----------------	-------

Cutoff Point	3.000
Number of Outliers Detected	12

Robust R-Square	0.744
-----------------	-------

Ordinary Least Squares (OLS) Regression for Outlier Free Data

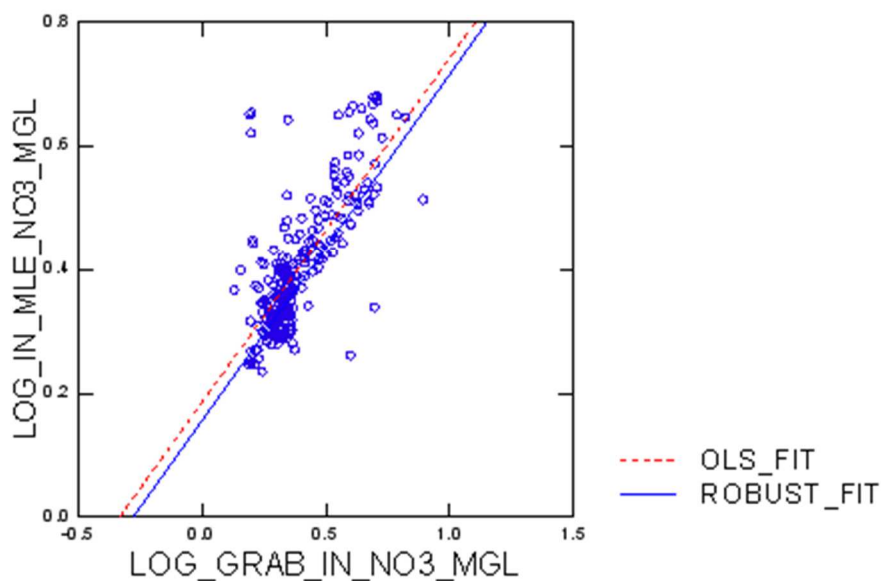
Multiple R	0.738
Squared Multiple R	0.545
Adjusted Squared Multiple R	0.543
Standard Error	0.073

OLS Parameter Estimates				
Effect	Coefficient	Standard Error	95.00% Confidence Interval	
			Lower	Upper
CONSTANT	0.188	0.014	0.162	0.215
LOG_GRAB_IN_NO3_MGL	0.542	0.033	0.478	0.606

Analysis of Variance					
Source	SS	df	Mean Squares	F-Ratio	p-Value
Regression	1.4531	1	1.453	275.825	0.000
Residual	1.2122	230	0.005		

Durbin-Watson D Statistic	0.547
First Order Autocorrelation	0.722

OLS and ROBUST Lines Plot



Plot of Residuals vs. Predicted Values

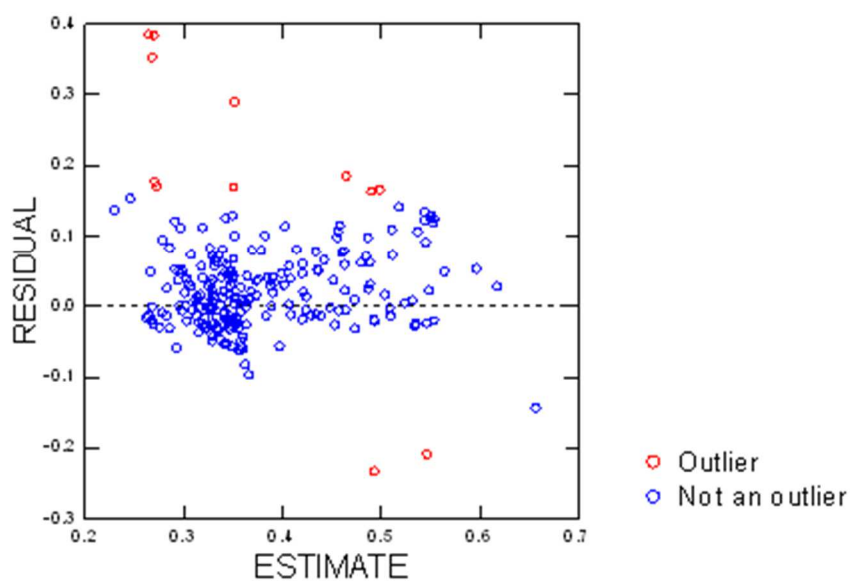


Figure J-5: Comparison of measured and predicted inflow nitrate-N concentration. Note that concentrations are expressed as log₁₀ values.

Nitrate-N Outflow models - Observed vs. predicted concentrations

Paired outflow concentrations predicted from measured inflow concentrations and measured outflow concentrations

Data for the following results were selected according to
SELECT GRAB_NITRATE_IN_MGL <>.

Dependent Variable	LOG_AMLE_IN_2_N- O3_OUT_PROC_MOD- EL_MGL
No. of cases	106
No. of Regressors	1

Least Absolute Deviations (LAD) Regression

Method of Estimation	IRLS
----------------------	------

Raw R-square (1-Residual/Total)	0.584
R-square(Observed vs. Predicted)	0.584

LAD Parameter Estimates	
Effect	Coefficient
CONSTANT	0.222
LOG_GRAB_NITRATE_OUT_MGL	0.429

Scale Estimates	0.208
-----------------	-------

Cutoff Point	3.000
Number of Outliers Detected	12

Ordinary Least Squares (OLS) Regression for Outlier Free Data

Multiple R	0.889
Squared Multiple R	0.790
Adjusted Squared Multiple R	0.788
Standard Error	0.240

OLS Parameter Estimates				
Effect	Coefficient	Standard Error	95.00% Confidence Interval	
			Lower	Upper
CONSTANT	0.233	0.026	0.182	0.284
LOG_GRAB_NITRATE_OUT_MGL	0.385	0.021	0.344	0.426

Analysis of Variance					
Source	SS	df	Mean Squares	F-Ratio	p-Value
Regression	20.045	1	20.045	346.655	0.000

Analysis of Variance					
Source	SS	df	Mean Squares	F-Ratio	p-Value
Residual	5.320	92	0.058		

Durbin-Watson D Statistic	0.942
First Order Autocorrelation	0.528

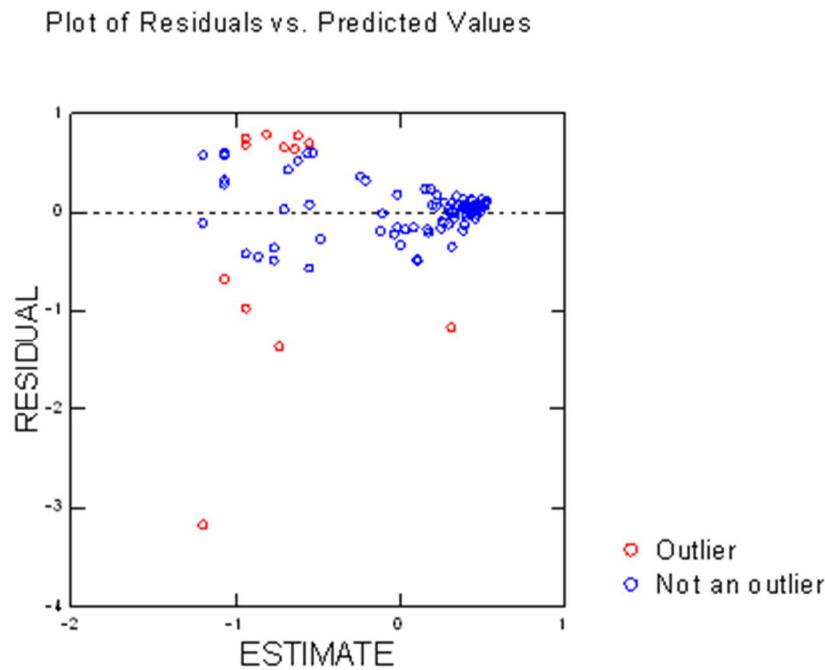
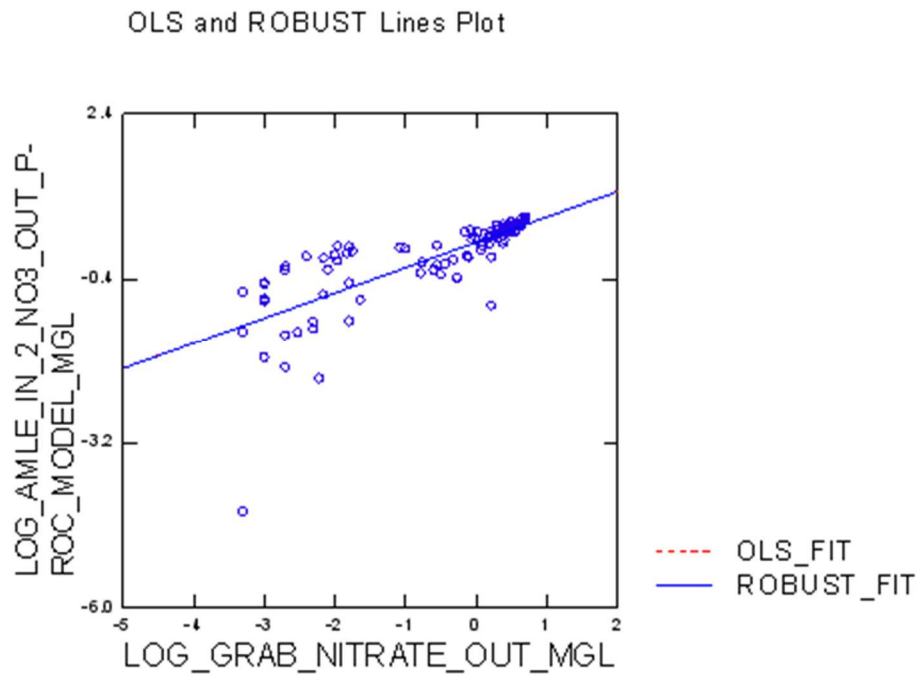


Figure J-6: Comparison of measured and process-model predicted outflow nitrate-N concentration. Note that concentrations are expressed as \log_{10} values.

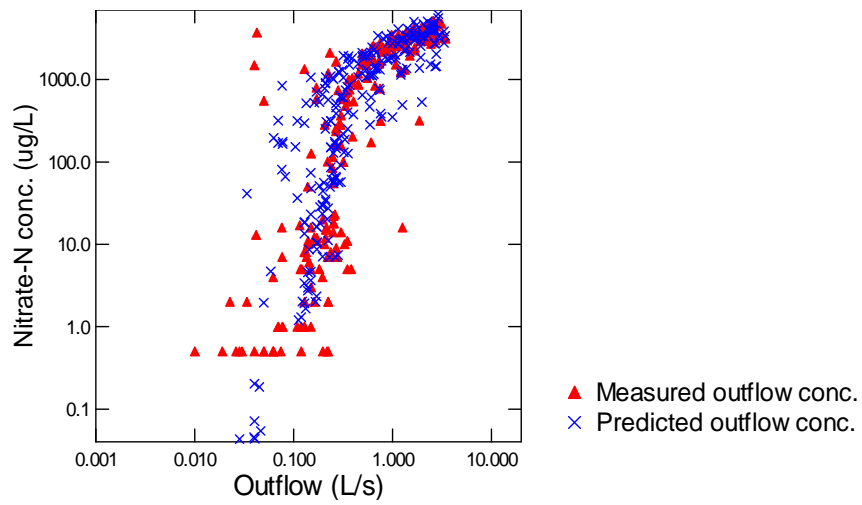


Figure J-7: Relationship of measured and process-model predicted outflow nitrate-N concentrations and flow, all values. Note that concentrations and flows are expressed as \log_{10} values.

Total -N – Inflow model

▼ Robust Regression

Dependent Variable	Log10 inflow TN conc. (mg/L) [AMLE]
No. of cases	222
No. of Regressors	1

Least Median of Squares (LMS) Regression

Method of Estimation	Quick Search
----------------------	--------------

Number of Subsamples	1226
----------------------	------

LMS Parameter Estimates	
Effect	Coefficient
CONSTANT	0.011
Log10 inflow TN conc. (mg/L) [Grab]	0.998

Scale Estimates	0.060
-----------------	-------

Cutoff Point	3.000
Number of Outliers Detected	14

Robust R-Square	0.998
-----------------	-------

Ordinary Least Squares (OLS) Regression for Outlier Free Data

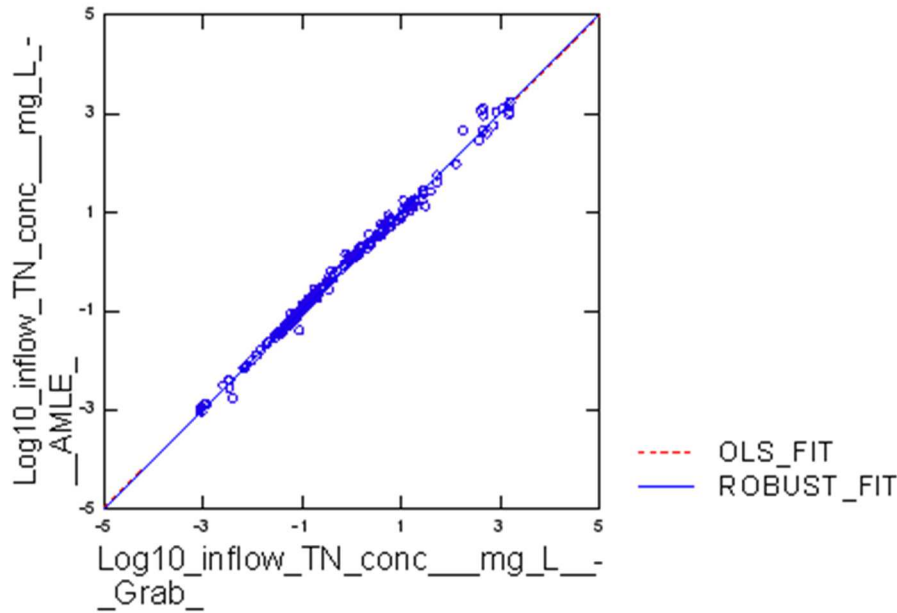
Multiple R	0.997
Squared Multiple R	0.995
Adjusted Squared Multiple R	0.995
Standard Error	0.099

OLS Parameter Estimates				
Effect	Coefficient	Standard Error	95.00% Confidence Interval	
			Lower	Upper
CONSTANT	0.011	0.007	-0.002	0.025
Log10 inflow TN conc. (mg/L) [Grab]	0.996	0.005	0.986	1.006

Analysis of Variance					
Source	SS	df	Mean Squares	F-Ratio	p-Value
Regression	374.820	1	374.820	37946.113	0.000
Residual	2.035	206	0.010		

Durbin-Watson D Statistic	0.810
First Order Autocorrelation	0.587

OLS and ROBUST Lines Plot



Plot of Residuals vs. Predicted Values

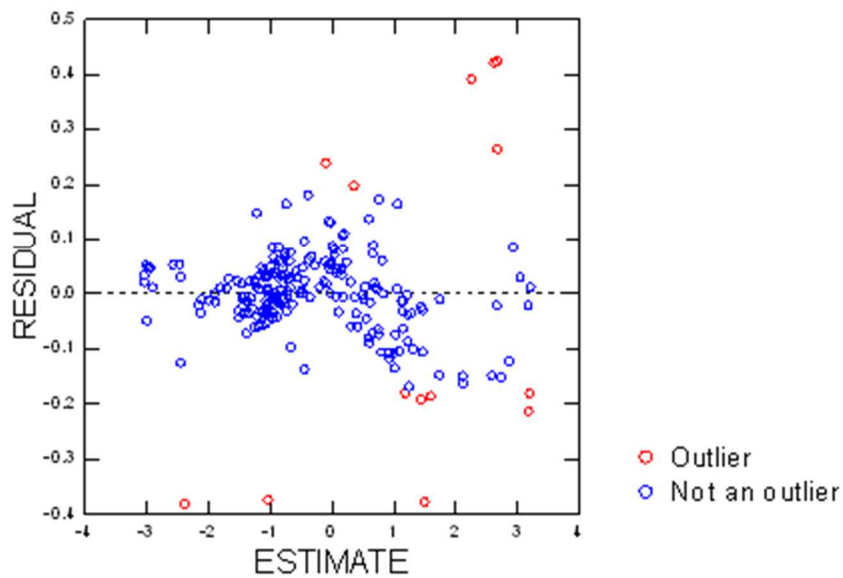


Figure J-8: Comparison of measured and predicted inflow total-N concentration. Note that concentrations are expressed as \log_{10} values.

Total-N - Outflow model

▼ Robust Regression

Dependent Variable	LOG_OUT_AMLE_TN-MGL
No. of cases	183
No. of Regressors	1

Least Median of Squares (LMS) Regression

Method of Estimation	Quick Search
----------------------	--------------

Number of Subsamples	832
----------------------	-----

LMS Parameter Estimates	
Effect	Coefficient
CONSTANT	0.067
LOG_GRAB_OUT_TN_MGL	0.433

Scale Estimates	0.149
-----------------	-------

Cutoff Point	3.000
Number of Outliers Detected	9

Robust R-Square	0.677
-----------------	-------

Ordinary Least Squares (OLS) Regression for Outlier Free Data

Multiple R	0.691
Squared Multiple R	0.477
Adjusted Squared Multiple R	0.474
Standard Error	0.182

OLS Parameter Estimates				
Effect	Coefficient	Standard Error	95.00% Confidence Interval	
			Lower	Upper
CONSTANT	0.118	0.014	0.091	0.146
LOG_GRAB_OUT_TN_MGL	0.463	0.037	0.390	0.536

Analysis of Variance					
Source	SS	df	Mean Squares	F-Ratio	p-Value
Regression	5.2031	5.203	156.749	0.000	
Residual	5.709172	0.033			

Durbin-Watson D Statistic	0.820
First Order Autocorrelation	0.581

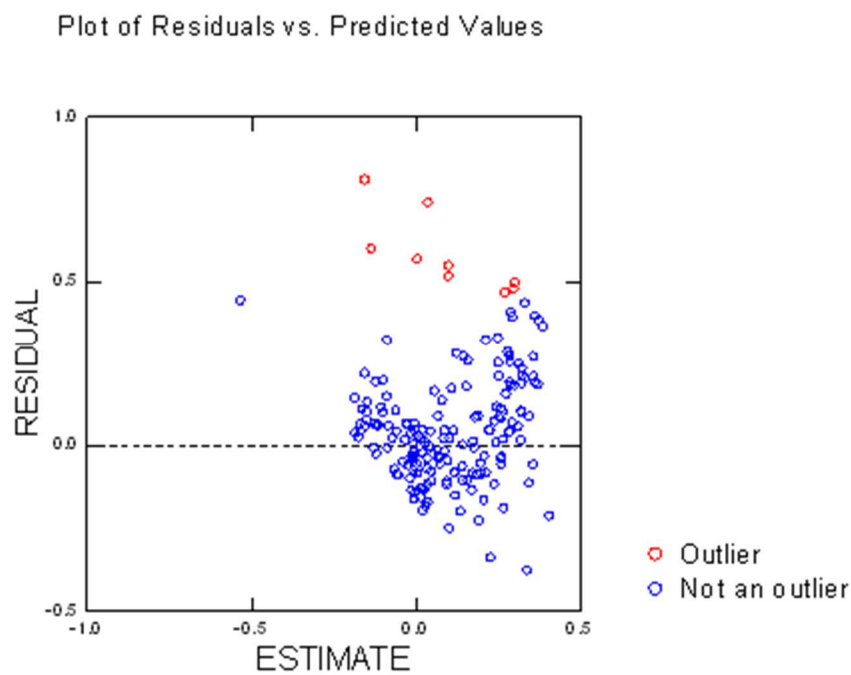
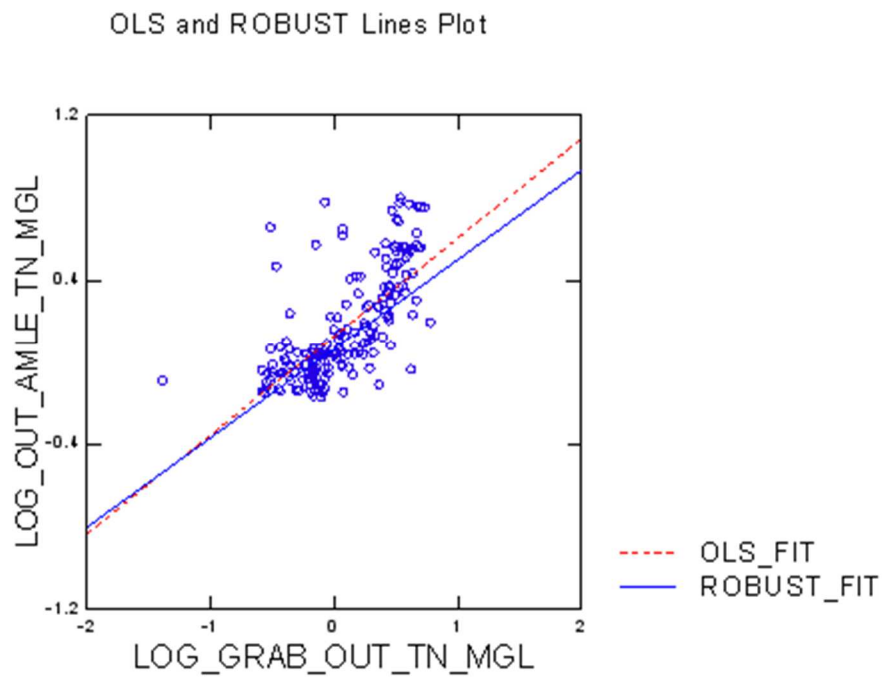


Figure J-9: Comparison of measured and predicted outflow total-N concentration. Note that concentrations are expressed as \log_{10} values.

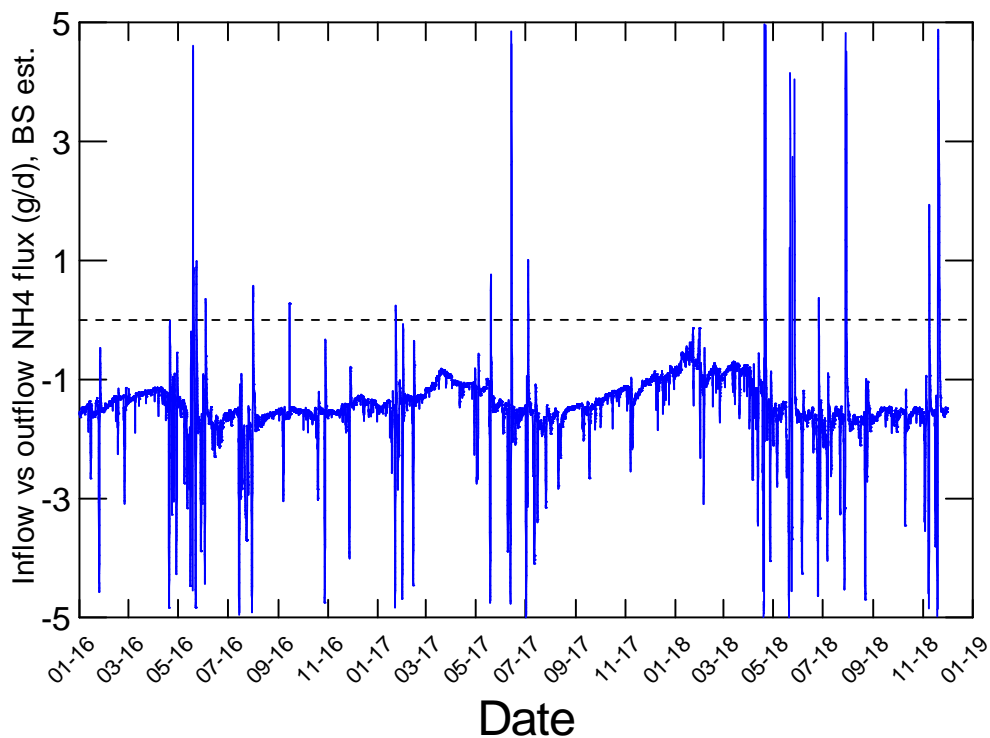


Figure J-10: Performance of the woodchip filter in terms of ammoniacal-N removal, grams per day. Negative values indicate that the filter is a net source of ammoniacal-N. The spikes are artefacts of timing differences between the two models.

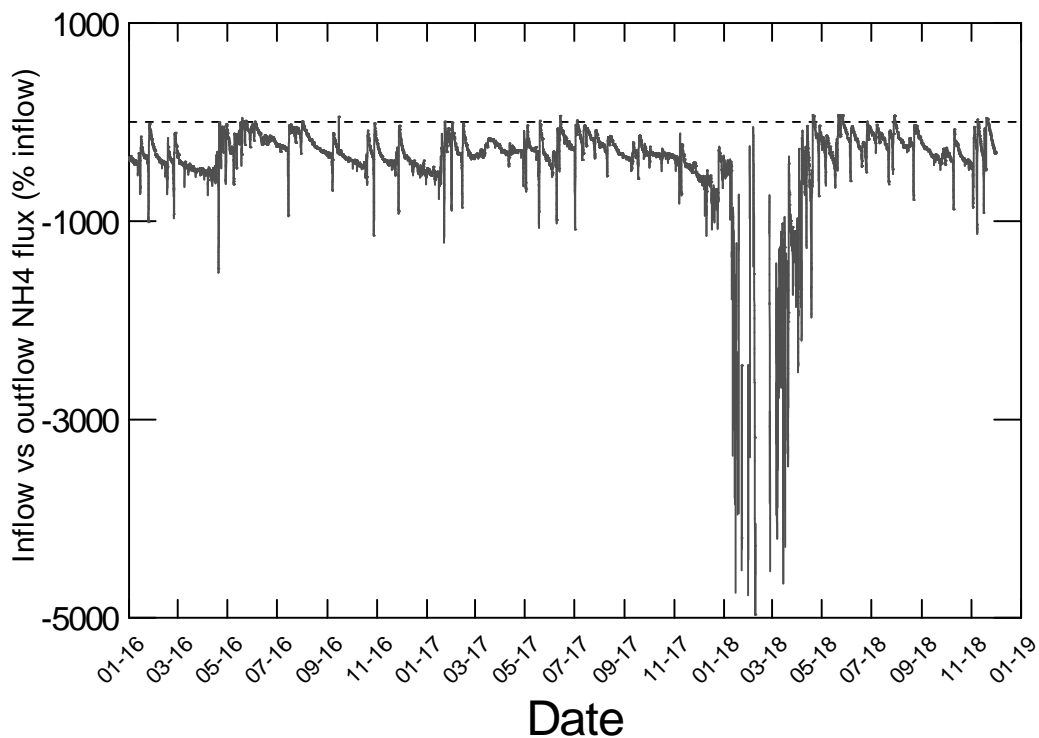


Figure J-11: Performance of the woodchip filter in terms of ammoniacal-N removal, reported as proportion of inflow load. Negative values indicate that the filter is a net source of ammoniacal-N. The spikes and large negative values are artefacts of timing differences between the two models and extremely low flows that occurred in summer 2017/2018.

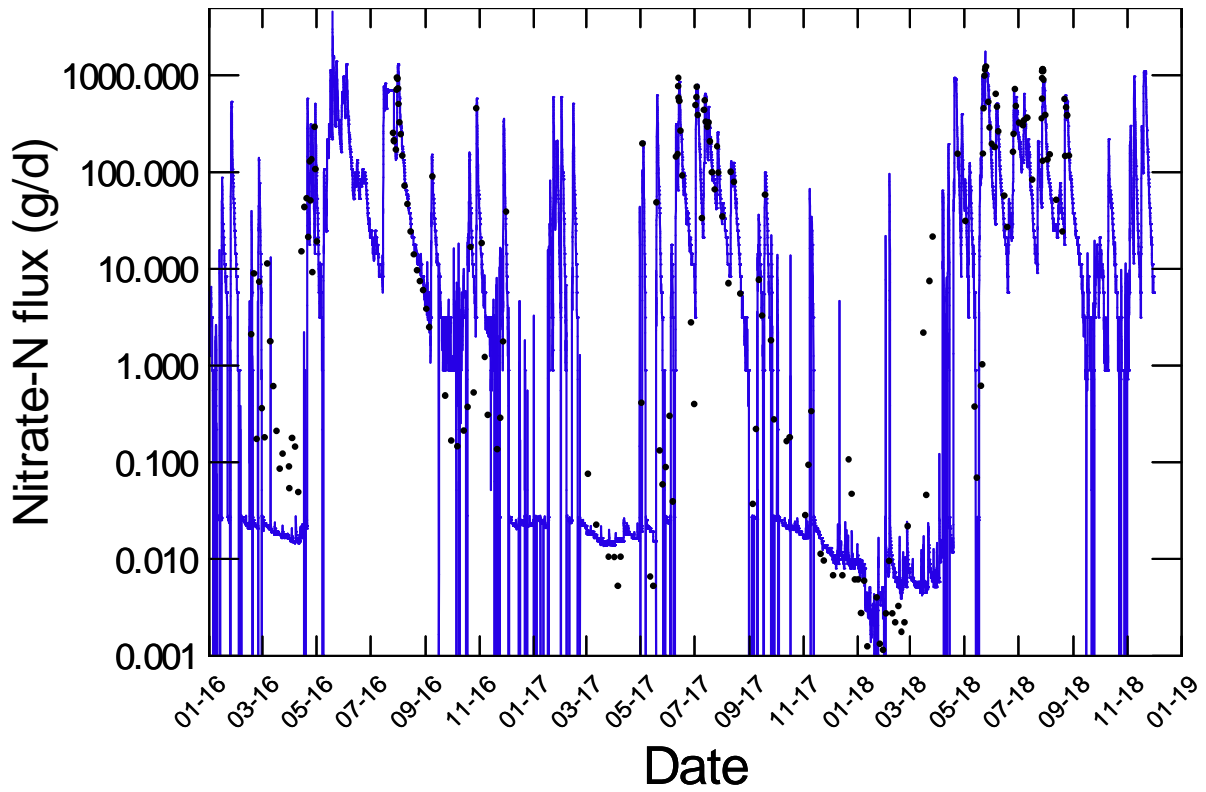


Figure J-12: Time-series of hourly average outflow nitrate-N flux derived from a mixed regression model. The black dots are grab sample flux estimates. The spikes <0.001 are artefacts of the calculation process, and were removed from the performance calculations. These are hourly average values derived from five-minute data.

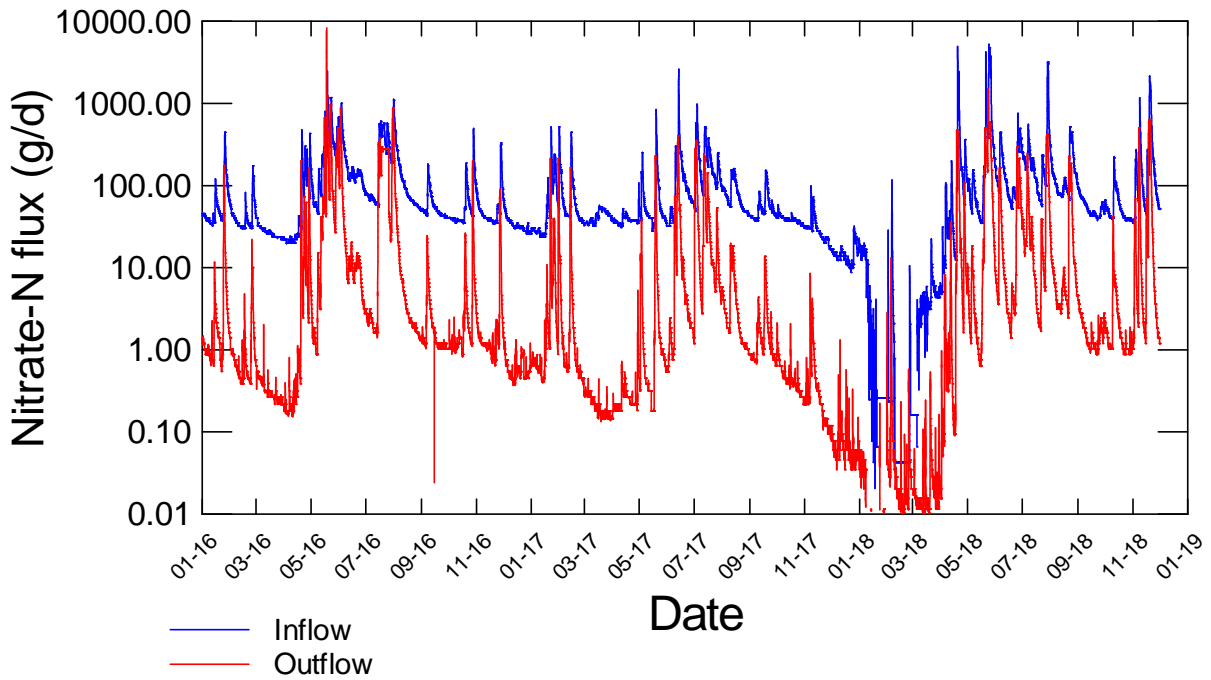


Figure J-13: Time-series of hourly average inflow and outflow nitrate-N flux derived from two bootstrap regression models. These are hourly average values derived from five-minute data.

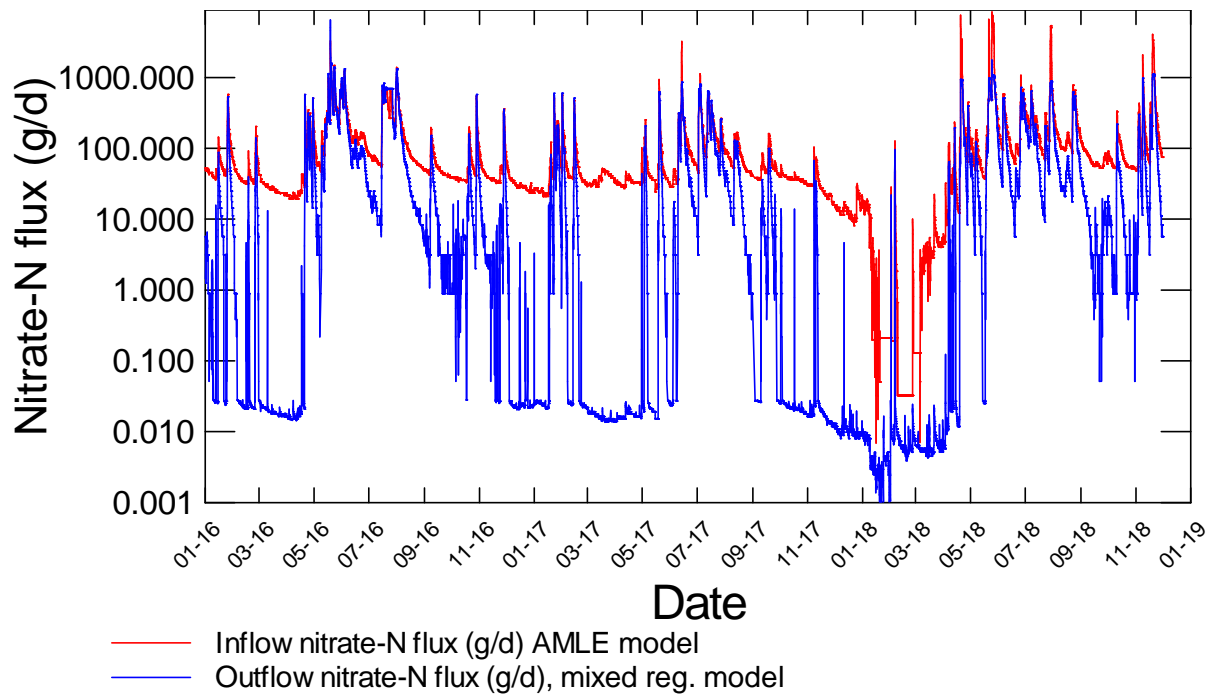


Figure J-14: Nitrate-N inflow and outflow flux from woodchip filter, estimated using two models. AMLE = model from LOADEST modelling package (Runkel et al. 2013), and the mixed regression model uses two relationships between discharge and concentration classified according to flow conditions. The relationship between model estimates and grab sample measurements are shown in Figure J-12.

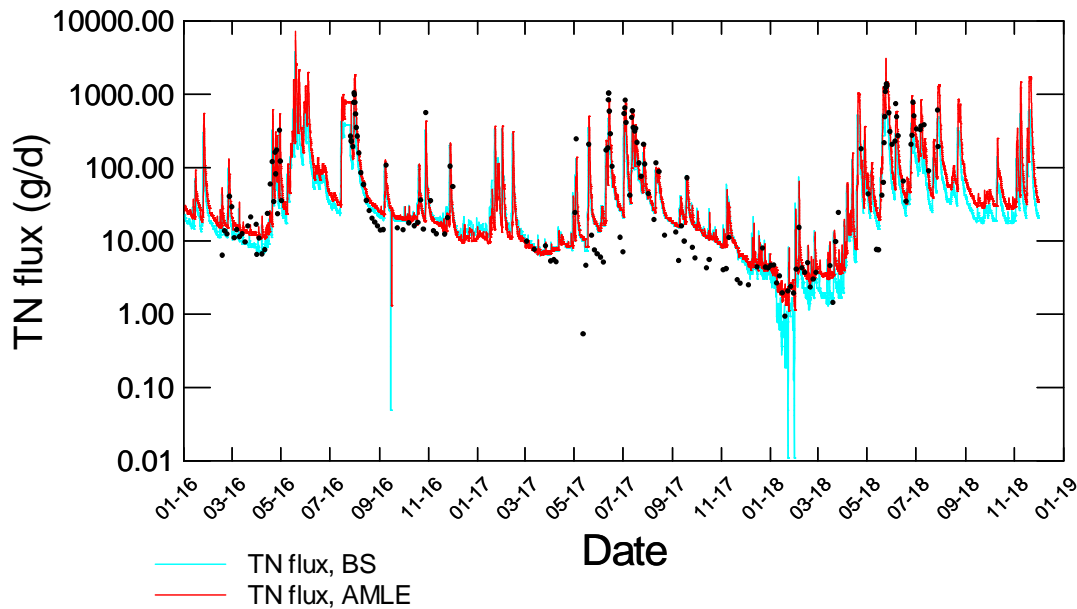


Figure J-15: TN outflow flux from the woodchip filter, estimated using two models. The black dots indicate instantaneous flux estimated from grab samples used to calibrate the models. BS=bootstrap regression model, AMLE = model from LOADEST modelling package (Runkel et al. 2013).

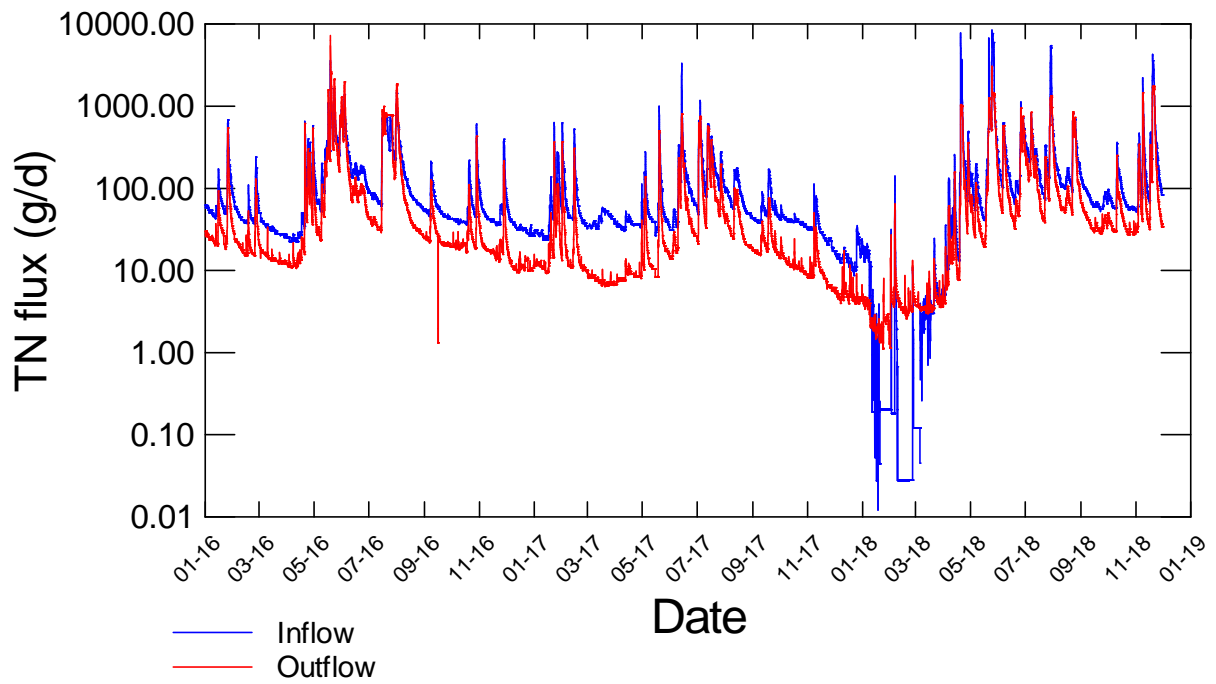


Figure J-16: Comparison of woodchip filter inflow and outflow TN flux estimated using AMLE regression models.

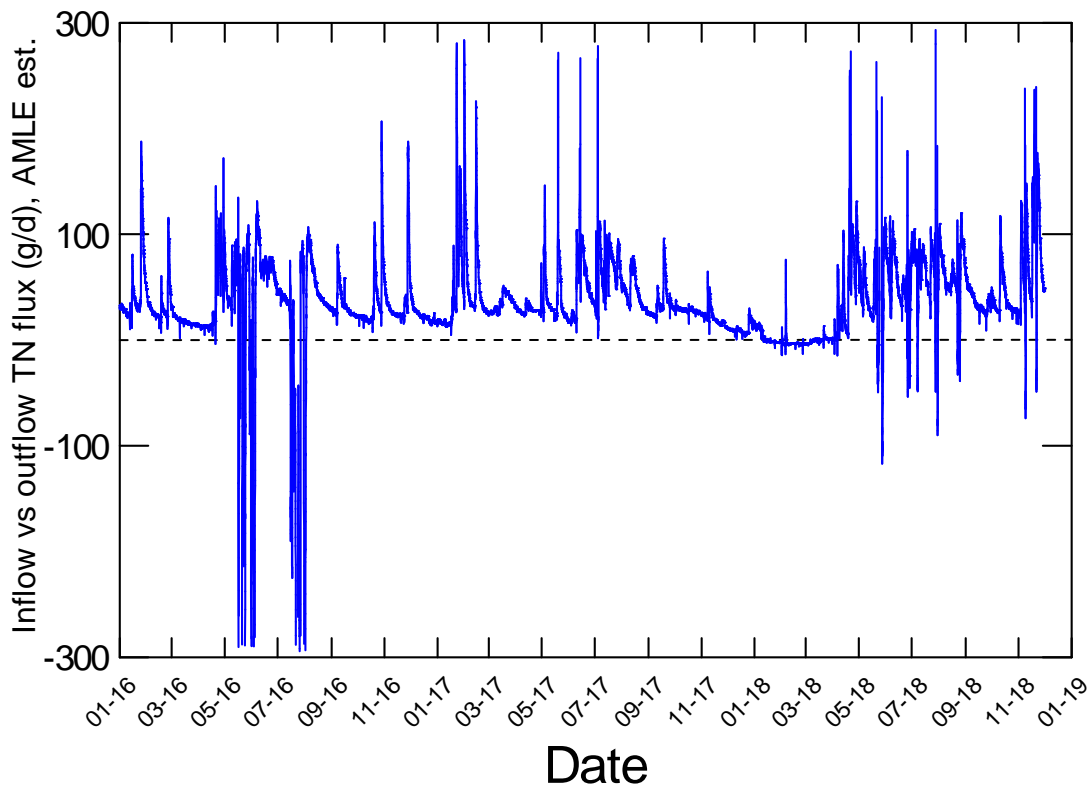


Figure J-17: TN removal by woodchip filter - inflow minus outflow TN flux, estimated using bootstrap regression models.

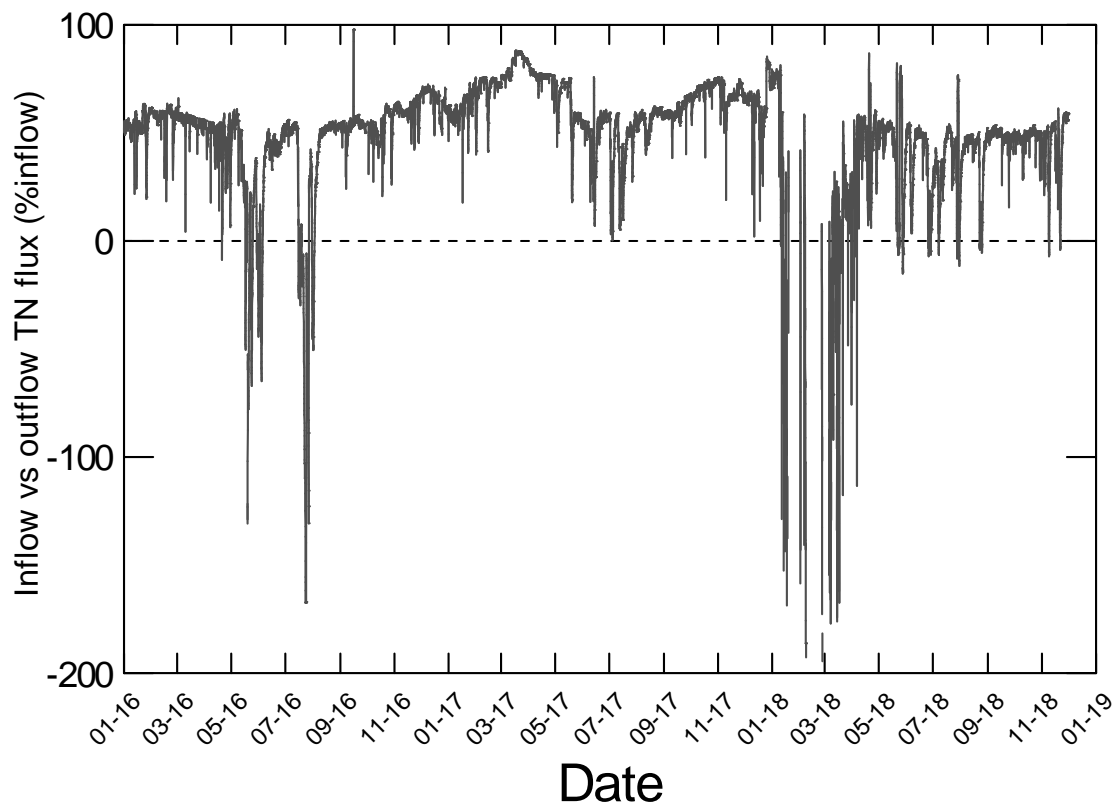


Figure J-18: Efficacy of TN removal by woodchip filter, expressed as proportion of inflow flux removed , estimated using bootstrap regression models.

Table J-2: Woodchip filter performance data - ammoniacal-N. Data derived from AMLE models.

Est. Period	Ammoniacal-N inflow						Ammoniacal-N outflow					
	No. results/ period	Mean load (g/d)	95% LCI	95% UCI	SE Prediction	Std. Error	No. results/ period	Mean load (g/d)	95% LCI	95% UCI	SE Prediction	Std. Error
Entire record	25584	1.19	1.05	1.34	0.07	0.07	25584	3.48	2.73	4.37	0.42	0.42
Autumn	6624	1.35	1.13	1.6	0.12	0.12	6624	2.43	1.74	3.31	0.4	0.4
Winter	6624	1.23	1.08	1.39	0.08	0.08	6624	3.64	3.08	4.27	0.3	0.3
Spring	6552	1.16	0.94	1.42	0.12	0.12	6552	4.97	3.57	6.75	0.81	0.81
Summer	5784	0.99	0.8	1.2	0.1	0.1	5784	2.82	1.71	4.38	0.68	0.68
Dec. 2015	24	1.19	0.82	1.66	0.21	0.12	24	4.99	1.68	11.62	2.62	2.49
Jan. 2016	744	1.74	1.38	2.17	0.2	0.19	744	5.02	1.81	11.19	2.46	2.45
Feb. 2016	696	1.01	0.82	1.23	0.1	0.1	696	3.42	1.34	7.26	1.55	1.55
Mar. 2016	744	0.48	0.39	0.58	0.05	0.05	744	2.17	0.94	4.3	0.87	0.87
Apr. 2016	720	0.86	0.71	1.03	0.08	0.08	720	2.33	1.17	4.2	0.78	0.78
May. 2016	744	2.5	2.09	2.96	0.22	0.2	744	3.82	2.2	6.2	1.03	1.02
June. 2016	720	1.43	1.22	1.66	0.11	0.1	720	3.06	1.95	4.57	0.67	0.66
July. 2016	744	1.55	1.33	1.79	0.12	0.11	744	3.48	2.49	4.74	0.58	0.57
Aug. 2016	744	0.98	0.83	1.15	0.08	0.07	744	2.86	2.15	3.73	0.4	0.39
Sep. 2016	720	0.55	0.46	0.66	0.05	0.05	720	2.51	1.93	3.21	0.33	0.32
Oct. 2016	744	0.99	0.81	1.21	0.1	0.1	744	3.24	2.48	4.16	0.43	0.42
Nov. 2016	720	1.2	0.96	1.47	0.13	0.12	720	3.42	2.47	4.61	0.55	0.54
Dec. 2016	744	0.84	0.68	1.02	0.09	0.08	744	2.79	1.97	3.84	0.48	0.47
Jan. 2017	744	1.78	1.4	2.23	0.21	0.2	744	3.27	2.09	4.87	0.71	0.71
Feb. 2017	672	1.95	1.53	2.44	0.23	0.22	672	2.86	1.84	4.26	0.62	0.61
Mar. 2017	744	0.73	0.6	0.89	0.07	0.07	744	1.45	1.06	1.93	0.22	0.22
Apr. 2017	720	0.46	0.38	0.56	0.05	0.05	720	1.23	0.92	1.6	0.17	0.17

Est. Period	Ammoniacal-N inflow						Ammoniacal-N outflow					
	No. results/ period	Mean load (g/d)	95% LCI	95% UCI	SE Prediction	Std. Error	No. results/ period	Mean load (g/d)	95% LCI	95% UCI	SE Prediction	Std. Error
May. 2016	744	0.66	0.55	0.79	0.06	0.05	744	1.58	1.22	2	0.2	0.19
June. 2016	720	1.01	0.85	1.2	0.09	0.07	720	2.05	1.62	2.56	0.24	0.23
July. 2016	744	1.32	1.14	1.53	0.1	0.09	744	2.88	2.27	3.61	0.34	0.33
Aug. 2017	744	0.55	0.46	0.65	0.05	0.05	744	2.26	1.71	2.92	0.31	0.3
Sep. 2017	720	0.54	0.45	0.65	0.05	0.05	720	2.47	1.86	3.22	0.35	0.34
Oct. 2017	744	0.54	0.44	0.65	0.05	0.05	744	2.45	1.84	3.2	0.35	0.34
Nov. 2017	720	0.57	0.47	0.69	0.06	0.06	720	2.71	2.03	3.56	0.39	0.38
Dec. 2017	744	0.38	0.31	0.46	0.04	0.04	744	2.14	1.63	2.75	0.28	0.28
Jan. 2018	744	0.14	0.11	0.17	0.01	0.01	744	1.24	0.9	1.67	0.2	0.19
Feb. 2018	672	0.05652	0.0407	0.07647	0.009151	0.005555	672	1.69	1.3	2.17	0.22	0.22
Mar. 2018	744	0.06488	0.04954	0.08349	0.00868	0.008411	744	1.25	0.93	1.64	0.18	0.18
Apr. 2018	720	2.19	1.69	2.8	0.28	0.23	720	3.47	2.58	4.57	0.51	0.5
May. 2016	744	4.18	3.3	5.22	0.49	0.43	744	4.58	3.6	5.74	0.54	0.52
June. 2016	720	1.15	0.99	1.34	0.09	0.08	720	4.36	3.47	5.41	0.5	0.48
July. 2016	744	1.96	1.64	2.33	0.18	0.14	744	5.57	4.42	6.94	0.64	0.62
Aug. 2018	744	1.09	0.93	1.28	0.09	0.08	744	6.15	4.6	8.06	0.88	0.86
Sep. 2018	720	0.52	0.43	0.62	0.05	0.05	720	5.49	3.75	7.78	1.03	1.02
Oct. 2018	744	0.77	0.63	0.93	0.08	0.07	744	7.55	4.82	11.28	1.66	1.64
Nov. 2018	720	4.8	3.55	6.35	0.72	0.67	720	14.96	8.44	24.61	4.16	4.13

Table J-3: Summary statistics for woodchip filter performance - nitrate-N removal, entire assessment period. Data derived from AMLE model (inflow) and process model (outflow).

Statistic entire assessment period	Inflow nitrate-N conc. (mg/L) [AMLE]	Outflow nitrate-N conc. (mg/L) [Proc. model]	Inflow nitrate-N flux (g/d) [AMLE]	Outflow nitrate-N flux (g/d) [Proc. model]	Nitrate-N removal (g/d) (inflow-outflow)	Nitrate-N removal efficacy. (% inflow removed)	Nitrate-N removal rate (g/m3/d)
N of Cases	24391	24391	24391	24391	24391	24391	24391
Minimum	1.0	0.0	0.0	0.0	0.0	0.0	0.0
Maximum	5.3	4.8	8364.3	2628.0	6961.2	100.0	305.5
Median	2.3	0.7	51.3	15.3	32.7	71.9	0.9
Arithmetic Mean	2.4	1.0	146.1	72.9	73.3	66.2	2.4
Std Error of Mean	0.0	0.0	2.8	1.0	2.1	0.2	0.1
95.0% LCL of Mean	2.4	1.0	140.7	70.9	69.2	65.8	2.2
95.0% UCL of Mean	2.4	1.0	151.5	74.8	77.4	66.5	2.6
Std Deviation	0.5	1.0	432.8	151.9	327.1	31.0	14.7
Cleveland percentiles							
1.00%	1.7	0.0	2.6	0.0	2.4	6.7	0.1
5.00%	1.9	0.0	12.1	0.0	10.5	13.1	0.3
10.00%	1.9	0.0	21.6	0.1	15.9	20.0	0.4
20.00%	2.0	0.0	30.6	0.4	21.3	32.6	0.5
25.00%	2.1	0.1	33.2	0.8	23.2	39.3	0.6
30.00%	2.1	0.1	35.8	1.3	24.7	44.5	0.6
40.00%	2.2	0.3	41.5	5.4	28.4	57.5	0.7
50.00%	2.3	0.7	51.3	15.3	32.7	71.9	0.9
60.00%	2.4	1.1	65.8	28.0	36.5	86.9	1.0
70.00%	2.5	1.5	93.5	50.4	41.6	95.5	1.3
75.00%	2.7	1.7	116.8	69.1	46.1	97.7	1.4
80.00%	2.9	1.9	143.8	91.6	52.4	98.9	1.5
90.00%	3.1	2.5	285.3	201.1	88.6	99.6	2.2
95.00%	3.3	2.9	503.4	402.2	150.5	99.9	3.2
99.00%	4.0	3.6	1464.5	781.1	654.0	100.0	25.1

Table J-4: Summary statistics for woodchip filter performance - nitrate-N removal, by season. Data derived from AMLE model (inflow) and process model (outflow).

Statistic	Summer only	Inflow nitrate-N conc. (mg/L) [AMLE]	Outflow nitrate-N conc. (mg/L) [Proc. model]	Inflow nitrate-N flux (g/d) [AMLE]	Outflow nitrate-N flux (g/d) [Proc. model]	Nitrate-N removal (g/d) (inflow-outflow)	Nitrate-N removal efficacy. (% inflow removed)	Nitrate-N removal rate (g/m3/d)
N of Cases		4809	4809	4809	4809	4809	4809	4809
Minimum		1.0	0.0	0.0	0.0	0.0	0.2	0.0
Maximum		3.3	2.2	575.9	345.3	406.6	100.0	6.3
Median		2.0	0.1	33.8	0.8	33.0	97.3	0.6
Arithmetic Mean		2.2	0.2	49.0	6.8	42.2	93.6	0.8
Std Error of Mean		0.0	0.0	1.0	0.4	0.6	0.1	0.0
95.0% LCL of Mean		2.1	0.2	47.1	6.1	40.9	93.4	0.8
95.0% UCL of Mean		2.2	0.2	50.9	7.6	43.4	93.9	0.8
Std Deviation		0.3	0.3	66.5	26.3	44.6	8.8	0.7
Cleveland percentiles								
1.00%		1.5	0.0	1.0	0.0	1.0	57.4	0.1
5.00%		1.9	0.0	9.3	0.0	8.9	79.0	0.3
10.00%		1.9	0.0	11.6	0.1	11.0	83.0	0.4
20.00%		2.0	0.0	15.9	0.2	14.4	88.5	0.4
25.00%		2.0	0.0	22.3	0.2	21.0	91.0	0.5
30.00%		2.0	0.0	25.1	0.3	24.3	92.3	0.5
40.00%		2.0	0.0	29.3	0.5	28.6	94.8	0.6
50.00%		2.0	0.1	33.8	0.8	33.0	97.3	0.6
60.00%		2.1	0.1	38.6	1.2	36.6	98.5	0.7
70.00%		2.3	0.2	43.9	2.0	40.4	99.0	0.8
75.00%		2.4	0.2	47.9	3.1	44.3	99.3	0.8
80.00%		2.4	0.3	52.2	5.0	49.7	99.4	0.9
90.00%		2.5	0.4	88.4	9.9	79.7	99.7	1.3
95.00%		2.6	0.6	149.1	27.8	122.4	99.9	2.0
99.00%		2.9	1.2	430.9	131.1	241.6	100.0	4.0

Table J-4: Summary statistics for woodchip filter performance - nitrate-N removal, by season. (continued)

Statistic	Inflow nitrate-N conc. (mg/L) [AMLE]	Outflow nitrate-N conc. (mg/L) [Proc. model]	Inflow nitrate-N flux (g/d) [AMLE]	Outflow nitrate-N flux (g/d) [Proc. model]	Nitrate-N removal (g/d) (inflow-outflow)	Nitrate-N removal efficacy. (% inflow removed)	Nitrate-N removal rate (g/m3/d)
N of Cases	6506	6506	6506	6506	6506	6506	6506
Minimum	1.0	0.0	0.0	0.0	0.0	0.0	0.0
Maximum	4.7	4.2	8364.3	2628.0	6961.2	100.0	305.5
Median	2.1	0.0	35.8	0.5	30.8	98.7	0.6
Arithmetic Mean	2.3	0.6	191.8	72.2	119.6	79.9	4.2
Std Error of Mean	0.0	0.0	8.5	2.3	6.7	0.4	0.3
95.0% LCL of Mean	2.3	0.6	175.2	67.8	106.3	79.2	3.6
95.0% UCL of Mean	2.3	0.7	208.4	76.7	132.8	80.5	4.8
Std Deviation	0.5	1.0	682.8	184.4	543.3	28.5	24.7
Cleveland percentiles							
1.00%	1.6	0.0	1.9	0.0	1.9	8.0	0.1
5.00%	1.8	0.0	4.0	0.0	4.0	16.6	0.2
10.00%	1.9	0.0	8.2	0.0	7.3	32.4	0.3
20.00%	1.9	0.0	23.6	0.1	21.4	50.6	0.4
25.00%	2.0	0.0	26.1	0.1	23.1	59.2	0.4
30.00%	2.0	0.0	28.5	0.1	23.7	74.7	0.5
40.00%	2.0	0.0	32.9	0.2	28.1	92.1	0.5
50.00%	2.1	0.0	35.8	0.5	30.8	98.7	0.6
60.00%	2.2	0.2	42.2	3.3	33.2	99.4	0.8
70.00%	2.4	0.6	60.8	19.1	40.1	99.6	1.2
75.00%	2.5	1.1	91.8	36.7	44.7	99.7	1.3
80.00%	2.6	1.4	136.2	75.0	54.6	99.8	1.6
90.00%	2.9	2.2	342.6	207.4	146.7	99.9	2.5
95.00%	3.2	2.9	646.9	497.0	225.6	100.0	3.9
99.00%	4.3	3.8	4458.6	951.7	3532.3	100.0	164.8

Table J-4: Summary statistics for woodchip filter performance - nitrate-N removal, by season. (continued)

Statistic	Winter only	Inflow nitrate-N conc. (mg/L) [AMLE]	Outflow nitrate-N conc. (mg/L) [Proc. model]	Inflow nitrate-N flux (g/d) [AMLE]	Outflow nitrate-N flux (g/d) [Proc. model]	Nitrate-N removal (g/d) (inflow-outflow)	Nitrate-N removal efficacy. (% inflow removed)	Nitrate-N removal rate (g/m3/d)
N of Cases		6524	6524	6524	6524	6524	6524	6524
Minimum		1.9	0.2	28.6	3.8	0.0	0.0	0.0
Maximum		4.8	4.3	5394.7	962.3	4452.6	86.7	203.3
Median		2.5	2.0	127.6	84.2	35.6	28.4	1.2
Arithmetic Mean		2.6	1.9	222.4	149.1	73.3	34.3	2.5
Std Error of Mean		0.0	0.0	4.7	2.0	3.5	0.3	0.2
95.0% LCL of Mean		2.6	1.9	213.1	145.2	66.5	33.8	2.2
95.0% UCL of Mean		2.7	2.0	231.7	153.1	80.1	34.8	2.8
Std Deviation		0.4	0.8	383.6	163.0	281.1	20.9	12.2
Cleveland percentiles								
1.00%		1.9	0.3	28.7	5.9	9.0	3.6	0.4
5.00%		2.1	0.6	47.0	15.8	15.8	7.7	0.7
10.00%		2.2	0.8	56.4	21.0	18.2	10.5	0.7
20.00%		2.3	1.2	69.6	32.9	21.0	15.7	0.8
25.00%		2.3	1.3	76.8	42.0	22.8	18.0	0.8
30.00%		2.3	1.4	84.2	52.0	24.6	20.1	0.9
40.00%		2.4	1.7	102.7	68.7	28.9	23.7	1.0
50.00%		2.5	2.0	127.6	84.2	35.6	28.4	1.2
60.00%		2.7	2.3	150.7	111.3	42.6	35.3	1.4
70.00%		2.9	2.5	196.8	149.0	50.2	43.3	1.5
75.00%		3.0	2.6	232.0	183.4	56.6	49.1	1.7
80.00%		3.0	2.7	285.0	232.7	69.6	55.7	1.9
90.00%		3.2	3.0	494.7	424.0	95.9	68.4	2.5
95.00%		3.4	3.3	632.1	498.3	149.3	72.5	3.4
99.00%		3.8	3.6	1235.5	704.8	502.2	81.7	16.7

Table J-4: Summary statistics for woodchip filter performance - nitrate-N removal, by season. (continued)

Statistic Spring only	Inflow nitrate-N conc. (mg/L) [AMLE]	Outflow nitrate-N conc. (mg/L) [Proc. model]	Inflow nitrate-N flux (g/d) [AMLE]	Outflow nitrate-N flux (g/d) [Proc. model]	Nitrate-N removal (g/d) (inflow-outflow)	Nitrate-N removal efficacy. (% inflow removed)	Nitrate-N removal rate (g/m3/d)
N of Cases	6552	6552	6552	6552	6552	6552	6552
Minimum	2.0	0.0	15.9	0.1	7.2	6.6	0.3
Maximum	5.3	4.8	4069.7	1214.2	2878.4	99.9	130.7
Median	2.2	0.9	49.5	18.8	32.7	63.0	1.0
Arithmetic Mean	2.5	1.0	96.1	46.0	50.1	64.1	1.8
Std Error of Mean	0.0	0.0	3.2	1.5	1.8	0.3	0.1
95.0% LCL of Mean	2.5	1.0	89.8	43.0	46.5	63.6	1.6
95.0% UCL of Mean	2.5	1.0	102.3	49.0	53.6	64.7	2.0
Std Deviation	0.6	0.8	259.3	124.6	147.3	23.0	6.7
Cleveland percentiles							
1.00%	2.0	0.0	17.6	0.5	14.5	19.1	0.5
5.00%	2.1	0.1	25.2	1.1	16.7	28.5	0.5
10.00%	2.1	0.1	31.5	1.4	18.7	34.8	0.5
20.00%	2.1	0.2	35.8	2.9	23.2	42.9	0.6
25.00%	2.1	0.3	36.9	4.3	24.3	44.9	0.7
30.00%	2.2	0.5	38.7	6.8	25.3	47.5	0.7
40.00%	2.2	0.7	42.0	11.5	29.1	54.5	0.9
50.00%	2.2	0.9	49.5	18.8	32.7	63.0	1.0
60.00%	2.3	1.1	54.7	24.0	34.7	70.1	1.0
70.00%	2.9	1.3	62.5	31.5	38.4	79.7	1.4
75.00%	3.0	1.4	70.0	36.3	40.4	88.2	1.5
80.00%	3.0	1.6	80.0	43.5	43.6	92.3	1.5
90.00%	3.2	2.0	127.9	79.0	58.3	96.0	2.1
95.00%	3.6	2.4	245.9	153.7	88.8	97.0	3.3
99.00%	4.4	3.8	1151.0	838.5	307.4	98.4	14.2

Table J-5: Woodchip filter performance data - nitrate-N. Data derived from AMLE model (inlet) and process model (outlet).

Period	Nitrate-N inflow						Nitrate-N Outflow					
	No. results/ period	Mean load (g/d)	95.0% LCL	95.0% UCL	Std Dev.	Std Error	No. results/ period	Mean load (g/d)	95.0% LCL	95.0% UCL	Std Dev.	Std Error
Entire record	24391	146.1	140.7	151.5	432.8	2.8	24391	72.9	70.9	74.8	151.9	1.0
Autumn	6506	191.8	175.2	208.4	682.8	8.5	6506	72.2	67.8	76.7	184.4	2.3
Winter	6524	222.4	213.1	231.7	383.6	4.7	6524	149.1	145.2	153.1	163.0	2.0
Spring	6552	96.1	89.8	102.3	259.3	3.2	6552	46.0	43.0	49.0	124.6	1.5
Summer	4809	49.0	47.1	50.9	66.5	1.0	4809	6.8	6.1	7.6	26.3	0.4
Jan-16	744	79.2	72.8	85.7	90.1	3.3	744	20.0	16.1	23.9	53.8	2.0
Feb-16	696	48.2	46.1	50.3	27.9	1.1	696	2.9	2.3	3.5	8.1	0.3
Mar-16	744	27.4	27.1	27.8	4.8	0.2	744	0.1	0.1	0.1	0.1	0.0
Apr-16	720	85.5	77.5	93.6	110.2	4.1	720	26.7	22.6	30.9	57.0	2.1
May-16	744	368.4	340.5	396.3	387.3	14.2	744	197.4	178.9	215.8	256.4	9.4
Jun-16	720	233.8	218.6	249.1	207.9	7.7	720	120.5	110.8	130.3	133.9	5.0
Jul-16	656	270.8	251.2	290.4	255.7	10.0	656	190.8	174.5	207.1	212.4	8.3
Aug-16	744	156.7	142.3	171.1	200.0	7.3	744	94.5	83.3	105.6	155.1	5.7
Sep-16	720	57.1	55.0	59.3	29.2	1.1	720	15.1	13.4	16.8	23.1	0.9
Oct-16	744	68.1	62.6	73.6	76.2	2.8	744	19.1	15.5	22.7	49.8	1.8
Nov-16	720	58.3	54.1	62.5	57.5	2.1	720	10.7	8.3	13.1	32.5	1.2
Dec-16	744	31.3	30.7	31.8	7.5	0.3	744	0.6	0.5	0.7	0.9	0.0
Jan-17	744	67.1	61.1	73.1	83.2	3.1	744	8.5	6.9	10.1	22.5	0.8
Feb-17	672	81.0	73.8	88.1	94.1	3.6	672	10.4	8.3	12.4	26.9	1.0
Mar-17	744	37.7	37.3	38.2	6.7	0.2	744	0.2	0.2	0.2	0.1	0.0
Apr-17	720	33.9	33.4	34.5	7.1	0.3	720	0.3	0.2	0.4	0.7	0.0
May-17	744	74.7	66.9	82.4	107.2	3.9	744	19.1	15.8	22.4	46.3	1.7
Jun-17	720	161.1	135.6	186.5	347.9	13.0	720	91.7	82.6	100.8	124.2	4.6
Jul-17	738	221.6	209.3	233.9	169.8	6.3	738	186.9	176.9	196.8	137.6	5.1
Aug-17	744	76.2	73.8	78.6	33.5	1.2	744	57.9	55.4	60.4	34.9	1.3
Sep-17	720	55.0	53.1	56.8	25.7	1.0	720	36.1	34.2	38.0	26.1	1.0

Period	Nitrate-N inflow						Nitrate-N Outflow					
	No. results/ period	Mean load (g/d)	95.0% LCL	95.0% UCL	Std Dev.	Std Error	No. results/ period	Mean load (g/d)	95.0% LCL	95.0% UCL	Std Dev.	Std Error
Oct-17	744	37.6	37.3	37.9	4.1	0.2	744	13.0	12.6	13.3	4.4	0.2
Nov-17	720	28.7	27.8	29.6	12.3	0.5	720	8.8	8.0	9.7	11.2	0.4
Dec-17	744	14.1	13.8	14.4	4.0	0.1	744	1.6	1.5	1.7	1.3	0.0
Jan-18	347	10.0	9.3	10.6	6.4	0.3	347	0.6	0.5	0.6	0.6	0.0
Feb-18	118	12.8	8.5	17.1	23.5	2.2	118	6.7	3.2	10.2	19.2	1.8
Mar-18	626	4.2	4.0	4.4	2.7	0.1	626	0.1	0.0	0.1	0.4	0.0
Apr-18	720	260.8	207.5	314.0	727.4	27.1	720	122.0	107.1	136.8	202.9	7.6
May-18	744	797.5	675.7	919.3	1692.5	62.0	744	270.7	247.4	294.0	323.5	11.9
Jun-18	719	221.4	208.0	234.8	183.2	6.8	719	185.5	173.5	197.5	164.1	6.1
Jul-18	742	458.4	391.5	525.4	929.1	34.1	742	248.3	233.4	263.2	206.3	7.6
Aug-18	741	206.5	195.2	217.9	157.1	5.8	741	169.9	160.0	179.9	137.7	5.1
Sep-18	720	71.8	70.5	73.1	17.8	0.7	720	42.5	41.3	43.6	15.7	0.6
Oct-18	744	77.3	74.0	80.6	45.9	1.7	744	41.2	38.6	43.8	36.7	1.3
Nov-18	720	414.0	363.2	464.9	695.4	25.9	720	229.6	207.0	252.2	308.9	11.5

Table J-6: Woodchip filter performance data - total-N. Data derived from bootstrap regression models.

Est. Period	Total-N inflow						Total N outflow					
	No. results/ period	Mean load (g/d)	95% LCI	95% UCI	SE Prediction	Std. Error	No. results/ period	Mean load (g/d)	95% LCI	95% UCI	SE Prediction	Std. Error
Entire record	25584	151.66	144.08	159.54	3.94	3.89	25584	98.44	81.69	117.62	9.17	9.04
Autumn	6624	202.84	190.21	216.07	6.6	6.26	6624	127.25	98.39	161.95	16.24	15.44
Winter	6624	239.51	226.61	252.93	6.71	6.59	6624	179.46	150.38	212.51	15.86	15.61
Spring	6552	103.55	91.5	116.73	6.44	6.38	6552	56.4	35.69	84.89	12.62	12.51
Summer	5784	46.97	44.14	49.93	1.48	1.45	5784	20.29	14.86	27.06	3.12	3.09
Dec. 2015	24	61.48	53.63	70.14	4.21	3.05	24	28.82	17.24	45.33	7.22	5.88
Jan. 2016	744	94.24	85.94	103.13	4.39	4.22	744	49.38	32.41	72.14	10.18	9.89
Feb. 2016	696	57.28	53.14	61.65	2.17	2.09	696	24.57	17.83	33.04	3.89	3.81
Mar. 2016	744	32.22	30.02	34.54	1.15	1.12	744	14.38	11.08	18.34	1.86	1.82
Apr. 2016	720	98.83	92.22	105.79	3.46	3.17	720	62.62	48.72	79.25	7.8	7.12
May. 2016	744	414.38	385.3	445.04	15.24	14.38	744	546.61	367.94	782.5	106.2	97.76
June. 2016	720	261.43	244.43	279.29	8.89	8.37	720	227.15	175.71	288.94	28.94	26.75
July. 2016	744	304.43	283.21	326.8	11.12	10.59	744	361.64	275.57	466.12	48.71	46.76
Aug. 2016	744	170.44	158.21	183.36	6.42	5.98	744	139.66	106.13	180.43	18.99	16.97
Sep. 2016	720	62.25	57.85	66.88	2.3	2.22	720	29.4	23.51	36.3	3.27	3.13
Oct. 2016	744	74.59	69.36	80.12	2.75	2.58	744	37.02	28.52	47.26	4.79	4.48
Nov. 2016	720	64.46	59.96	69.2	2.36	2.22	720	26.71	19.69	35.41	4.02	3.86
Dec. 2016	744	34.84	32.6	37.19	1.17	1.13	744	11.81	8.86	15.44	1.68	1.65
Jan. 2017	744	75.45	69.06	82.28	3.37	3.21	744	29.56	19.31	43.36	6.16	5.99
Feb. 2017	672	91.17	83.1	99.8	4.26	4.08	672	34.11	22.03	50.5	7.3	7.05
Mar. 2017	744	42.32	39.01	45.83	1.74	1.7	744	7.55	5.75	9.73	1.02	1
Apr. 2017	720	37.61	34.72	40.69	1.52	1.49	720	9.02	6.91	11.58	1.2	1.17
May. 2016	744	81.4	75.39	87.74	3.15	2.91	744	38.66	29.58	49.67	5.14	4.62

Est. Period	Total-N inflow						Total N outflow					
	No. results/ period	Mean load (g/d)	95% LCI	95% UCI	SE Prediction	Std. Error	No. results/ period	Mean load (g/d)	95% LCI	95% UCI	SE Prediction	Std. Error
June. 2016	720	171.19	158.82	184.26	6.49	5.5	720	88.87	70.32	110.81	10.35	9.33
July. 2016	744	235.37	221.6	249.77	7.19	6.74	744	163.09	132.9	198.07	16.64	15.5
Aug. 2017	744	80.6	75.68	85.74	2.57	2.45	744	36.88	30.15	44.67	3.71	3.54
Sep. 2017	720	58.11	54.29	62.13	2	1.92	720	23.11	18.71	28.24	2.43	2.33
Oct. 2017	744	40.02	37.25	42.95	1.45	1.41	744	11.91	9.51	14.73	1.33	1.3
Nov. 2017	720	30.81	28.6	33.16	1.16	1.13	720	10.15	7.85	12.92	1.3	1.26
Dec. 2017	744	15.26	14.17	16.42	0.57	0.56	744	5	3.93	6.27	0.6	0.58
Jan. 2018	744	5.14	4.75	5.55	0.21	0.19	744	2.66	1.96	3.53	0.4	0.4
Feb. 2018	672	2.54	2.26	2.83	0.15	0.09	672	5.09	4	6.4	0.61	0.58
Mar. 2018	744	3.79	3.39	4.22	0.21	0.21	744	4.03	3.15	5.09	0.5	0.48
Apr. 2018	720	279.41	254.39	306.21	13.22	11.21	720	126.35	92.95	167.89	19.16	17.72
May. 2016	744	829.38	751.88	912.63	41.02	37.63	744	330.13	253.55	422.62	43.21	40.54
June. 2016	720	236.8	215.67	259.43	11.17	10.85	720	179.92	140.05	227.63	22.38	21.21
July. 2016	744	475.48	426.88	528.05	25.82	24.22	744	261.57	191.68	348.73	40.17	38.74
Aug. 2018	744	218.23	191.14	248.06	14.53	14.34	744	155.04	105.13	220.6	29.58	28.94
Sep. 2018	720	76.41	65.45	88.66	5.93	5.89	720	39.24	24.24	60.19	9.23	9.16
Oct. 2018	744	83.19	69.96	98.2	7.21	7.16	744	44.2	25.76	70.95	11.62	11.53
Nov. 2018	720	445.83	368.42	534.66	42.45	41.79	720	288.43	149.45	505.39	91.86	90.7

Appendix K Efficacy of woodchip filter, inflow AMLE vs outflow process model estimates – Nitrate-N only

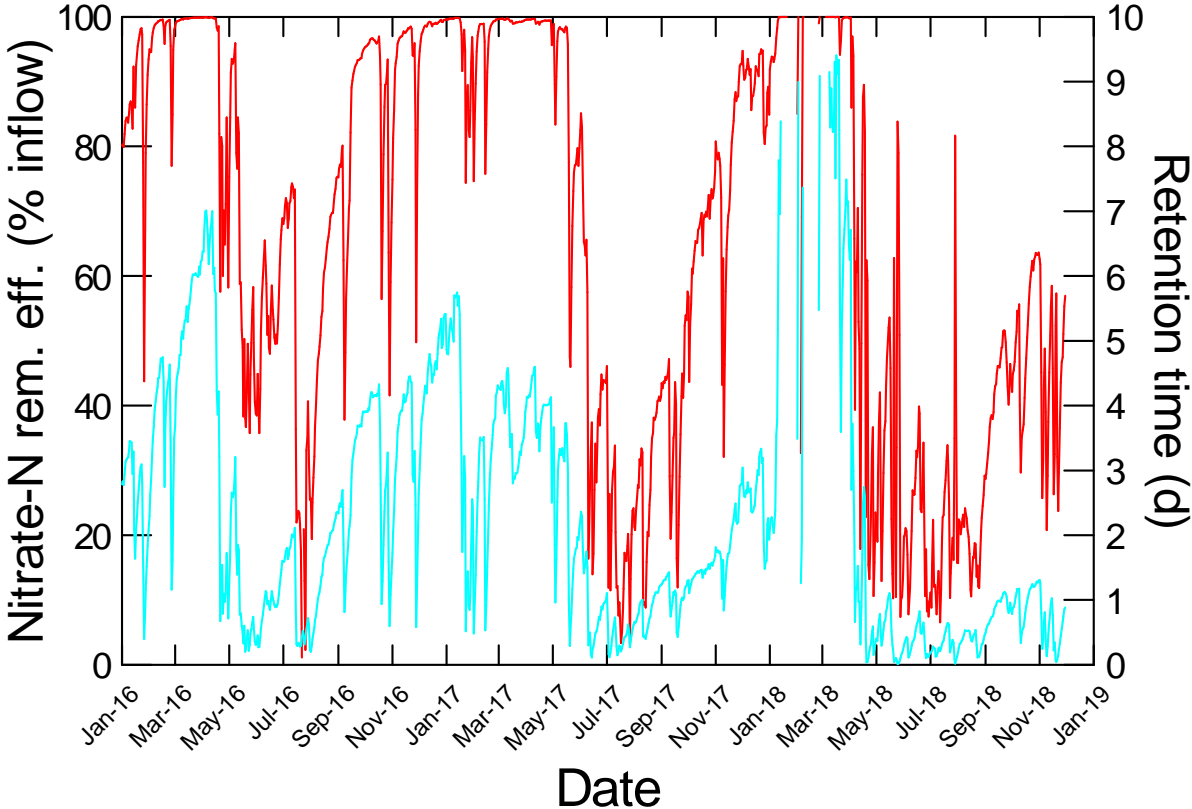


Figure K-1: Relationship between nitrate-N removal (red) and hydraulic retention time (cyan). Nitrate-N removal was estimated as the difference between inflow and outflow mass. Hydraulic retention time was estimated as the quotient of active biofilter volume and inflow, expressed in days after correcting for units. The relationship between water level and retention time was discussed in section 4. The inflow flux was estimated using the LOADEST AMLE model, and the outflow flux was estimated from inflow concentrations using the process described in section 2.5.2.

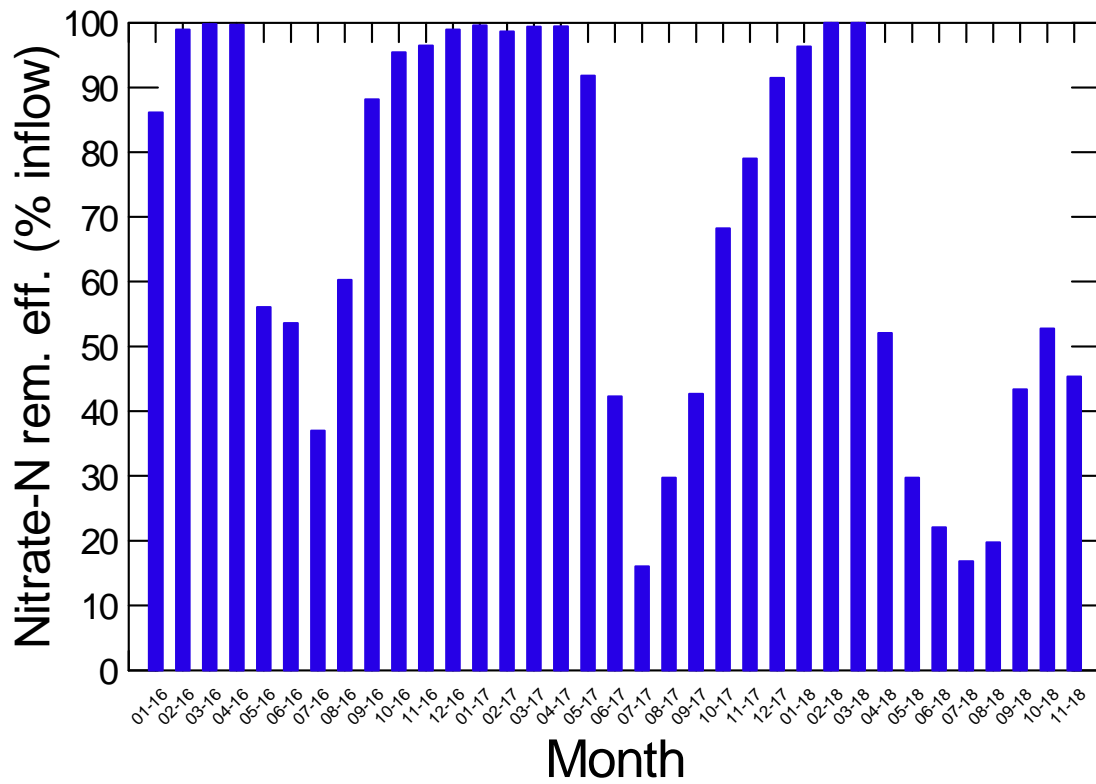


Figure K-2: Median nitrate-N removal efficacy, estimated as the percent of inflow flux removed by the filter by month.

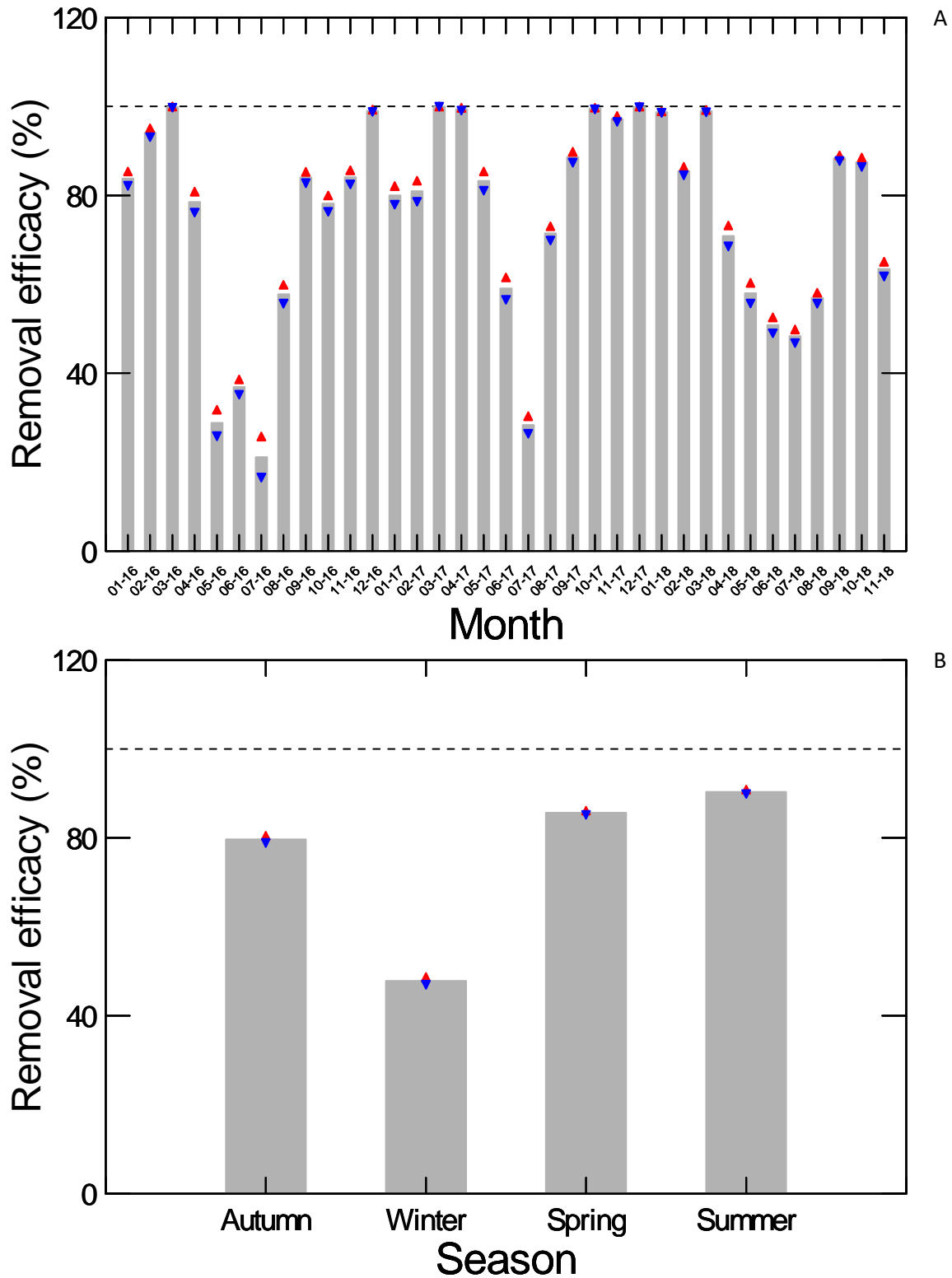


Figure K-3: Nitrate-N removal efficacy for various time periods. A = average efficacy at monthly time step, plus confidence limits; B = seasonal mean plus confidence limits.

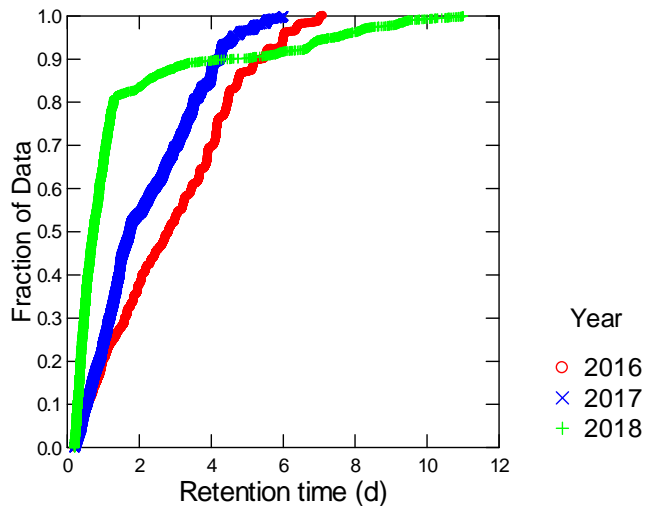


Figure K-4: Distribution of retention time by year.

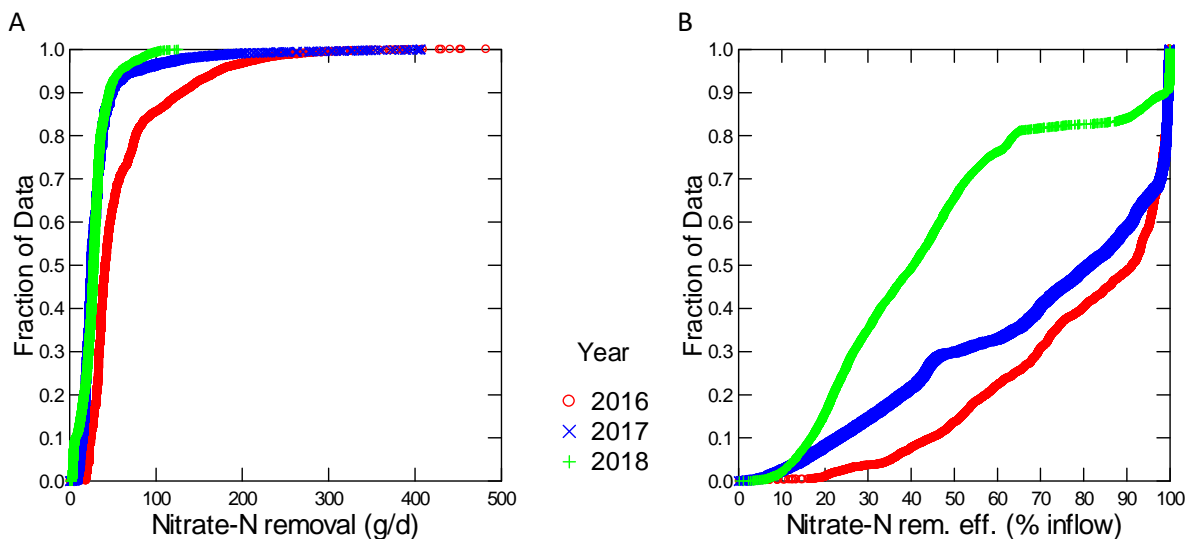


Figure K-5: Distribution of nitrate-N removal performance data by year.

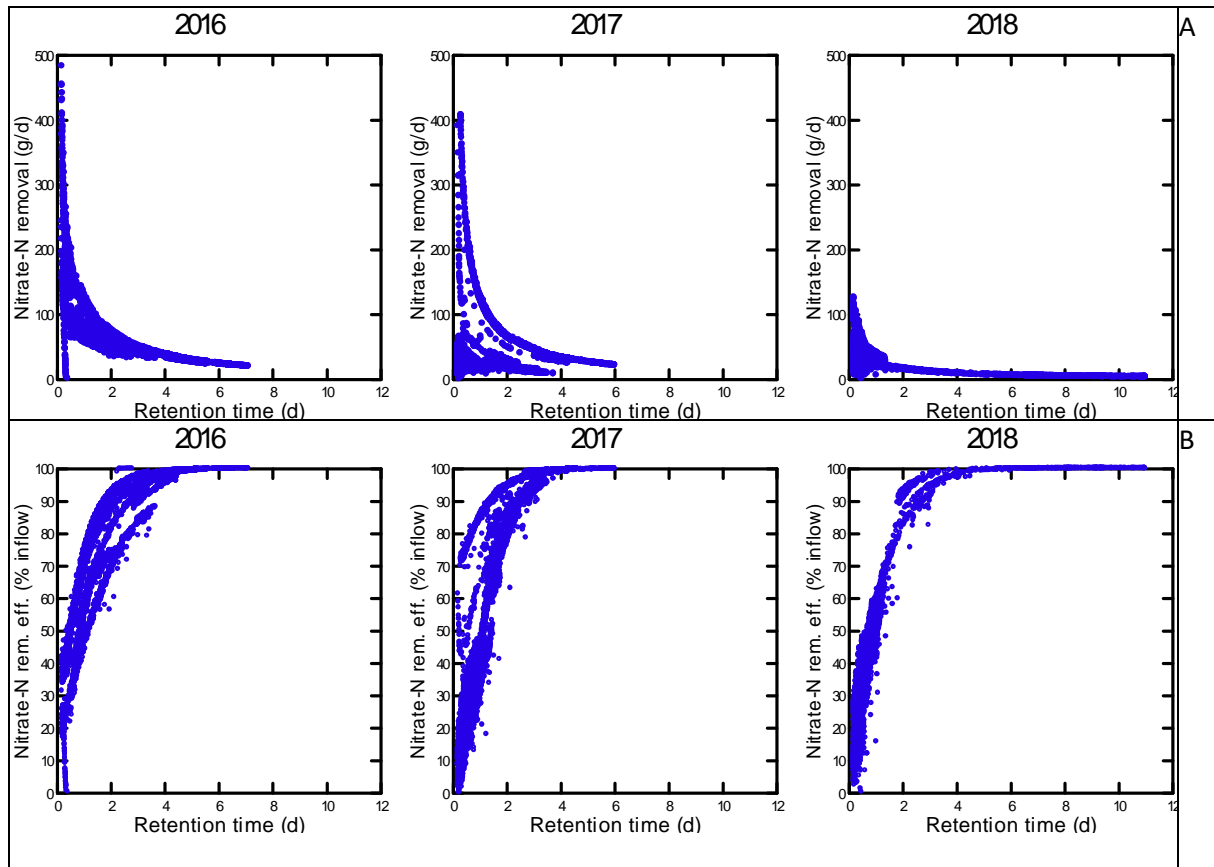


Figure K-6: Relationship between nitrate-N removal performance and retention time by year. A) Nitrate-N removal rate (g/d), and B) nitrate-N removal efficacy in terms of proportion of influent load removed.

Appendix L Nitrate-N removal performance

Three year period	Nitrate-N removal rate (g/m ³ /d)	Nitrate-N removal (g/d)
N of Cases	24391	24391
Minimum	0.0	0.0
Maximum	305.5	6961.2
Median	0.9	32.7
Arithmetic Mean	2.4	73.3
Standard Error of Arithmetic Mean	0.1	2.1
95.0% LCL of Arithmetic Mean	2.2	69.2
95.0% UCL of Arithmetic Mean	2.6	77.4
Standard Deviation	14.7	327.1
Method = CLEVELAND		
1.00%	0.1	2.4
5.00%	0.3	10.5
10.00%	0.4	15.9
20.00%	0.5	21.3
25.00%	0.6	23.2
30.00%	0.6	24.7
40.00%	0.7	28.4
50.00%	0.9	32.7
60.00%	1.0	36.5
70.00%	1.3	41.6
75.00%	1.4	46.1
80.00%	1.5	52.4
90.00%	2.2	88.6
95.00%	3.2	150.5
99.00%	25.1	654.0

Year = 2016	Nitrate-N removal rate (g/m³/d)	Nitrate-N removal (g/d)
N of Cases	8696	8696
Minimum	0.0	0.9
Maximum	19.6	1550.5
Median	0.7	41.9
Arithmetic Mean	1.0	65.5
Standard Error of Arithmetic Mean	0.0	0.7
95.0% LCL of Arithmetic Mean	1.0	64.1
95.0% UCL of Arithmetic Mean	1.1	67.0
Standard Deviation	1.0	69.1
Method = CLEVELAND		
1.00%	0.3	19.5
5.00%	0.4	23.3
10.00%	0.4	25.3
20.00%	0.5	32.0
25.00%	0.5	34.1
30.00%	0.5	34.9
40.00%	0.6	38.3
50.00%	0.7	41.9
60.00%	0.8	48.1
70.00%	1.0	59.0
75.00%	1.2	71.1
80.00%	1.4	78.4
90.00%	2.1	136.2
95.00%	2.8	181.1
99.00%	4.8	329.3

Year = 2017	Nitrate-N removal rate (g/m³/d)	Nitrate-N removal (g/d)
N of Cases	8754	8754
Minimum	0.0	0.0
Maximum	76.8	2560.4
Median	0.8	25.3
Arithmetic Mean	1.0	37.6
Standard Error of Arithmetic Mean	0.0	0.9
95.0% LCL of Arithmetic Mean	0.9	35.9
95.0% UCL of Arithmetic Mean	1.0	39.4
Standard Deviation	2.4	83.4
Method = CLEVELAND		
1.00%	0.3	9.0
5.00%	0.4	12.0
10.00%	0.5	14.7
20.00%	0.5	18.3
25.00%	0.6	19.5
30.00%	0.6	20.9
40.00%	0.7	23.4
50.00%	0.8	25.3
60.00%	0.8	29.9
70.00%	0.9	32.9
75.00%	1.0	35.4
80.00%	1.0	38.2
90.00%	1.3	49.7
95.00%	1.8	86.3
99.00%	4.7	247.5

Year = 2018	Nitrate-N removal rate (g/m³/d)	Nitrate-N removal (g/d)
N of Cases	6941	6941
Minimum	0.0	0.0
Maximum	305.5	6961.2
Median	1.5	28.6
Arithmetic Mean	6.0	127.9
Standard Error of Arithmetic Mean	0.3	7.2
95.0% LCL of Arithmetic Mean	5.4	113.9
95.0% UCL of Arithmetic Mean	6.6	142.0
Standard Deviation	27.1	597.2
Method = CLEVELAND		
1.00%	0.1	1.1
5.00%	0.2	3.2
10.00%	0.3	4.7
20.00%	0.9	16.1
25.00%	1.1	19.9
30.00%	1.2	22.2
40.00%	1.4	25.9
50.00%	1.5	28.6
60.00%	1.6	31.7
70.00%	1.8	34.7
75.00%	2.0	38.3
80.00%	2.2	43.4
90.00%	3.5	71.9
95.00%	7.1	142.8
99.00%	184.7	4128.7

Season = Summer	Nitrate-N removal rate (g/m ³ /d)	Nitrate-N removal (g/d)
N of Cases	4809	4809
Minimum	0.0	0.0
Maximum	6.3	406.6
Median	0.6	33.0
Arithmetic Mean	0.8	42.2
Standard Error of Arithmetic Mean	0.0	0.6
95.0% LCL of Arithmetic Mean	0.8	40.9
95.0% UCL of Arithmetic Mean	0.8	43.4
Standard Deviation	0.7	44.6
Method = CLEVELAND		
1.00%	0.1	1.0
5.00%	0.3	8.9
10.00%	0.4	11.0
20.00%	0.4	14.4
25.00%	0.5	21.0
30.00%	0.5	24.3
40.00%	0.6	28.6
50.00%	0.6	33.0
60.00%	0.7	36.6
70.00%	0.8	40.4
75.00%	0.8	44.3
80.00%	0.9	49.7
90.00%	1.3	79.7
95.00%	2.0	122.4
99.00%	4.0	241.6

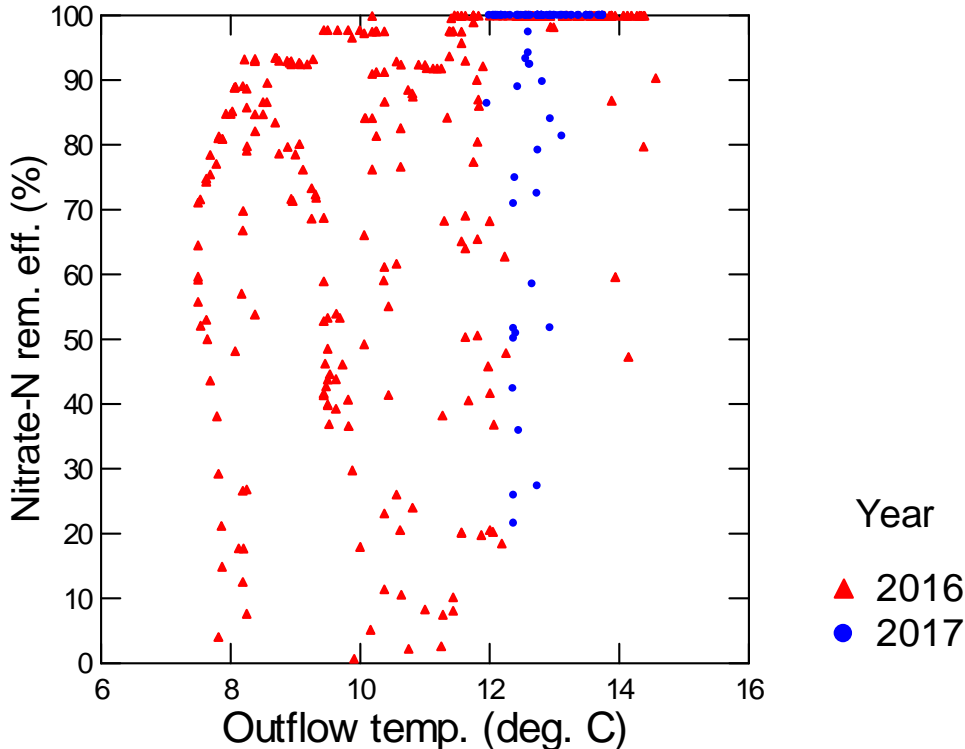
Season = Autumn	Nitrate-N removal rate (g/m ³ /d)	Nitrate-N removal (g/d)
N of Cases	6506	6506
Minimum	0.0	0.0
Maximum	305.5	6961.2
Median	0.6	30.8
Arithmetic Mean	4.2	119.6
Standard Error of Arithmetic Mean	0.3	6.7
95.0% LCL of Arithmetic Mean	3.6	106.3
95.0% UCL of Arithmetic Mean	4.8	132.8
Standard Deviation	24.7	543.3
Method = CLEVELAND		
1.00%	0.1	1.9
5.00%	0.2	4.0
10.00%	0.3	7.3
20.00%	0.4	21.4
25.00%	0.4	23.1
30.00%	0.5	23.7
40.00%	0.5	28.1
50.00%	0.6	30.8
60.00%	0.8	33.2
70.00%	1.2	40.1
75.00%	1.3	44.7
80.00%	1.6	54.6
90.00%	2.5	146.7
95.00%	3.9	225.6
99.00%	164.8	3532.3

Season = Winter	Nitrate-N removal rate (g/m3/d)	Nitrate-N removal (g/d)
N of Cases	6524	6524
Minimum	0.00	0.02
Maximum	203.30	4452.62
Median	1.25	35.61
Arithmetic Mean	2.49	73.32
Standard Error of Arithmetic Mean	0.15	3.48
95.0% LCL of Arithmetic Mean	2.19	66.50
95.0% UCL of Arithmetic Mean	2.78	80.15
Standard Deviation	12.19	281.11
Method = CLEVELAND		
1.00%	0.37	9.04
5.00%	0.68	15.79
10.00%	0.73	18.15
20.00%	0.81	21.02
25.00%	0.84	22.78
30.00%	0.90	24.55
40.00%	1.04	28.86
50.00%	1.25	35.61
60.00%	1.37	42.65
70.00%	1.54	50.23
75.00%	1.71	56.57
80.00%	1.93	69.59
90.00%	2.54	95.86
95.00%	3.41	149.29
99.00%	16.73	502.19

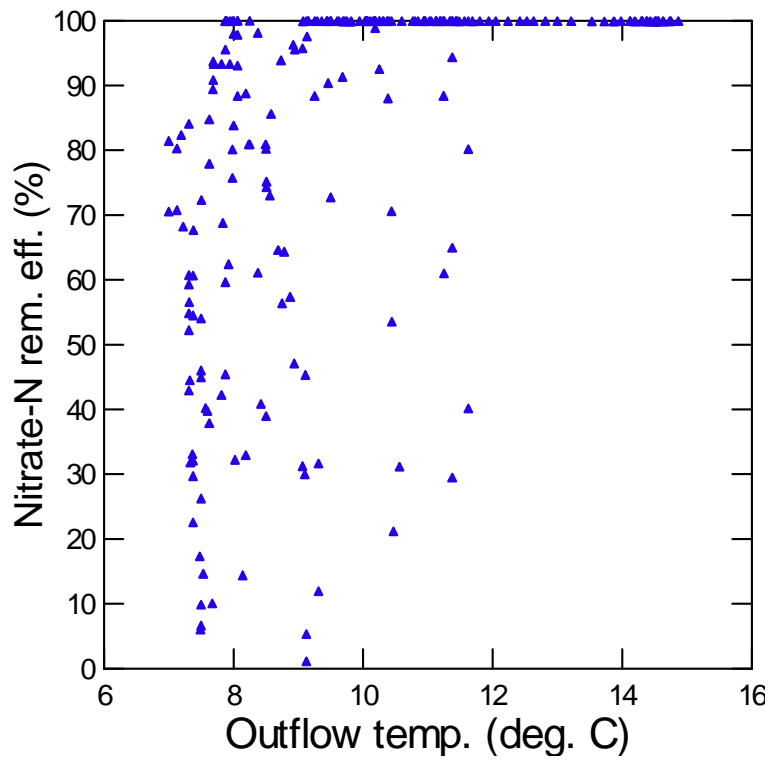
Season = Spring	Nitrate-N removal rate (g/m³/d)	Nitrate-N removal (g/d)
N of Cases	6552	6552
Minimum	0.3	7.2
Maximum	130.7	2878.4
Median	1.0	32.7
Arithmetic Mean	1.8	50.1
Standard Error of Arithmetic Mean	0.1	1.8
95.0% LCL of Arithmetic Mean	1.6	46.5
95.0% UCL of Arithmetic Mean	2.0	53.6
Standard Deviation	6.7	147.3
Method = CLEVELAND		
1.00%	0.5	14.5
5.00%	0.5	16.7
10.00%	0.5	18.7
20.00%	0.6	23.2
25.00%	0.7	24.3
30.00%	0.7	25.3
40.00%	0.9	29.1
50.00%	1.0	32.7
60.00%	1.0	34.7
70.00%	1.4	38.4
75.00%	1.5	40.4
80.00%	1.5	43.6
90.00%	2.1	58.3
95.00%	3.3	88.8
99.00%	14.2	307.4

Appendix M Relationship between woodchip filter performance and temperature

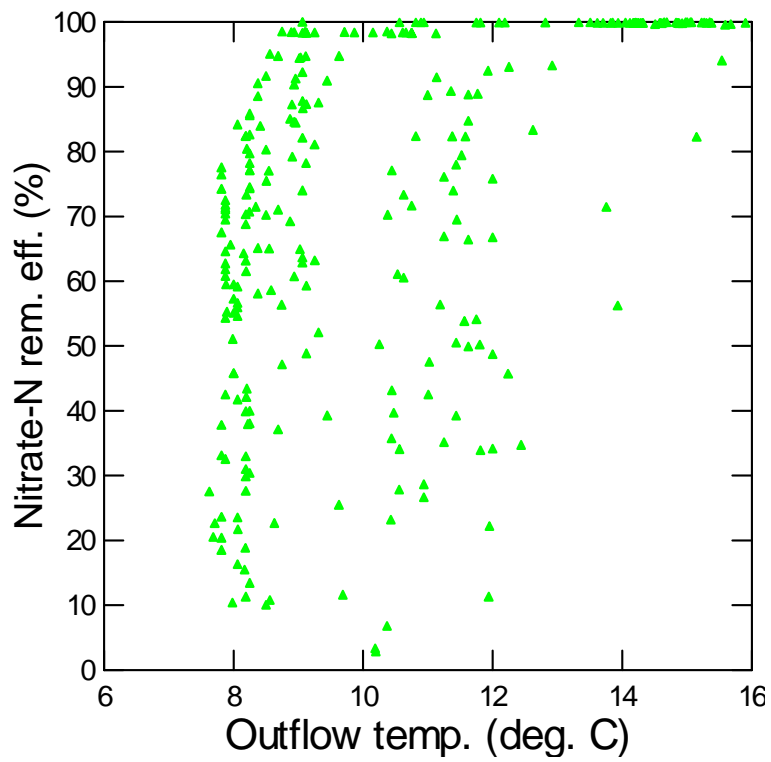
Level = high



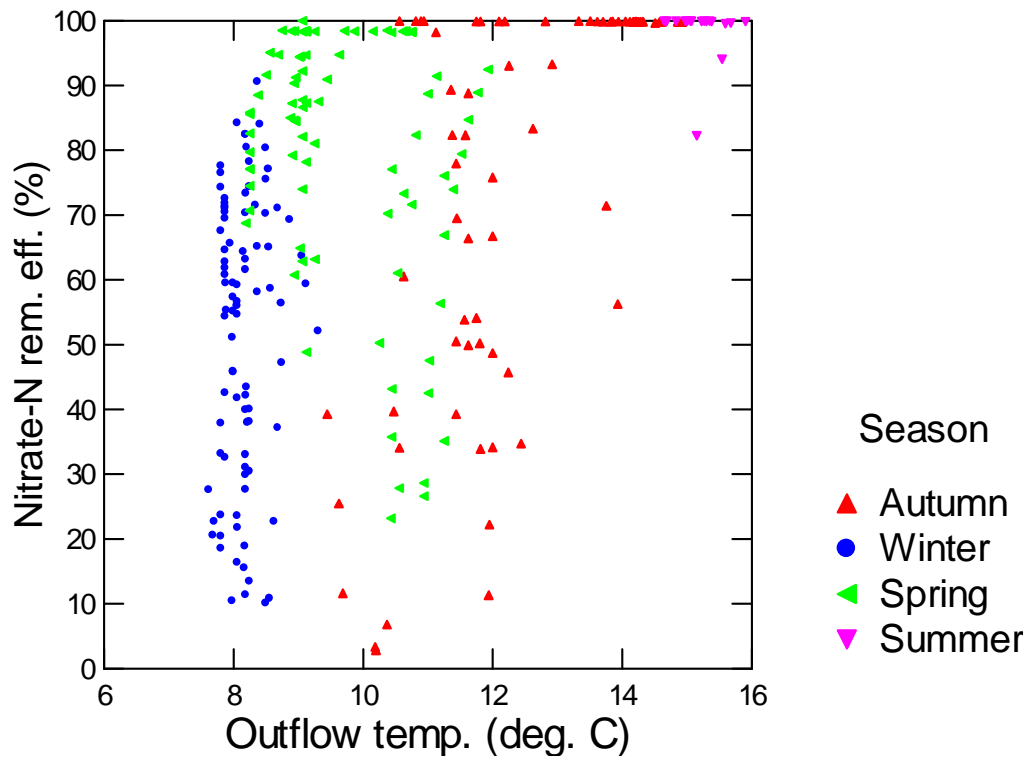
Level = medium



Level = low



Level = low



Level = high

